Translating torpor into a neuroprotective therapy for acute stroke:

an investigation of its electrophysiological and neuroprotective properties

Dr. Yi-Ge Huang

St. John's College

University of Oxford

A thesis submitted for the degree of

Doctor of Philosophy

Hilary Term 2024

Translating torpor into a neuroprotective therapy for acute stroke: an investigation of its electrophysiological and neuroprotective properties

Dr. Yi-Ge Huang

St. John's College, University of Oxford

A thesis submitted for the degree of *Doctor of Philosophy*, Hilary Term 2024

Abstract

Acute ischaemic stroke is a leading cause of adult disability and mortality globally. Meta-analyses of preclinical studies indicate that hypothermia is the most potent neuroprotective strategy for stroke. However, existing hypothermic therapies have so far been largely unsuccessful in clinical trials, with compensatory thermogenesis being a contributing factor. However, thermogenesis is suppressed in torpor, which is a regulated state of hypothermia and hypometabolism occurring naturally in some mammals in response to actual or perceived food shortage. Recent studies demonstrate that torpor can be pharmacologically-induced via activation of central nervous system A_1-adenosine receptors (A_1AR), even in animals incapable of natural torpor. Consequently, there is growing promise of successfully-harnessing torpor's neuroprotective potential to develop novel therapies for acute stroke. However, relatively little is understood about torpor's impact on brain activity and its neuroprotective effects. Since these aspects are likely pertinent to the successful translation of torpor into a neuroprotective therapy, the overarching aim of this thesis is to investigate them. In Chapters 2 and 3, I observed that both natural (fasting-induced) and pharmacological (cyclohexyladenosine-induced) torpor *in vivo* in laboratory mice are characterised by reversible hypothermia and by slow-wave activity (SWA) on EEG that resembles NREM sleep, indicating decreased net cortical neuronal firing which may reflect decreased potential for an excitotoxic response to an ischaemic insult. In Chapter 4, I observed that both 33 °C hypothermia and cyclohexyladenosine (CHA) increase viability during oxygen glucose deprivation in *in vitro* SH-SY5Y neuronal cultures, with viability further increasing when 33 °C hypothermia and CHA are combined with one another. Finally, in Chapter 5, I observed that, although physically-induced 33 °C hypothermia was neuroprotective in a 2 h middle cerebral artery occlusion rat model of focal ischaemia, neither CHA-induced 33 °C hypothermia nor CHA given at normothermia were protective. Together,

these data provide further insight into the electrophysiological properties of torpor, as well as CHA-induced torpor's potential for translation into a neuroprotective therapy for acute ischaemic stroke and the possible challenges of doing this.

List of abbreviations

A_1AR	A_1 adenosine receptor
AMPA	A-amino-3-hydroxy-5- methyl-4-isoxazoleproprionate
ATP	Adenosine triphosphate
BAT	Brown adipose tissue
BBB	Blood brain barrier
CBF	Cerebral blood flow
CHA	N^6-cyclohexyladenosine
CIRP	Cold inducible binding protein
CNS	Central nervous system
CPA	N^6-cyclopentyladenosine
EEG	Encephalography
EMG	Electromyography
ET	Euthermic
FSC	Forward scatter
HT	Hypothermic
LD	Light-dark
LFP	Local field potential
MCA	Middle cerebral artery
MCAO	Middle cerebral artery occlusion
NDS	Neurological deficit score
NMDA	N-methyl-D-aspartate
NREM	Non-rapid eye movement
OGD	Oxygen glucose deprivation
PKC	Protein kinase C
PLC	Activation of phospholipase C
POA	Preoptic area
RBM3	RNA binding motif 3
REM	Rapid eye movement sleep
ROS	Reactive oxygen species
RPIA	R-phenylisopropyl-adenosine
SSC	Side scatter
STAIR	Stroke therapy academic industry roundtable

SWA	Slow-wave activity
T_a	Ambient temperature
T_b	Core body temperature
TH	Therapeutic hypothermia
$T_{surface}$	Surface body temperature
ZT	Zeitgeber time

Preface

The work presented in this thesis was carried out by the author from August 2018 to December 2023 at the Radcliffe Department of Medicine and the Department of Physiology, Anatomy and Genetics University of Oxford, under the supervision of Prof. Alastair M. Buchan, Dr. Paul M. Holloway and Prof. Vladyslav V. Vyazovskiy. No part of this thesis has been previously submitted for a degree at this or any other university. Some of the work has been published in peer-reviewed scientific publications:

- Huang YG, Flaherty SJ, Pothecary CA, Foster RG, Peirson SN, Vyazovskiy VV. The relationship between fasting-induced torpor, sleep, and wakefulness in laboratory mice. Sleep. 2021 Sep 13;44(9):zsab093. doi: 10.1093/sleep/zsab093. (Chapter 2; Statement of authorship provided within thesis).
- Liddle LJ, Huang YG, Kung TFC, Mergenthaler P, Colbourne F, Buchan AM. An Assessment of Physical and N6-Cyclohexyladenosine-Induced Hypothermia in Rodent Distal Focal Ischemic Stroke. Ther Hypothermia Temp Manag. 2023 Jun 20. doi: 10.1089/ther.2023.0025. Epub ahead of print. (Chapter 5; Statement of authorship within paper).

Acknowledgements

This thesis has been completed with the kind support and help from a network of generous people around me. I would like to take this opportunity to express my sincere thanks to all of them. First and foremost, I would like to express my profound gratitude towards my supervisors, Prof. Alastair Buchan and Dr. Paul Holloway for their kind and patient support, and exceptional supervision and perseverance, both of whom have been excellent and truly inspirational scientists to learn from. I would also like to thank Prof. Vladyslav Vyazovskiy for his guidance and sharing with me his invaluable knowledge and enthusiasm for torpor. Members of both labs have also given their precious time and efforts to help with experiments. My thanks also go to Prof. Fred Colbourne, Dr. Lane Liddle and Ms. Tiffany Kung at University of Alberta, Edmonton, for their collaboration. I am very grateful to the Medical Research Council and Stroke Association for sponsoring my DPhil. Most of all, I am forever indebted to my Peipei for her love, patience and understanding throughout my studies, and my mum and dad (particularly for introducing flow cytometry to me), my aunt and my sister for their invaluable support and encouragement.

Contents

1 Introduction

1.1 Stroke

Stroke is a sudden neurological deficit resulting from the loss of cerebral blood flow. It is a leading cause of morbidity and mortality globally, being the second leading cause of death after ischaemic heart disease.[1] Over the past several decades, stroke incidence and mortality have both fallen, but prevalence has remained stable at 2.5% due to improved survival. Increasing prevalence of predisposing factors such as hypertension and diabetes and the increasing average population age account for a projected mortality rate of 12 million globally by 2030.[2] Therefore, a major priority of the wider medical research community is to develop and improve strategies for prevention, acute treatment and chronic management of stroke.

Stroke is a heterogeneous disease, broadly classified into ischaemic and haemorrhagic types, where vascular occlusion and rupture are the respective causes. The vast majority of strokes are of the ischaemic type (~87%), which can be further subdivided by cause into thrombotic, embolic and due to hypoperfusion.[3] The clinical presentation and sequelae vary greatly depending upon the location of the occlusion, which determines which cerebral regions are affected. Whereas hypoperfusion (e.g., due to cardiac arrest) usually leads to global ischaemia, thrombosis or embolus (e.g., of cardiac origin) usually causes focal ischaemia. Focal ischaemia resulting from middle cerebral artery (MCA) occlusion accounts for approximately 67% of all ischaemic strokes, and classic symptoms and signs include: contralateral hemiparesis or hemiplegia; hemisensory impairment; visual disorders such as contralateral homonymous hemianopia; aphasia (resulting from a dominant hemisphere lesion); and perceptual deficits

such as hemispatial neglect, anosognosia, and apraxia (resulting from a non-dominant hemisphere lesion).[3] Recovery from such deficits depends on the severity of the original insult; in many cases permanent disability results. The neuropsychiatric sequelae of stroke, such as dementia and depression, are long-lasting and often as devastating as the neurological ones.[4]

1.1.1 Mechanisms of ischaemic cell death in stroke

Ischaemic cell death results from a cascade of events that begins with disruption of blood supply to the brain. The cerebrovascular system is crucial to normal brain function: as with other vascular systems, it delivers oxygen and nutrients and removes waste products. Under normal physiological conditions, cerebral vascular tone is directly regulated by the metabolic rate of brain cells. This so-called neurovascular coupling ensures that blood delivery matches metabolic demand.[5] When there is a primary decline in metabolic rate, there is a physiological secondary decrease in cerebral blood flow (CBF) by a similar magnitude. However, CBF can be *severely and abruptly* reduced due to pathological causes, such as vascular occlusion via thrombosis or embolus. In such cases, both duration and magnitude of CBF reduction, as well as presence of collateral blood supply, affect the survival rates of neurons and glia adjacent to the occlusion. Vulnerability to ischaemia also depends upon other factors such as the type of brain tissue in question (e.g., hippocampal CA1 neurons tolerate ischaemia worse than CA3 neurons).[6]

Decreased blood flow leads to decreased availability of oxygen, glucose and high-energy metabolites such as adenosine trisphosphate (ATP) and phosphocreatine. Such metabolites are required by neuronal transmembrane ion pumps (e.g., the Na-K-ATPase) for maintaining a resting membrane potential of approximately –70 mV.[7] Thus, as a consequence of decreased

metabolite supply, there is increased neuronal depolarisation and voltage-gated Ca^{2+} channel activation, leading to influx of Ca^{2+} ions. ATP deprivation also triggers intracellular acidosis, which further worsens ionic imbalance via activation of acid-sensing Na^{+} and Ca^{2+} ion channels.[8] Elevated Ca^{2+} drives excessive presynaptic release of excitatory amino acid neurotransmitters – the main ones being glutamate and glutamate-like amino acids – and these bind to ionotropic or metabotropic receptors. The former are ligand-gated cation channels, subdivided by their selectivity over glutamate for N-methyl-D-aspartate (NMDA), α-amino-3-hydroxy-5- methyl-4-isoxazoleproprionate (AMPA), and kainate (KA).[9] The latter are G-protein coupled and under non-ischaemic conditions participate in the modulation of synaptic transmission and neural plasticity, e.g., in learning and memory. However, under ischaemic conditions, they contribute (firstly via activation of phospholipase C (PLC), protein kinase C (PKC) and then inositol triphosphate (IP_3)) to a wide range of pro-cell death downstream effects. The result is a vicious circle leading to a further rise of intracellular calcium and increase in cell death.[9]

Ischaemic stroke also triggers an inflammatory response in the brain characterised by the release of pro-inflammatory cytokines, chemokines, damage-associated molecular patterns (DAMPs), and activation of immune cells, which contribute to the recruitment of leukocytes and amplification of tissue damage within the ischaemic region.[10,11] Microglia, as the resident immune cells of the central nervous system, respond swiftly to the ischaemic insult by transitioning into an activated state and releasing pro-inflammatory cytokines, including interleukin-1β (IL-1β), tumour necrosis factor-α (TNF-α), and interleukin-6 (IL-6), as well as chemokines and other inflammatory mediators, thereby amplifying the inflammatory response.[10,12] DAMPs, endogenous molecules released by stressed, injured, or dying cells, such as high-mobility group box 1 (HMGB1), nucleic acids, and heat shock proteins, act as danger

signals and activate pattern recognition receptors (PRRs) on microglia, astrocytes, and infiltrating leukocytes.[13,14] Activation of PRRs, including toll-like receptors (TLRs), triggers intracellular signalling cascades that further enhance the inflammatory response and contribute to tissue damage.[15,16] Furthermore, infiltrating leukocytes, such as neutrophils and monocytes, are attracted to the site of ischaemic injury in response to chemotactic signals released by activated microglia and resident astrocytes, contributing to the inflammatory cascade through the release of pro-inflammatory cytokines, proteolytic enzymes, and reactive oxygen species.[17] The activation of PRRs on infiltrating leukocytes also amplifies the immune response and exacerbates tissue damage.[18] The sustained production of pro-inflammatory cytokines, chemokines, DAMPs, and activation of PRRs promote the recruitment and activation of additional immune cells, creating a positive feedback loop that perpetuates the inflammatory response.

Disruption of the blood-brain barrier (BBB) plays an important role in stroke pathophysiology. The BBB, a layer of endothelial cells typified by high selectivity of tight junctions and lack of fenestrae, that regulates the movement of molecules and cells between the blood and brain tissue, maintaining a tightly controlled microenvironment essential for proper neuronal function.[19] However, during ischaemia, the integrity of the BBB is compromised through several interrelated mechanisms. While the aforementioned inflammatory responses activate endothelial cells, onset of oxidative stress (which initiates within minutes of an ischaemic event) starts to damage endothelial cells and tight junctions, as does the release of matrix metalloproteinases, which degrade extracellular matrix components and tight junction proteins, albeit over the timespan of hours.[19] These processes collectively lead to increased BBB permeability, further exacerbating the inflammatory response by facilitating the entry of inflammatory cells, DAMPs, and additional inflammatory mediators into the brain,

contributing to further tissue injury.[17] Thus these processes transition from being the initial cause of BBB disruption to being its consequences.

Reperfusion injury, occurring upon the restoration of blood flow after a period of ischaemia, encompasses a complex series of events that exacerbate tissue damage and neuronal injury. While reperfusion is necessary to salvage viable brain tissue, it also introduces its own set of detrimental effects, including further oxidative stress, inflammation, and excessive calcium release.[12,13] One of the key mechanisms contributing to reperfusion injury is the generation of reactive oxygen species (ROS) during the sudden reintroduction of oxygen to the ischaemic tissue. The restoration of blood flow leads to the formation of ROS, such as superoxide anions, hydroxyl radicals, and hydrogen peroxide, through various enzymatic and non-enzymatic processes.[16] ROS, in turn, cause oxidative damage to lipids, proteins, and DNA, leading to further tissue injury and neuronal dysfunction.[20] For instance, ROS can initiate lipid peroxidation, which results in the destruction of cellular membranes and compromises their integrity and function.[21] Protein oxidation and modification, another consequence of ROS formation, lead to the dysfunction of enzymes and structural proteins critical for cellular processes. DNA damage induced by ROS can result in mutations and disruptions in gene expression, further contributing to cellular dysfunction and death.[22] The reperfusion of ischaemic tissue results in the further activation of the inflammatory pathways previously mentioned. The sudden influx of oxygen and nutrients triggers the release of pro-inflammatory cytokines, such as interleukin-1β (IL-1β), interleukin-6 (IL-6), and tumour necrosis factor-α (TNF-α), from various immune cells, including microglia and infiltrating leukocytes. These cytokines act as signalling molecules to recruit and activate additional immune cells, amplifying the inflammatory response within the reperfused region.

In summary, ischaemic cell death in stroke results from a complex cascade of interrelated events. The initial disruption of blood supply triggers a series of pathophysiological processes including energy depletion, ionic imbalance, excitotoxicity, oxidative stress, and inflammation. These mechanisms are further complicated by BBB disruption and reperfusion injury. The temporal dynamics of these processes are critical, with acute effects generally being detrimental, while some later inflammatory responses may contribute to repair and regeneration.[23,24] This intricate interplay of mechanisms underscores the challenges in developing effective stroke treatments and highlights the importance of considering multiple therapeutic targets and intervention timepoints. Understanding these mechanisms provides a foundation for developing neuroprotective strategies and identifying potential windows for therapeutic intervention in acute ischaemic stroke.

1.2 Neuroprotective therapies

1.2.1 The salvageable ischaemic penumbra: an opportunity to achieve neuroprotection

Successful recanalisation therapy via drug (e.g., intravenous tissue-type plasminogen activator (IV tPA))-mediated thrombolysis or mechanical thrombectomy leads to restoration of CBF and reperfusion of the ischaemic tissue.[25,26] This consequently results in restoration of energy metabolite levels and normal ionic homeostasis. Within the volume of brain tissue affected by ischaemia and reperfusion injury, a certain proportion of neurons and glia at the very centre would have either already undergone or eventually will undergo irreversible cell death by the time of therapeutic restoration of CBF. Surrounding this is a penumbral layer of cells that are dying but are potentially rescuable, in the eventuality of CBF being restored. The ultimate goal

of neuroprotective therapies is to maximise the volume of penumbral tissue surviving by inhibiting and slowing down the processes resulting in cell death mentioned above.[27]

The concept of the ischaemic penumbra is based on the observation that blood flow reduction in the brain is not uniform and that there exists a transitional zone surrounding the core of the ischaemic lesion. This penumbra is characterised by *moderately* compromised perfusion, impaired (but not irreversible) cellular metabolism, and the potential for functional recovery if timely intervention is provided.[28] It is in this region that interventions targeting neuroprotection can have a profound impact on clinical outcomes post-stroke. It should be noted, however, that while the general concept of the penumbra focuses on a transitional zone, the reality may be more complex: the penumbra might not be uniformly affected across its entirety and there may be smaller areas or regions within this penumbra with varying degrees of compromised perfusion and metabolic activity, i.e., mini-penumbras. It is unclear whether or not there are any implications of this concept for targeted interventions.[29]

The ischaemic penumbra is a dynamic entity that evolves over time following the onset of ischaemia. Initially, the tissue within the penumbra experiences decreased oxygen and glucose availability, leading to a state of energy failure and impaired ion homeostasis.[28] However, unlike the irreversibly damaged core, the penumbra still maintains some degree of residual perfusion, albeit at reduced levels. This residual blood flow is critical for sustaining cellular viability and offers a therapeutic window during which interventions can be implemented to salvage the endangered tissue.[30]

In the ischaemic penumbra, there is a delicate balance between ongoing cell death processes and the potential for recovery. The key challenge lies in identifying and targeting the molecular

mechanisms that drive cellular injury within this region. Different molecular pathways and processes have been implicated in the pathophysiology of the ischaemic penumbra, including excitotoxicity, oxidative stress, inflammation, and apoptosis – which are described in the previous section.[5,13] Understanding the interplay between these processes and their temporal dynamics is crucial for the development of effective neuroprotective strategies.

In summary, the salvageable nature of the ischaemic penumbra provides opportunities for the development of therapeutic interventions aimed at halting or reversing the progression of tissue damage: neuroprotection. By targeting the underlying mechanisms of injury and promoting cellular resilience, neuroprotective therapies hold the potential to enhance the recovery of brain function and improve patient outcomes. However, as is described in the following section, translating preclinical findings into successful clinical interventions has proven challenging, and many neuroprotective therapies have failed to demonstrate efficacy in human trials.[12]

1.2.2 Neuroprotective therapies have so far failed in their translation to the clinic

Recanalisation of the occluded artery via thrombolysis with tissue plasminogen activator and/or thrombectomy is the current gold standard of treatment for acute ischaemic stroke. However, only a small proportion of patients can be treated via this route, due to specific contra-indications and patchy availability of the infrastructure required for delivery of such a treatment. As a result, the current therapeutic window is < 4.5 h after the ischaemic event.[31,32] For several decades, a parallel avenue of therapeutic development has been the development of neuroprotective agents and strategies to slow down and prevent ischaemia-induced neuronal injury in the ischaemic penumbra, with the goal of extending the therapeutic window in which recanalisation can occur.[27]

The overriding theme so far has been the failure to translate preclinical successes to efficacious clinical therapies. In some cases, there was purely lack of neuroprotective effect. In other cases, systematic reviews have suggested poor quality of trial design (including lack of proper randomisation, placebo controls and blinding), the lack of reproducibility of results and heterogeneity, and inconsistency in factors such as the type and strain of animal model and the precise endpoints used.[33,34] In 1999, the original set of recommendations from the stroke therapy academic industry roundtable (STAIR), an academia and industry joint collaborative effort, was published.[35] These were intended to be followed in order to advance stroke research in an evidence-based manner: randomisation and blinding of studies; demonstrating efficacy in two or more laboratories, as well as in a second species; attention to sex differences; attention to route of administration; and consideration of a clinically useful dose response and therapeutic window. Partly spurred by the continued difficulty of translating neuroprotectants, STAIR continued to document further recommendations for translating neuroprotective therapies, culminating in a further STAIR report (2009) that recommended several steps relating to the conduct of good science and laboratory practice. These included: elimination of randomisation and assessment bias; reporting on exclusion and inclusion criteria; using full power analyses; and disclosing potential conflicts of interest.[33] In the next paragraph, I mention notable examples of neuroprotectants that have failed translation to the clinic.

Neuroprotective agents developed so far have singularly targeted specific modes of stroke pathophysiology such as excitotoxicity and free radical generation. Early attempts to target the excitotoxic cascade using NMDA antagonists yielded limited success due to factors such as adverse clinical effects and limited understanding of the actual mechanism of action of the neuroprotectant.[36] For example, i.p. injection of MK-801, an NMDA receptor antagonist, in a

Mongolian gerbil model of global cerebral ischaemia was shown to be neuroprotective.[37] However, this effect was shown to be a consequence of MK-801 triggering hypothermia, which itself was well-known to be neuroprotective, rather than global antagonism of NMDA receptors. Indeed, MK-801 given in gerbils whose core body temperature (T_b) was maintained at 37 ˚C did not lead to neuroprotection.[38,39] In another gerbil study, it was shown that NBQX, an AMPA receptor antagonist, protected hippocampal CA1 neurons against ischaemia-induced damage. However, this drug was found to have significant nephrotoxicity.[40] More recently, NA-1 (or nerinetide), a peptide that disrupts the NMDAR-PSD95-nNOS complex and thus dissociates NMDARs from downstream neurotoxic nitric oxide production, demonstrated efficacy in a non-human primate model of ischaemic stroke. However, results of the phase 3 ESCAPE-NA1 trial showed no benefit when combined with alteplase-mediated thrombolysis and endovascular thrombectomy.[41,42] More recently, the phase 3 ESCAPE-NEXT trial failed to show a benefit of NA-1 (given an average of 4 to 5 hours after stroke onset) for stroke patients undergoing endovascular therapy, but the smaller FRONTIER study (with the same drug but given 1 hour from symptom onset in a pre-hospital setting) showed beneficial effects on functional outcomes.[43,44] As a further example, the nitrone free radical scavenger NXY-059 is another drug that both demonstrated preclinical neuroprotective efficacy and satisfied almost all STAIR criteria for preclinical research quality, but then failed in a high-profile clinical trial.[45]

The mixed results from the NA-1 trials are significant as they highlight key challenges in translating neuroprotective agents from preclinical models to clinical stroke treatment. Whilst NA-1 showed promise in non-human primates, its efficacy was not replicated in large clinical trials when combined with standard reperfusion therapies. Notably, the ESCAPE-NA1 trial revealed a potential drug-drug interaction between NA-1 and alteplase, with better outcomes

observed in patients who received NA-1 without alteplase. This unexpected finding underscores the importance of considering potential pharmacological interactions in combination therapies. The positive outcomes from the smaller FRONTIER trial, where NA-1 was administered earlier and pre-hospital without alteplase, further support this interaction hypothesis and emphasise the critical role of treatment timing. These results demonstrate the complexity of stroke pathophysiology and treatment, highlighting the need for careful consideration of how neuroprotective agents are integrated into existing stroke care pathways and the value of targeted trials to identify optimal treatment scenarios.

1.3 Therapeutic hypothermia

1.3.1 Therapeutic hypothermia acts upon a broad range of pathophysiological mechanisms mediating ischaemia-induced injury

Hypothermia has been used as a therapy long before the advent of modern medicine. Hippocrates described the use of snow and ice in reducing haemorrhage resulting from traumatic injury and whole-body cooling was touted as a cure for tetanus around 300–400 BC.[46] There has also been a steady stream of anecdotal evidence for hypothermia's life-saving properties, with remarkable stories of survivors of drowning and avalanches who underwent accidental hypothermia.[47] However, it is only in recent times that hypothermia has been systematically studied as a medical therapy. Studies in rodent stroke models have demonstrated that varying degrees of hypothermia can limit the extent of neuronal injury.[48] For decades, hypothermia has been used as a neuroprotective and cardioprotective adjunct for cardiac arrest and elective cardiothoracic and neurosurgery patients, as well as in neonatal hypoxaemia. It has been widely believed that similar success can be achieved for therapeutic hypothermia in acute stroke.[49,50]

Unlike most drugs with neuroprotective potential, hypothermia acts upon a broad range of pathophysiological mechanisms mediating ischaemia-induced injury.[47,51] It has effects on cerebral metabolic rate (CMR), glutamate release and reuptake, free radical generation, inflammation and the BBB. For example, hypothermia decreases the rate of ATP hydrolysis as well as the cerebral metabolic rates of oxygen (CMRO2) and glucose (CMRglu). Per °C decrease in T_b, CMRO2 falls by ~5%.[52] Hypothermia inhibits processes driving the excitotoxic cascade: it prevents both glutamate release and intracellular calcium build-up.[53] Hypothermia is anti-inflammatory: it suppresses granulocyte, leukocyte and ICAM-1 (an intercellular adhesion molecule) accumulation. It also reduces iNOS, nitric oxide and peroxynitrite mediated oxidative damage.[54] However, protective effects generally only occur over the duration of hypothermia; post-hypothermia there is a rebound in immune cell infiltration and loss of neuroprotective effect.[55] Intra-ischaemic hypothermia reduces the generation of hydroxyl free radicals and activation of pro-apoptotic factor caspase-3 whilst increasing expression of the anti-apoptotic factor bcl-2.[56,57] On the other hand, evidence that milder hypothermia reduces necrosis is that cytochrome *c* release is reduced in the *absence* of pro-apoptotic changes in bcl-2 expression or caspase activation.[58] Finally, hypothermia likely maintains BBB integrity: at 33 °C it reduces BBB leakage of the tracer horseradish peroxidase in rats undergoing transient forebrain ischaemia.[59]

Via the aforementioned mechanisms, hypothermia could potentially act synergistically with thrombolysis and thrombectomy to achieve better histological and neurological outcome, as well as enlarge the window of opportunity for recanalisation. Ultimately, timely cooling may preserve a greater proportion of the penumbra and may also decrease the inflammatory response generated due to post-reperfusion oedema.[47]

1.3.2 Preclinical findings

Consistent with hypothermia's purported broad action outlined above, successive meta-analyses of preclinical hypothermia studies in focal ischaemic models have indicated that hypothermia is strongly neuroprotective against both global and focal ischaemia. Indeed, they suggest that, of all preclinical neuroprotective treatments for focal ischaemia, hypothermia is the most potent.[49,60] Recent meta-analyses have focused on understanding how different factors relating to application of therapeutic hypothermia (e.g., delay between ischaemia onset and hypothermia initiation, target temperature, hypothermia duration, and regional versus whole-body cooling etc.) affect various measures of outcome (e.g., infarct volume, cerebral oedema volume, level of apoptosis and necrosis of neurons and glia, and neurobehavioural scores). Even taking into account considerable heterogeneity of these factors between studies, there is a significant and powerful treatment effect of hypothermia at all levels (mild, moderate and severe).[49]

The relative effect of individual variables on outcome remains unclear, however, and there is still no consensus from both preclinical and clinical studies on whether, for example, a target temperature of 34 ˚C is more beneficial than 36 ˚C, or a treatment duration of 24 h is more beneficial than 12 h. Whilst a general trend is that shallower target temperatures generally need lengthier durations to achieve the same therapeutic effect, the very awareness of this has in some cases generated bias in experimental design: shallower temperature has tended to be paired with longer duration and vice versa, leading to a loss of independence between these two factors.[61] More recently, however, it has become clearer that longer delays to hypothermia from ischaemia-onset lead to longer duration of hypothermia required to achieve equivalent treatment effect. Furthermore, the latest clinical trial data from ESCAPE-NEXT and

FRONTIER trials (mentioned in 1.2.1) showed that, for the same neuroprotectant, protection is achieved at 1 h post-stroke but not at 3–4 h post-stroke; it is possible that the same is applicable to hypothermia, though this remains to be determined.[61]

1.3.3 Clinical trials

Despite preclinical success in achieving neuroprotection with hypothermia, progress in clinical trials has been limited. In addition to problems common to the development of many neuroprotective agents described above, there are several hypothermia-specific challenges that affect efficacy and have not yet been fully addressed. Clinical trials so far have been unsuccessful. For example, ICTuS-2, was a Phase 2 trial of intravascular cooling as a hypothermic therapy for acute stroke, which ended prematurely primarily due to high pneumonia-associated mortality: the use of sedatives and/or narcotics to suppress shivering interferes with swallowing and increases risk of aspiration-related pneumonia.[62,63] Hypothermia is immunosuppressive, and – aside from requiring improved infection control measures in the clinical setting – more work needs to be done to optimise hypothermia depth and duration in order to achieve an adequate balance between too much and too little cooling.[64]

Clinical use of hypothermia has also been limited by the homeostatic mechanisms that control T_b. Humans, like all mammals, are endotherms and T_b is maintained at an equilibrium of approximately 37 ˚C. This is done via a negative feedback system consisting of thermosensory afferents and thermoeffector elements, which are coordinated by the CNS with the median preoptic (MnPO) nucleus of the hypothalamus, dorsomedial hypothalamus (DMH), raphe pallidus and paraventricular nucleus playing key roles.[65–68] Thermosensory afferents are specialised nerve endings that detect temperature changes both internally and externally, and transmit signals to the CNS when temperature shifts occur. Thermoeffector elements are

responsible for physiological responses like vasodilation, vasoconstriction, shivering, and sweating, aimed at heat conservation or dissipation. Central control is primarily by the MnPO nucleus of the hypothalamus, which processes input from thermosensory afferents to determine the body's temperature status. For a basic but elegant illustration of current and previous understandings of CNS thermoregulatory pathways, please refer to Figure 1 from Saper and Machado, 2020.[69] The raphe pallidus coordinates autonomic responses, while the paraventricular nucleus integrates temperature signals with other factors (e.g., hydration levels, metabolic demands, and circadian rhythms). The result is maintenance of T_b within an optimal range for normal physiology and function.[65–68]

Therapeutic hypothermia via *extrinsic* cooling (e.g., application of ice packs or administration of intravascular cold saline) displaces T_b downwards from its equilibrium, which ultimately results in a sympathetic-driven thermo*genic* response in order to return T_b to 37 ˚C. The thermogenic response is more of a problem in humans than in smaller mammals like rodents because humans have a much lower surface area:volume ratio through which to lose heat.[70] Therefore, more cooling per unit volume of tissue is required to decrease in T_b by the same magnitude per unit time. Thermogenesis is achieved via shivering (a stereotyped movement caused by rapid alternating contraction and relaxation of antagonistic muscles mediated by sympathetic nervous system efferents) and non-shivering generation of heat in brown adipose cells (BAT) (which occurs via the conversion of the mitochondrial transmembrane proton gradient into thermal energy by the transmembrane uncoupling protein (UCP1)). The shivering component is also unpleasant for the patient and requires control by antimuscarinics and narcotic opioid analgesics such as meperidine; this has the knock-on effect of respiratory depression and exacerbates the risk of pneumonia. Specifically, reduced respiratory function impairs the lungs' ability to clear mucus and other secretions from the airways, creating an

environment conducive to bacterial growth.[62] As a result of the above, a potentially more effective way of achieving cooling would be to suppress thermogenesis and lower the body's theoretical "set-point" temperature.

1.4 Torpor

1.4.1 Torpor is physiologically-regulated and reversible hypothermia

Torpor is a regulated and reversible state of metabolic suppression used as a strategy by many animals to conserve energy.[71–73] It has evolved multiple times across the animal kingdom – not only as derivations along individual phyletic lineages – but also independently across phyla that had become well-separated.[74,75] There are two types of torpor: fasting-induced torpor and hibernation torpor. Hibernation is defined as prolonged torpor, lasting more than 24h. Hibernation is either obligate or facultative. Obligate hibernation is driven by an endogenous circannual rhythm. Facultative hibernation is induced by short days and subsequent gonadal regression and encouraged by food and/or water restriction.[70,76] In all cases, the torpid mammal appears quiescent, has reduced mobility and has decreased responsiveness to sensory stimuli – characteristics in common with sleep. Unlike sleep, the torpid mammal experiences substantially greater decreases in metabolic, heart and breathing rates (sometimes down to just 1% of baseline values).[77]

Arguably, the most recognisable feature of torpor is whole body hypothermia. The overarching mechanism responsible is suppression of thermogenesis. Mammals and birds are endotherms: most species maintain a core body temperature (T_b) of 36–37 °C across a wide range of ambient temperatures (T_a). This is achieved by actively regulating the balance between heat loss (e.g., via vasodilatation and piloerection) and thermogenesis. At the molecular level, thermogenesis

occurs via respiration – an exothermic set of reactions of which heat and ATP are by-products resulting from the conversion of oxygen and glucose to carbon dioxide and water.[78] At the whole organism level, as described in 1.3.3, thermogenesis in endotherms occurs through two main mechanisms: shivering, which involves rapid antagonistic muscle contractions, and non-shivering thermogenesis in BAT, where inner mitochondrial membrane uncoupling protein 1 (UCP1) converts the proton gradient derived from oxidative phosphorylation into heat.[79]

At the organism level, provided that T_b is above T_a, there is a net loss of heat to the environment over a temperature gradient as per thermodynamic principles. Neuroanatomical studies suggest that the lateral and median preoptic area of the anterior hypothalamus is thought to act as the thermoregulatory "control centre", which integrates information about T_b and peripheral body temperature from afferent sensory neurons located within both the hypothalamus itself and key thermoregulatory tissues (e.g., abdominal viscera, skin and spinal cord).[65–68,80–82] According to whether the body is sensed to be too cool or too warm, different patterns of efferent signals are relayed to effector systems that promote heat retention or heat loss respectively. Such responses are broadly categorised as either physiological or behavioural. Physiological responses are involuntary and mostly autonomic; examples include evaporative heat loss via sweating, vasodilation/vasoconstriction, shivering and non-shivering or BAT thermogenesis. Behavioural responses are voluntary, goal/reward-orientated and learnt by positive reinforcement; examples include locomotor activity to either adopt postures that alter surface area:volume ratio (e.g., curling up into a ball) or move into or out of direct sunlight.[80,83] Suppression of thermogenesis during torpor is A_1AR-dependent and leads to disruption of physiological temperature homeostasis, akin to lowering the set-point temperature of a thermostat. As a result, T_b is no longer actively maintained at any temperature set-point, and, purely following thermodynamically principles, heat contained within the body is lost so that

it equilibrates with the external environment. T_b thus tends towards T_a, with its rate of decrease depending upon body surface area:volume ratio and T_b:T_a gradient.[70,84,85]

Associated with hypothermia are a wide range of physiological effects: decreased metabolic, cardiac and respiratory rates; leucopaenia and thrombocytopaenia; suppression of inflammatory and immune responses; hyperglycaemia and decreased carbohydrate metabolism.[64] These are outside the scope of this thesis and will not be discussed in any further detail here.

1.4.2 A_1 adenosine receptor signalling is sufficient and necessary for lowered T_b during torpor

Results from studies by Drew and colleagues suggested that activation of CNS A_1 adenosine receptors (A_1AR) is both sufficient and necessary for torpor. In the Arctic ground squirrel (AGS), activation of A_1AR by the agonist N^6-cyclohexyladenosine (CHA) administered via a pre-implanted cannula led to lowered T_b, whereas antagonism of A_1AR by theophylline during entrance into torpor led to sustained reversal of hypothermia.[86] These experiments employed measures to minimise handling-induced arousal, including prior habituation of AGSs to handling procedures. Consistent with these findings are those of previous studies in mice (which naturally undergo fasting-induced torpor), in which i.p. administration of the structurally similar A_1AR agonists, N^6-cyclopentyladenosine (CPA) and R-phenylisopropyl-adenosine (R-PIA), led to profound hypothermia.[87,88] More recently, it was found that activation of CNS A_1AR by CHA in the laboratory rat, a species naturally *incapable* of torpor, also leads to suppression of thermogenesis and a drop in T_b.[89] A subsequent study found that deep hypothermia induced by CHA (down to a mean minimum T_b of 29.7 ˚C) reduced mortality

in a rat model of global ischaemia.[90] However, to date, the effect of CHA-induced hypothermia on focal ischaemia has not been studied.

The precise neural circuitry behind CNS control of thermogenesis is complex and has not yet been fully elucidated. However, as mentioned previously, hypothalamic nuclei, specifically those in the MnPO, are likely to play a key role, as are other centres such as the raphe pallidus and paraventricular nucleus.[87,91–93] Further discussion of how CNS controls thermoregulation will not be discussed here as it lies outside the scope of this thesis. However, evidence suggests that the neural mechanisms controlling thermoregulation are evolutionarily conserved between mammals including rodents and humans.[94] Crucially, this lends support to the hypothesis that, as in all mammals studied so far, hypothermia can be pharmacologically induced in humans via CNS A_1AR-mediated suppression of thermogenesis.[95–97]

1.4.3 Rationale behind thesis and key objectives

The discovery that normal thermoregulation can be subverted by pharmacological activation of CNS A_1AR has led to optimism that a more effective means of inducing therapeutic hypothermia can be developed, which can potentially be deployed relatively early (e.g., pre-hospitalisation). This may be particularly important in the context of acute ischaemic stroke, since in most patients normal thermoregulation is largely intact, unlike in the cardiac arrest scenario.[98] However, more work needs to be done to uncover the mechanisms and consequences of hypothermia induced by CNS A_1AR activation. In particular, for successful translation, there is firstly a need to study its effects on brain activity and determine if it would indeed be protective against acute ischaemic stroke.

Therefore, in this thesis, I study the effects of torpor on brain activity as measured by electroencephalography (EEG), which is an established method of chronically recording overall activity of the brain. This is done in both in models of natural torpor (fasting-induced torpor in the laboratory mouse) and in pharmacological torpor (CHA-induced torpor), in order for phenotypic comparisons to be made. Next, I evaluate the neuroprotective effects of A_1AR agonist-induced hypothermia in both *in vitro* and *in vivo* models of ischaemia. As explained above, both impact on brain activity and neuroprotective efficacy of torpor are important aspects to investigate if such a treatment were to be successfully translated to the clinic. Therefore, to address these, I propose the following hypothesis-driven objectives:

1. Electrophysiology of fasting-induced torpor in mice (Ch. 2)
    - Hypothesis: Fasting-induced torpor in mice shares key electrophysiological characteristics with hibernation, including entrance via NREM sleep, predominance of slow-wave activity (SWA) during the hypothermic state, and suppression of REM sleep at low body temperatures.
    - Rationale: While hibernation has been extensively studied electrophysiologically, less is known about fasting-induced torpor. Understanding the similarities and differences could provide insights into the underlying mechanisms and evolutionary relationships between these energy-conserving states.
    - Expected results: Based on prior literature on hibernation, I expect to observe that fasting-induced torpor is entered via NREM sleep, exhibits predominantly slow-wave EEG activity that decreases in amplitude with declining body temperature, and shows suppression of REM sleep during deep torpor.
2. Electrophysiology of cyclohexyladenosine-induced torpor in mice (Ch. 3)

- Hypothesis: Pharmacologically-induced torpor using the A_1 adenosine receptor agonist CHA produces a state electrophysiologically similar to natural fasting-induced torpor.
- Rationale: Understanding the electrophysiological properties of CHA-induced torpor and comparing these with those of fasting-induced torpor could provide insights into similarities and differences in terms of underlying mechanisms. It would also indirectly provide insights into the potential impacts on brain activity should a similar approach eventually be used in humans for inducing therapeutic hypothermia (e.g., for acute stroke).
- Expected results: I anticipate CHA-induced torpor will show similar EEG characteristics to fasting-induced torpor, including SWA decreasing with body temperature. However, I expect some differences in induction and arousal dynamics due to its pharmacological nature. These findings would validate CHA-induced torpor as a model for studying torpor mechanisms and support its potential therapeutic applications.

3. Neuroprotective properties of hypothermia and cyclohexyladenosine in a neuronal culture model of ischaemia (Ch. 4)
    - Hypothesis: Both hypothermia and CHA provide neuroprotection against oxygen-glucose deprivation (OGD) in vitro, with potentially additive effects when combined.
    - Rationale: Understanding the neuroprotective effects of hypothermia and CHA individually and in combination could inform the development of treatments for ischaemic conditions like acute stroke.
    - Expected results: I anticipate both hypothermia and CHA will improve neuronal survival after OGD, with potentially greater protection when combined. I expect

CHA to show some neuroprotective effects at normothermia, suggesting mechanisms independent of hypothermia. These findings would provide a strong rationale for further investigation of combined hypothermia and CHA treatment in more complex models of ischaemia.

4. Neuroprotective properties of cyclohexyladenosine-induced torpor in a rat model of cerebral ischaemia (Ch. 5)
    - Hypothesis: CHA-induced torpor provides neuroprotection in a rat model of focal cerebral ischaemia, comparable to the effects of physical hypothermia.
    - Rationale: If CHA-induced torpor proves neuroprotective in vivo, it could offer a pharmacological alternative to physical cooling for treating ischaemic stroke.
    - Expected results: I anticipate CHA-induced torpor will reduce infarct volume and improve functional outcomes compared to normothermia, with effects similar to physical hypothermia. I expect some neuroprotection from CHA even when body temperature is maintained, suggesting temperature-independent mechanisms. These findings would support the potential of pharmacologically-induced torpor-like states as a neuroprotective strategy for stroke.

2 Electrophysiological properties of natural torpor

2.1 Introduction

As discussed in Chapter 1, torpor is a regulated and reversible state of metabolic suppression used as a strategy by many animals to conserve energy, having evolved multiple times across the animal kingdom.[71–73] There are two types of torpor, fasting-induced torpor and hibernation torpor. Hibernation is defined as prolonged torpor, lasting more than 24h. Hibernation is either obligate or facultative. Obligate hibernation is driven by an endogenous circannual rhythm. Facultative hibernation is induced by short days and subsequent gonadal regression and encouraged by food and/or water restriction.[70,76]

Also discussed in Chapter 1 was that the most recognisable feature of torpor is whole body hypothermia, caused by suppression of thermogenesis. Mammals and birds, as endotherms, typically maintain a T_b of 36–37 °C across a wide range of Ta. This is due to their ability to maintain T_b homeostasis via active regulation of heat loss and thermogenesis (both shivering and non-shivering types; described in more detail in 1.4.1).[79] The MnPO of the anterior hypothalamus is thought to act as the CNS thermoregulatory "control centre", which integrates information about T_b and peripheral body temperature from afferent sensory neurons.[65–68,80–82] This leads to physiological and behavioural responses to maintain temperature homeostasis.

[80,83] During torpor, A_1AR-dependent suppression of thermogenesis disrupts this homeostasis, causing T_b to eventually equilibrate with T_a[70,84,85]

The effects of hypothermia – whether through physical cooling or through torpor – upon brain activity have been the subject of a number of studies. Chronic cortical encephalography (EEG) has been recorded during whole body physical cooling in rodents, monkeys and humans. The general finding of these studies has been that the hypothermic EEG is predominantly characterised by SWA, with EEG power decreasing with decreasing T_b.[99–101] Studies in animals undergoing hibernation (e.g., alpine and Arctic ground squirrels, marmots, hedgehogs and dwarf lemurs) and seasonal-daily torpor (e.g., Djungarian hamsters, round-tailed ground squirrels and grey mouse lemurs) have yielded similar findings.[102–109]

The effects of hypothermia on states of vigilance have been investigated in a limited number of studies. EEG can be used to distinguish between different states of vigilance: sleep and wakefulness have characteristic patterns of brain activity, which arise from a dynamic interplay among numerous cortical and subcortical sleep-wake controlling circuits. During wakefulness, EEG activity is characterised by fast, low amplitude oscillations, dominated by theta-frequency activity (4–7 Hz), whilst non-rapid eye movement (NREM) sleep is defined by the occurrence of slow waves (typically 0.5–4 Hz), arising within thalamocortical networks.[73,110] The amplitude of slow-waves during NREM sleep is an established marker of the homeostatic sleep drive, which increases with prolonged wake and decreases with sleep.[111] Additionally, NREM sleep exhibits other distinctive EEG features such as sleep spindles (brief 12–14 Hz oscillations lasting 0.5–3 s) and K-complexes (large amplitude, biphasic waves lasting >0.5 s). By contrast, rapid eye-movement (REM) sleep is typically characterised by lower amplitude, theta-frequency oscillations, i.e. similar to the waking state.[73] While these EEG characteristics are

broadly similar across mammals, important species differences exist between rodents and humans that must be considered for clinical translation.[112] Human sleep architecture is more complex, comprising three distinct NREM stages (N1–N3) and REM sleep, whereas rodents exhibit a simpler architecture with single NREM and REM states. Stage N1 represents drowsiness and sleep onset in humans, characterised by slowing of alpha rhythm (8–12 Hz) and appearance of vertex sharp waves. Stage N2 features distinctive sleep spindles and K-complexes, whilst N3 (slow-wave sleep) is dominated by high-amplitude delta waves. This progressive deepening of NREM sleep seen in humans is not observed in rodents, which transition directly into a state most closely resembling N3. The temporal organisation of sleep also differs substantially between species. Humans typically experience a single consolidated 7–9 hour sleep period comprising 4–5 cycles of NREM-REM sleep. In contrast, laboratory mice exhibit polyphasic sleep patterns consisting of multiple shorter episodes throughout the 24-hour period, totalling approximately 12 hours of sleep.[113] These shorter cycles may reflect evolutionary adaptations to predation pressure, requiring more frequent periods of arousal. These differences, summarised in Table 1, have implications for detection, recognition and scoring of vigilance states between humans and mice.

Table 1: Comparison of vigilance state scoring criteria between humans and laboratory mice, highlighting key differences relevant for clinical translation.

State	Human Criteria	Mouse Criteria	Key difference
Wake	High frequency (>13 Hz), high EMG tone, eye movements	High frequency (>7 Hz), high EMG, prominent theta (4–7 Hz)	Theta rhythm prominence in rodents
NREM	Three stages (N1–N3), progressive delta (0.5–4 Hz), spindles (12–14 Hz)	Single state, high delta (0.5–4 Hz), spindles (12–14 Hz)	Simpler NREM architecture in rodents

REM	Mixed frequency EEG, muscle atonia, eye movements	Theta-dominated (4–7 Hz), muscle atonia	Theta rhythm prominence in rodents
Scoring Epochs	30 second epochs	4–10 second epochs	Smaller temporal resolutions allow more sensitive detection of short-term transitions in vigilance state

Beginning with Walker et al. in 1979, several studies have documented that torpor is entered via normothermic NREM sleep. It was concluded, that "hibernation is continuous with and homologous to sleep; more specifically, it is primarily an extension of the thermoregulatory adjustments of slow wave sleep".[114] In studies that recorded electromyography (EMG) during torpor, upon entrance into torpor there is a marked reduction in EMG activity that accompanies a suppression of shivering thermogenesis and the drop in T_b. The reverse occurs during rewarming: there is a progressive increase in EMG activity that accompanies disinhibition of shivering thermogenesis.[102,103,114–119] EEG obtained during pharmacologically-induced hypothermia is similarly predominantly NREM-like SWA, the amplitude of which decreases with T_b, whilst the EMG shows inhibition and disinhibition of shivering thermogenesis upon entry into and emergence from torpor, respectively.[92,120]

Notably, relatively fewer studies have recorded EEG and EMG in animals undergoing hypothermic torpor triggered by *fasting,* e.g., the pocket mouse and the laboratory mouse, rather than photoperiodic changes.[109,121,122] That fasting-induced torpor is triggered by *actual* and acute rather than seasonally-perceived lack of food is significant, not least because the selection pressures that drove its evolution are likely to be quite different, i.e., fluctuations in food availability that are decoupled from seasonal variations.[76,123] The other dimension that I considered when choosing to study torpor in murine rodents such as mice and rats is their

relevance to overarching aim of this thesis: to translate torpor, a naturally-occurring phenomenon, into a neuroprotective treatment for acute stroke. Unlike for the Arctic ground squirrel, models of both global and focal ischaemia have been established in both rats and mice. For the studies described in Chapters 2 and 3, the mouse is chosen rather than the rat because rats do not naturally undergo torpor whereas mice do, and this allows for a direct comparison of natural (fasting-induced) torpor with pharmacologically (A_1AR agonist) induced torpor.

Thus, in this study, I perform chronic recordings of EEG, EMG and surface body temperature ($T_{surface}$) in laboratory mice undergoing torpor induced by food restriction. I hypothesise that fasting-induced torpor shares key electrophysiological characteristics with hibernation, including NREM sleep entry, SWA predominance during hypothermia, and REM sleep suppression at low body temperatures. The primary aims are to characterise EEG morphology throughout torpor and compare these patterns with non-torpid (euthermic) states. These analyses aim to enhance our understanding of natural torpor, which is pertinent to its potential translation into a neuroprotective therapy for acute stroke.

2.2 Materials and methods

2.2.1 Animals and recording conditions

Adult, male C57BL/6 mice were used in this study (Charles River; n = 6; aged 12 weeks). Throughout the experiment, mice were individually housed in custom-made clear Plexiglas cages (20 x 30 x 35 cm) on a 12:12 h light-dark (12:12 LD) cycle for the duration of the experiment (Figure 1a) inside sound-attenuated, ventilated recording chambers (Campden Instruments, Loughborough, UK; two cages per chamber). Each chamber was illuminated at approximately 200 lux by a warm white LED strip lamp during the light phase of the 12:12 LD cycle. Room temperature and relative humidity were regulated at 20 ± 1 °C and 60 ± 10%, respectively. $T_{surface}$ was continually recorded from the hottest pixel detected by thermal imaging cameras (Optris Xi 80 compact spot finder thermal imaging camera with 80° wide angle lens, Optris GmbH, Berlin, Germany) mounted at the top of each cage (Figure 1a). *Ad libitum* water was provided throughout the study. All procedures were performed in compliance with the United Kingdom Animals (Scientific Procedures) Act of 1986, as well as the University of Oxford Policy on the Use of Animals in Scientific Research (PPL P828B64BC). All experiments had approval from the University of Oxford Animal Welfare and Ethical Review Board.

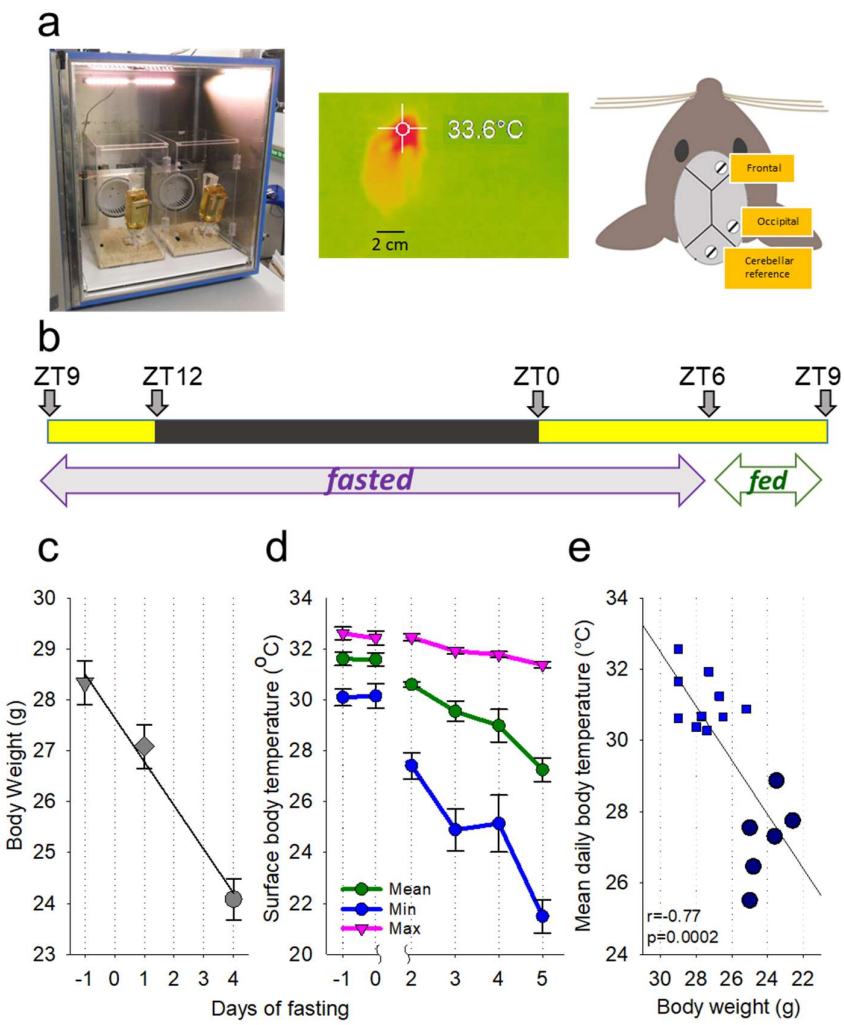

Figure 1. The experimental design and effects of food restriction on body weight and surface body temperature. a, Left: photograph showing the recording chamber with two Plexiglas cages for individually housed mice. Middle: a representative thermal image of a mouse acquired with the thermal imaging camera. Right: schematic diagram showing the position of EEG electrodes. b, Experimental design illustrating the timing of feeding and fasting relative to the LD cycle. c, The time course of body weight across the experiment. d, The time course of surface body temperature, shown separately for the maximum, mean and minimum daily temperature values, irrespective of the time of day or behavioural state. e, The relationship between body weight and mean daily surface body temperature. The data points correspond to individual animals. Each animal contributes three data points, corresponding to the days when body weight was measured. The data for Day 5 of fasting are depicted as large dark blue circles. Mean values, n = 6, SEM where relevant.

2.2.2 Surgical procedure and experimental design

Animals underwent cranial surgery to implant custom-made EEG and EMG head-mounts as described previously.[124–126] Each head-mount consisted of three stainless steel screw EEG electrodes (SelfTapping Bone Screws, length 4 mm, shaft diameter 0.85 mm; InterFocus Ltd, Cambridge, UK) and two stainless steel EMG wires, all attached to an 8-pin surface mount connector (8415-SM, Pinnacle Technology Inc, Kansas, USA). Surgical procedures were carried out using aseptic technique under isoflurane anaesthesia (5% for induction; 1.5–2.5% for maintenance). Animals were head-fixed during surgical procedures using a stereotaxic frame (David Kopf Instruments, California, USA). Viscotears liquid gel (Alcon Laboratories Limited, Hemel Hempstead, UK) was applied at regular intervals to protect the eyes. Two head-mount screws were implanted epidurally over the frontal (M1 motor area, anteroposterior (AP) +2 mm, mediolateral (ML) 2 mm) and occipital (V1 visual area, AP -3.5–4 mm, ML +2.5 mm) cortical areas (Figure 1a). The third screw acted as a reference electrode and was implanted over the cerebellum; additionally, an anchor screw was implanted contralaterally to the frontal screw (with the tip within the cranium) to stabilise the head implant. Two stainless steel wires were inserted either side of the nuchal muscle for recording EMG. All head-mount screws and wires were stabilised using dental cement (Associated Dental Products Ltd, Swindon, UK). Overall, this configuration gave two EEG derivations (frontal vs. cerebellum and occipital vs. cerebellum) and one EMG derivation. All animals were given subcutaneous (s.c.) normal saline and maintained on thermal support throughout surgery and for the subsequent 1–2 h. Analgesics were administered pre- and post-operatively (meloxicam 1–2 mg/kg, s.c., Metacam, Boehringer Ingelheim Ltd, Bracknell, UK). A 7-day recovery period was permitted prior to cabling the animals for recording. Mice were habituated to the recording cable for 2 days before recordings were used in analyses.[22-24]

2.2.3 Restricted feeding paradigm

A restricted feeding paradigm, partly based upon a previous protocol, was used.[126] Recordings began at ZT9 (Zeitgeber time; ZT0 = lights on, ZT12 = lights off). After obtaining two stable baseline 24 h recordings with food provided *ad libitum* (defined from here as Days –1 and 0 of fasting), food was removed at ZT9 and subsequently 1.5 g food was made available to the animals only between ZT6–9 each day (Figure 1b). This paradigm was chosen because, as demonstrated previously, it results in an occurrence of hypothermic bouts.[126] Animals were weighed at ZT6 on Days –1, 2 and 5. The experiment was terminated at the end of Day 5. On Day 5 of fasting some of the animals were woken up if they were still in torpor at the time of feeding, and therefore these data were not included in the analysis of sleep latency.

2.2.4 Signal processing

EEG data were acquired as described previously using the Multi-channel Neurophysiology Recording System (TDT, Alachua FL, USA).[126] EEG and EMG data were sampled at 256.9 Hz (filtered between 0.1–100 Hz), amplified (PZ5 NeuroDigitizer pre-amplifier, TDT, Alachua FL, USA) and stored on a local PC. Data were resampled offline at 256 Hz. Signal conversion was performed using custom-written MATLAB (version 2019a; The MathWorks Inc, Natick, Massachusetts, USA) scripts based upon previous studies[125,126] and tailored to this study, and the output was converted into European Data Format for offline analysis. For each 24 h recording, EEG power spectra were calculated via Fast Fourier Transform (FFT) for 4 s epochs, at a 0.25 Hz resolution (SleepSign Kissei Comtec, Nagano, Japan). All computer clocks were calibrated to real time prior to recording, and subsequently all recordings of EEG and temperature were precisely aligned prior to further analysis.

2.2.5 Detection of hypothermic bouts

In this study, $T_{surface}$ was recorded using thermal imaging cameras, and used for detecting the occurrence of hypothermic bouts, defined by transient decreases of $T_{surface}$ (see below). I have chosen thermal imaging cameras as a non-invasive tool to monitor body temperature. This is an important refinement relevant for both animal welfare and the scientific aims of the study, as this allowed us to avoid implanting an i.p. device to record core body temperature, in addition to cranial EEG electrodes. The thermal imaging cameras were fit-for-purpose in detecting relatively large changes in $T_{surface}$ such as those that occur during fasting-induced torpor, as previously published,[126,127] but could also detect its minor fluctuations. I noted that the absolute values of $T_{surface}$ obtained in this study (Figure 1c) were variable between animals and consistently lower than previously reported temperature values recorded in small rodents from the brain or intraperitoneally placed thermistors. Although the values of $T_{surface}$ reported here cannot be interpreted as a proxy of absolute core body or brain temperature, relative state-dependent changes in $T_{surface}$ could be reliably detected and compared within an animal across experimental days. Since $T_{surface}$ recordings are prone to artifacts, arising from changes in piloerection, movement and changes in the visibility of the "hot-spot" to the cameras depending on the animal's position (Figure 1a), I smoothed the data as described below with the aim to minimise artefactual temperature fluctuations, and to improve detection of physiological temperature changes.

Transient superficial decreases in $T_{surface}$ occurred in all 6 animals at baseline, and were generally within 1–2 °C below the median temperature during baseline. These drops in $T_{surface}$ typically corresponded to prolonged bouts of sleep, when the core body temperature is decreased and $T_{surface}$ is expected to be even lower and likely influenced by piloerection.[113,128,129] Occasionally, deeper incursions of $T_{surface}$ occurred at baseline, but they

were never as deep as during days with fasting. All changes in $T_{surface}$, including relatively minor dips during baseline were considered as putative hypothermia bouts, which were subsequently analysed based on the magnitude of temperature decrease.

As fasting progressed, the bouts of hypothermia became progressively deeper and longer, and unequivocal torpor bouts occurred in all animals on Day 5 of fasting. Due to camera software malfunction, no $T_{surface}$ data was recorded for Day 1. Hypothermic bouts were detected using custom-made MATLAB scripts based on $T_{surface}$ data averaged in 1 min bins and smoothed with a 20 min moving average, which removed artefacts occurring as a result of movement. During days of fasting, hypothermic bouts were defined as time periods during which $T_{surface}$ was more than 3 SD below the median temperature value, and which ended when $T_{surface}$ reached at least the level of 1 SD below the mean $T_{surface}$ recorded on baseline days. Upon inspection, it was revealed that such periods sometimes consisted of "sub-bouts" that were demarcated by noticeable increases in $T_{surface}$, while remaining well below normothermic levels. These "sub-bouts" were not considered as interruptions of hypothermic bouts. Substantial variability was observed across hypothermic bouts with respect to minimal $T_{surface}$ achieved. For some specific analyses, I identified epochs of "deep hypothermia" on the days of food restriction, where $T_{surface}$ was decreased by more than 4 °C relative to the median $T_{surface}$ calculated at baseline.

2.2.6 Scoring of vigilance states

Scoring of vigilance states was performed offline by visual inspection of consecutive 4 s epochs (SleepSign, Kissei Comtec, Nagano, Japan). Frontal and occipital EEG derivations and EMG were displayed simultaneously to facilitate scoring. Vigilance states were classified as wake (high frequency, low-amplitude irregular EEG pattern dominated by theta-activity, 4–7 Hz),

non-rapid eye movement sleep (NREM; EEG dominated by high amplitude, low frequency waves), or rapid eye movement sleep (REM; EEG is dominated by theta-activity, most prominent in the occipital derivation, with a low level of EMG activity). Epochs where EEG signals were contaminated by artefacts due to movement were excluded from spectral analyses (7.1 ± 3.2% of total recording time). The onset of individual NREM sleep episodes was defined by the first occurrence of slow waves in at least one EEG channel, along with the absence of EMG activity. Vigilance states annotation was performed across all days, including the time periods when $T_{surface}$ was low (see Results). As EEG amplitude decreased in association with a drop in $T_{surface}$, it was not used as a key criterion for vigilance state annotation and the scoring was based on frequency content and the overall pattern of EEG activity, in addition to the presence or absence of EMG activity.

2.2.7 Statistics

Statistical analyses were performed using MATLAB (The MathWorks Inc, Natick, Massachusetts, USA). Since EEG spectral power values are not normally distributed, data were log-transformed prior to statistical comparison.[130] Data are presented as mean values with standard error of the mean (SEM). To assess the effect of fasting across days, one-way repeated measures ANOVA was used. Pair-wise comparisons were calculated based on parametric (paired Student's T) tests.

2.3 Results

2.3.1 Body weight and temperature

Body weight and $T_{surface}$ were recorded throughout the experiment (Figure 1c). As restricted feeding progressed, a decrease in mean body weight was observed. Over 5 days of restricted feeding, mean body weight fell from 28.3 ± 1.17 g during baseline to 24.1 ± 0.94 g on Day 5 ($p < 0.001$; $F(2, 10) = 233.99$, $p = 4.01$ e-09, repeated measures ANOVA; Figure 1c). Over the same time period, daily $T_{surface}$ values also decreases: maximum $T_{surface}$ decreased slightly from 32.6 ± 0.24 °C to 31.4 ± 0.075 °C ($p = 0.005$; $F(5, 25) = 12.5$, $p = 3.94$ e-06), mean $T_{surface}$ dropped from 31.6 ± 0.27 °C to 27.2 ± 0.47 °C ($p = 0.001$; $F(5, 25) = 17.7$, $p = 1.66$ e-07), whilst minimum $T_{surface}$ dropped substantially from 30.1 ± 0.36 °C to 21.5 ± 0.61 °C ($p < 0.001$; $F(5, 25) = 25.9$, $p = 3.84$ e-09) (Figure 1d). Overall, there was a positive correlation between body weight and mean daily $T_{surface}$ (Figure 1e).

2.3.2 Characteristics of hypothermic bouts

From $T_{surface}$ data, hypothermic bouts, e.g., any decreases of peripheral temperature by > 0.5 °C relative to median baseline value, were detected on all days (see Methods). As mentioned in the Methods section, relatively superficial periods of hypothermia (decreases of up to ~ 2.5 °C) were detected in some animals during baseline, which is likely to have occurred during NREM sleep, especially when bedding material obscured vision of the thermal cameras. As fasting progressed, there was a general trend of hypothermic bouts becoming progressively deeper (Figure 2a). Calculating the incidence of hypothermic bouts across consecutive days revealed that the number of bouts per 24 h did not change and averaged 3.8 ± 0.91 on Day –1 and 4.7 ±

0.61 on Day 5 ($F(5, 25) = 1.2$, n.s.; Figure 2b). There was an increase in the number of bouts on Day 2, before a subsequent decrease, possibly reflecting a progressive consolidation of the hypothermic bouts across the fasting days ($p = 0.001$; $F(5, 25) = 21.4$). Consistent with this notion, a marked increase in mean duration of hypothermic bouts was evident, starting from 121 ± 12 min on Day –1 and reaching 213 ± 37 min on Day 5 ($p = 0.020$; $F(5, 25) = 5.1$, $p = 0.002$; Figure 2c). The minimum temperature values attained during hypothermic bouts also decreased progressively from 30.2 ± 0.31 °C on Day –1 to 25.0 ± 0.52 °C ($p = 0.001$; $F(5, 25) = 14.9$, $p = 8.01$ e-07) on Day 5 (Figure 2d). This was reflected in a shift towards a more frequent occurrence of hypothermic bouts with lower values of $T_{surface}$ during days of fasting as compared with baseline days when food *ad libitum* was provided ($p = 0.006$; Figure 2e). Next, the cumulative daily hypothermia index was calculated,[103,108] which is the integral of the decrease in $T_{surface}$ relative to median baseline $T_{surface}$ for each hypothermia bout. This analysis revealed a progressive increase of hypothermia index across days ($F(5, 25) = 5.7$, $p = 0.010$; Figure 2f).

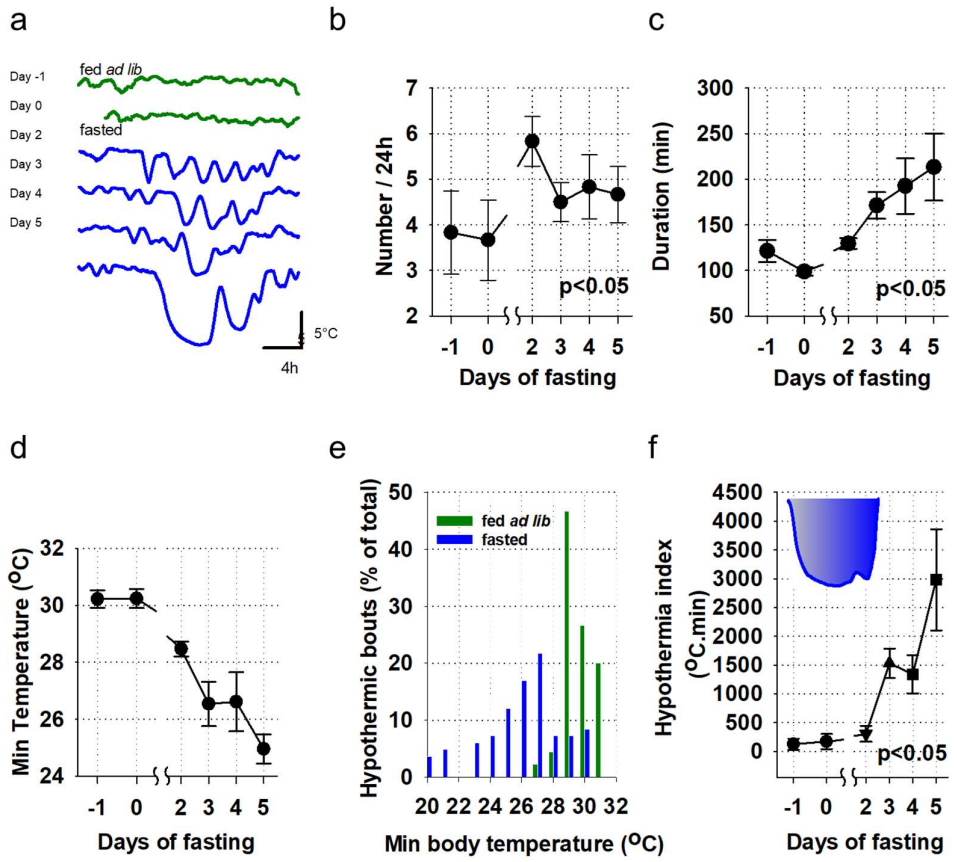

Figure 2. The characteristics of hypothermia bouts. a, Representative examples of hypothermia bouts in one individual animal (with each line representing a 24 h day) showing that hypothermic bouts became deeper as fasting progressed from Day 2 to Day 5. b,c,d, The time course of the number and duration of hypothermia bouts and the minimum surface body temperature attained during hypothermia bouts. Note that as restricted feeding progressed, hypothermia bouts increased in duration, became more frequent and deeper. e, Distribution of hypothermia bouts during baseline and fasted days. f, The time course of daily cumulative hypothermia index (equal to the integral of the decrease in $T_{surface}$ relative to median baseline $T_{surface}$ for each hypothermia bout; represented by the inset showing shaded area between curve and straight line) across the experiment. Note that as restricted feeding progressed, the hypothermia index increased. n = 6, mean values, SEM.

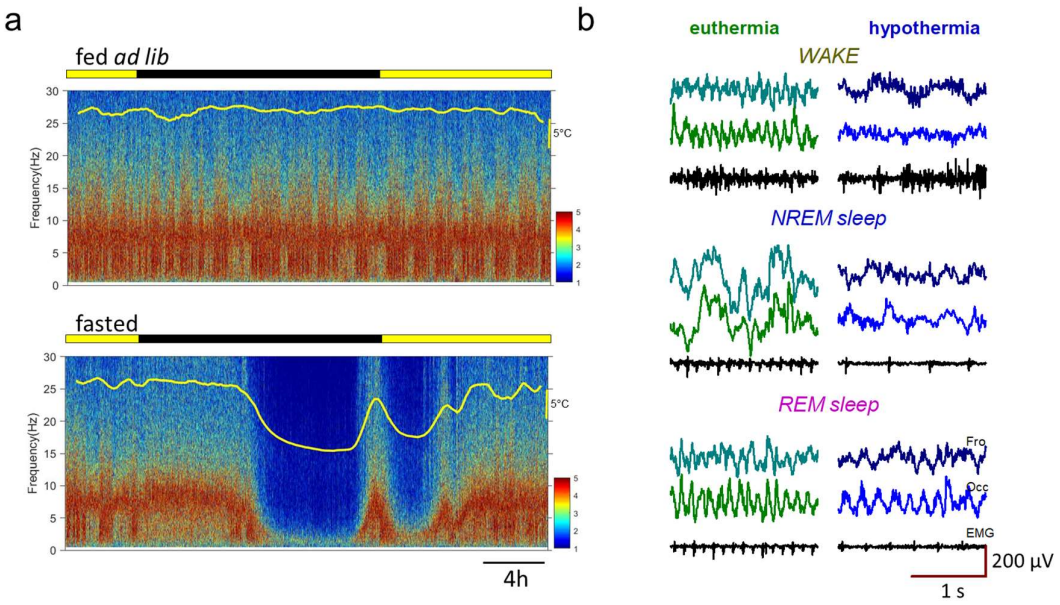

Figure 3. The timing of torpor bouts and corresponding changes in the EEG. a, Representative EEG power density spectra colour-coded on a logarithmic scale (μV^2/0.25 Hz) during baseline day and during the last day of fasting in one individual mouse. Note the substantial reduction in EEG power during hypothermia. b, Representative EEG and EMG traces taken from wakefulness, NREM sleep and REM sleep during euthermic conditions (surface body temperature > 36 °C) and during hypothermia (< 24 °C). EEG and EMG traces labelled as: Fro (frontal EEG); Occ (occipital EEG); EMG.

2.3.3 The relationship between hypothermia and vigilance states during fasting

Visual inspection of EEG spectra revealed that EEG power was generally depressed across all frequencies during hypothermic bouts, especially when $T_{surface}$ was reduced **(**Figure 3a**)**. However, the typical EEG and EMG signatures of wakefulness, NREM sleep and REM sleep

were apparent, which allowed vigilance state annotation throughout the recording period (Figure 3b).

As fasting progressed, the amount of wakefulness as expressed as a percentage of 24 h increased initially from 50.2 ± 2.4% to 59.7 ± 2.3% ($p = 0.002$) on Day 3, but then decreased on Day 5 to 51.3 ± 4.7% ($p = 0.180$, $F(6, 30) = 2.5$, $p = 0.042$; Figure 4a, top). At the same time, the daily amount of NREM sleep (including epochs during both normothermia and hypothermia) showed first a suppression but then returned to values similar to baseline (fed ad lib: 41.6 ± 1.8%, Day 5: 47.1 ± 4.7%, $p = 0.290$; $F(6, 30) = 4.9$, $p = 0.001$; Figure 4a middle). However, the amount of REM sleep decreased markedly from 8.1 ± 0.5% at baseline to 1.6 ± 0.2% ($p < 0.001$) on Day 5 ($F(6, 30) = 35.6$, $p = 2.42$ e-12; Figure 4a, bottom). These changes were evident from individual hypnograms (three days from a representative individual mouse shown on Figure 4b).

Focusing specifically on the proportion of each vigilance state within hypothermic bouts on Day 5 and during matching time periods on Day –1, revealed lower amounts of wake (31.2 ± 3.8% versus 45.6 ± 2.1%; $p = 0.012$) and REM sleep (0.96 ± 0.36% versus 8.2 ± 0.5%; $p < 0.001$), while the amount of NREM sleep was increased (61.8 ± 3.4% versus 42.5 ± 1.5%; $p = 0.002$). The decrease in $T_{surface}$ was strongly associated with the amount of REM sleep, which was proportionally decreased, while NREM sleep increased as a function of hypothermia deepening (Figure 4c). The $T_{surface}$ and the amount of wakefulness were only weakly related.

Next, it was asked whether fasting-induced torpor affects subsequent sleep. To enable direct comparisons with baseline it was important to ensure that body temperature reaches normothermia after emergence from torpor. However, this was not the case. When the time

courses of $T_{surface}$ across baseline day and during the last two days of fasting were calculated, when torpor bouts were especially prominent, it was apparent that the animals remain persistently hypothermic around feeding time (Figure 4d). Specifically, the mean $T_{surface}$ was below corresponding baseline values during the last hour before feeding on both days Day 4 and 5 ($p = 0.003$ and 0.009 respectively), and even during the first hour after the animals were provided with food and aroused ($p = 0.016$ and 0.019 for Day 4 and 5 respectively). Immediately before and post-feeding at ZT6, mice were generally observed to be awake, possibly because they developed food anticipation and also because they spent time feeding after food was provided. This was reflected in a reduced amount of NREM sleep before and immediately after food was provided (Figure 4e). This period of wakefulness is likely to include the rewarming phase of torpor, during which mice are known to shiver. Finally, the time at which mice entered the first period of sleep lasting 1 minute or longer was identified, and the duration between the start of feeding and the start of post-torpor sleep was calculated. This revealed that mice did not go to sleep immediately after feeding, and instead stayed awake on average for 49.5 ± 9.0 min. A large inter-individual variability in sleep latency was noted (range: 14.7–72.7 min) (Figure 4f).

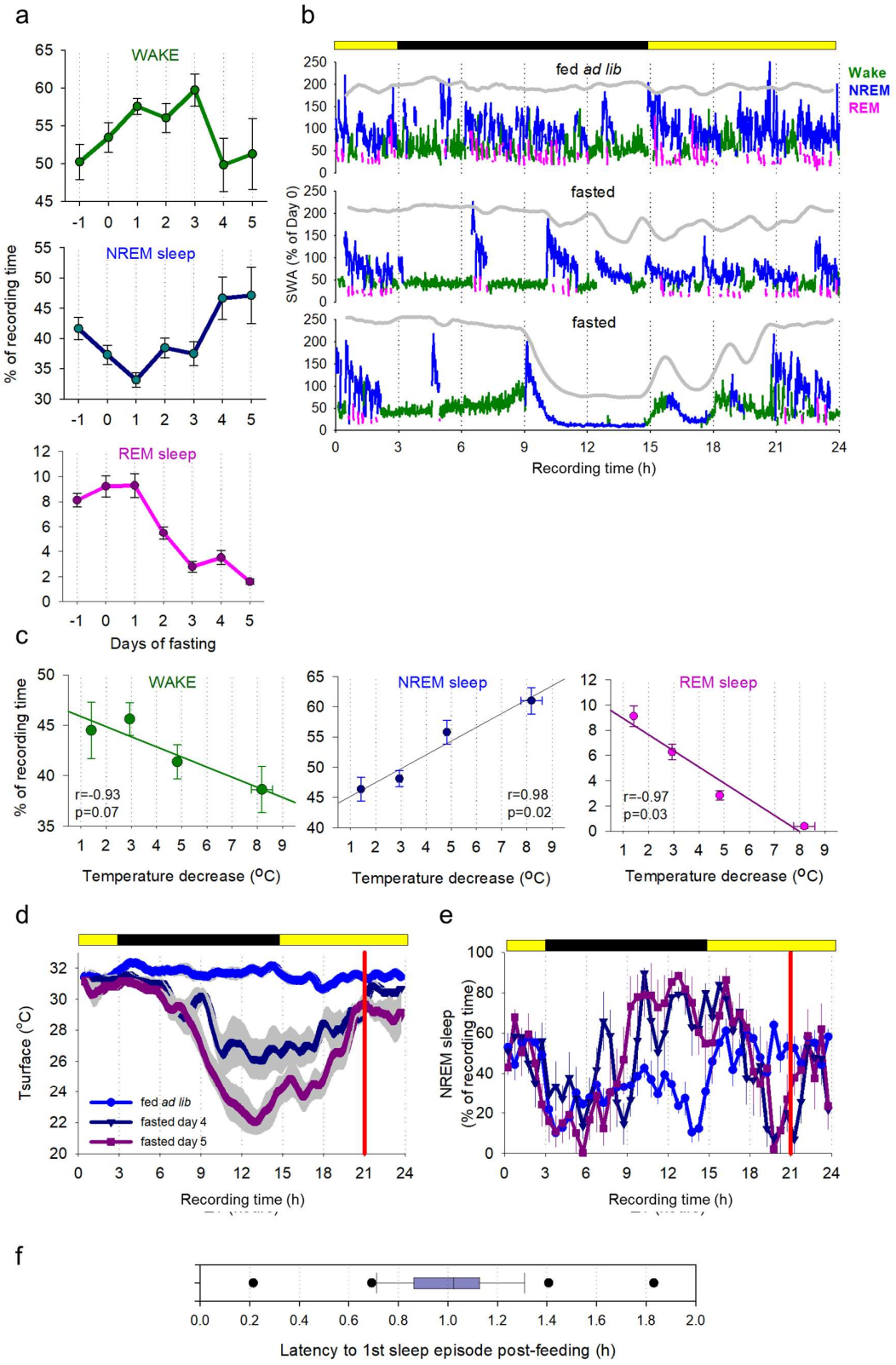

Figure 4. The effects of fasting and hypothermia on vigilance states. a, The time course of daily amounts of EEG/EMG defined wakefulness, NREM sleep and REM sleep.

Note a progressive increase in the amount of NREM sleep and decrease in REM sleep during fasting. b, The time course of EEG slow-wave activity (0.5–4Hz, SWA) during the 24 h period shown for baseline day (fed *ad lib*) and two days of food restriction (Day 3 and Day 5 of fasting) in an individual mouse. Mean SWA is plotted in 1-min epochs and is color-coded according to the vigilance state (waking: green, NREM sleep: blue, REM sleep: pink). The grey line at the top corresponds to surface body temperature. Note the drop in SWA when body temperature is low. c, The relationship between the amount of waking, NREM and REM sleep and peripheral body temperature. Note that when the temperature declines by more than approximately 5 °C, REM sleep virtually disappears. d,e Time course of $T_{surface}$ (d) and NREM sleep (e) during baseline day (fed *ad lib*) and during the last two days of fasting. Vertical red line indicates the approximate time when the animals were provided with food. f, Time from feeding to first episode of sleep across fasting days. Purple box indicates median and interquartile range; black circles indicate outliers. Mean values, n=6, SEM.

2.3.4 EEG spectral analysis during wake and sleep: effects of hypothermia

Next, I investigated the effects of fasting and hypothermia on EEG spectral power. I addressed whether the decrease in spectral power I observed earlier (Figure 3c) was state specific and whether it was primarily associated with $T_{surface}$ or resulted from changes in sleep intensity associated with fasting. I calculated EEG power spectra separately for epochs, scored as waking, NREM sleep and REM sleep during baseline when the animals were fed *ad libitum*, during epochs of deep hypothermia when the animals were fasted, and also during those epochs on fasting days when $T_{surface}$ was similar to baseline. I observed that EEG power generally showed a decrease during hypothermia on days when the animals were food restricted, but it was virtually identical between normothermia epochs on fasted days and during baseline (Figure 5a). The reduction in EEG power during hypothermia was especially pronounced during NREM sleep, which is consistent with previous findings in Djungarian hamsters (Figure 5b).[131] The decrease in EEG power during waking was also observed during hypothermia as compared with both baseline and normothermia in the frontal derivation and compared to normothermia

only in the occipital EEG (Figure 5a). The decrease in EEG power during REM sleep was somewhat more pronounced than during waking, but caution is warranted with interpreting this result as the total amount of REM sleep was drastically decreased when $T_{surface}$ was low. However, during those epochs of REM sleep that occurred during hypothermia, a marked left-ward shift of the theta peak was present, consistent with the observation made previously in Djungarian hamsters.[132] To further address whether the changes in the EEG observed were related to temperature changes rather than fasting, I clustered all waking, NREM and REM-scored epochs as a function of progressively decreasing $T_{surface}$, and calculated corresponding total spectral EEG power in the frequency range between 0.5–30 Hz (Figure 5b). I observed generally higher values of total EEG power during NREM sleep at normothermia, but in all three vigilance states EEG power decreased markedly as a function of $T_{surface}$ decrease (Figure 5b).

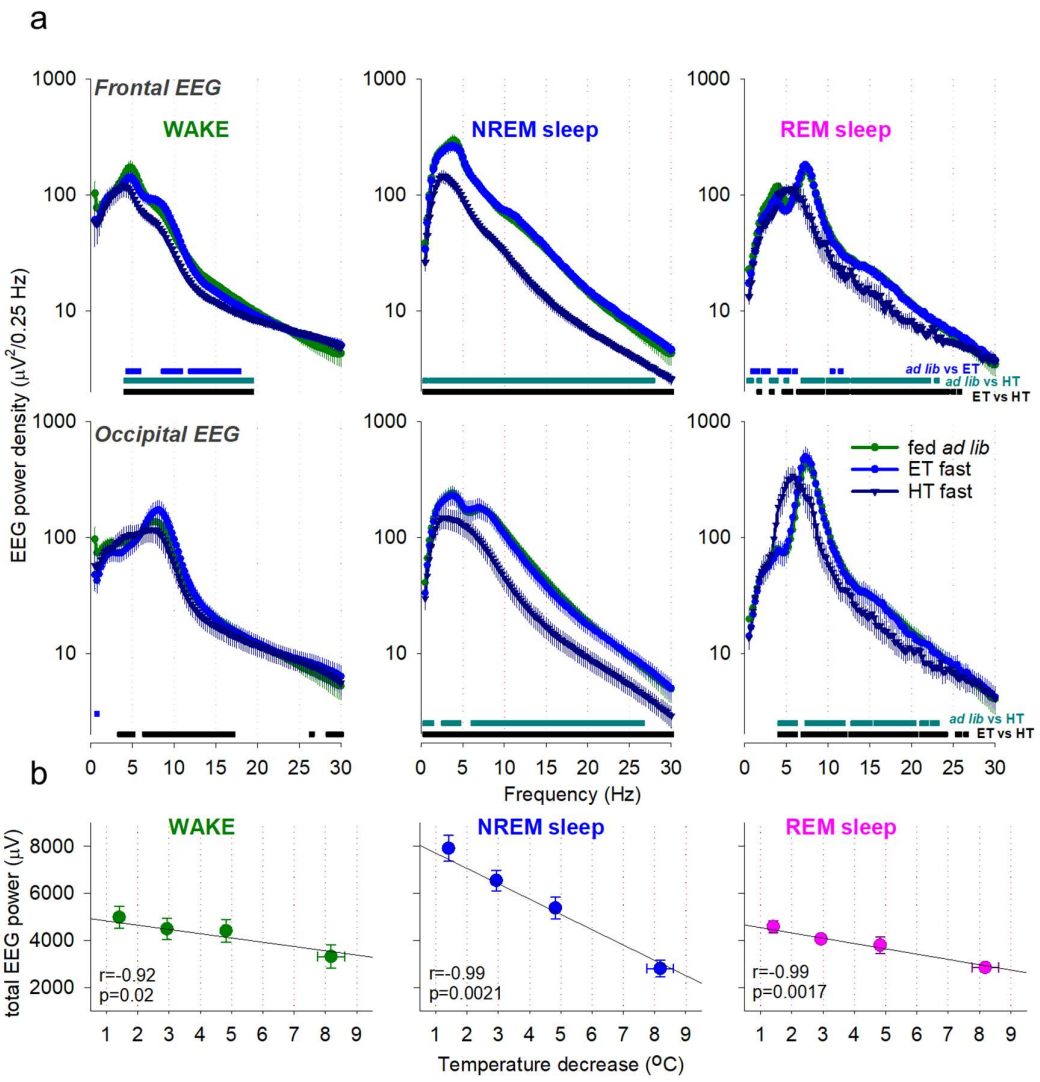

Figure 5. The effects of fasting and hypothermia on EEG power spectra. a, EEG power spectra during waking, NREM sleep and REM sleep during baseline (fed *ad lib*) and shown separately for euthermic (ET) and hypothermic (HT) episodes during fasting. Note that EEG power generally declines during hypothermia on fasted days but is virtually indistinguishable from spectra of the EEG recorded during the same days at euthermia. EEG power spectra during REM sleep highlight a marked slowing of theta peak frequency. Horizontal lines below the curves depict frequency bins where EEG power was different between days ($p < 0.05$; paired t-test on log-transformed values). b, The relationship between total EEG power during waking, NREM and REM sleep and surface body temperature. Note a strong negative relationship between surface body temperature and EEG power in all vigilance states. n = 6, mean values, SEM.

2.3.5 Hypothermic bouts are initiated from normothermic NREM sleep

For the following analyses, all episodes of decreased $T_{surface}$ lasting at least 2 h that occurred during baseline and fasting conditions were identified (denoted by 'fed ad lib' and 'fasting' respectively). These included minor decreases in $T_{surface}$ of less than 2 °C that were predominant during baseline conditions, and have been well-documented in earlier studies.[128,133,134] The visual inspection of individual hypnograms suggested that bouts of hypothermia during fasting days do not start from wakefulness or REM sleep, but rather commence during or just before NREM sleep with high SWA (Figure 4b, 6a). Notably, during the initial NREM sleep at the beginning of hypothermic bouts, the EEG signals were indistinguishable between those on fasting days (that predominantly progressed into deep hypothermia) or those on baseline days (associated with only a minor decrease in $T_{surface}$) (Figure 6b). In these two groups, the corresponding amount of sleep were calculated and compared **(**Figure 6c). In both cases, the onset of hypothermia was associated with a marked increase in the proportion of NREM sleep, which was especially pronounced at the onset of the (deeper) hypothermic bouts that occurred on fasting days (Figure 6d). Furthermore, a greater amount of NREM-like state was seen as $T_{surface}$ decreased further. At the same time, EEG SWA started with high values in both cases, and showed a similar decreasing trend during the following 60 min period (Figure 6e). Thus, these data suggest that the occurrence of bouts of hypothermia is closely linked to the occurrence of deep NREM sleep characterised by high SWA.

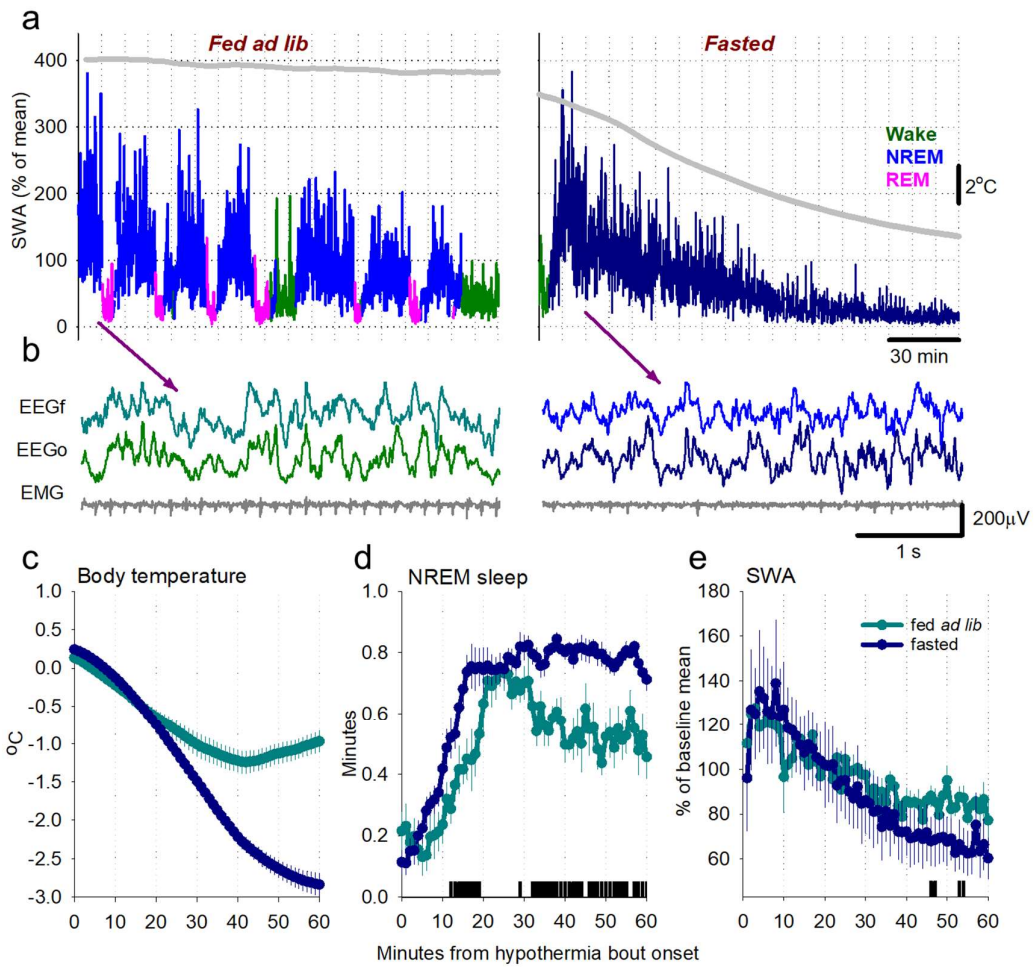

Figure 6. The relationship between surface body temperature, sleep and SWA at the onset of hypothermia episodes. a, A representative example of the time course of EEG slow-wave activity (0.5–4Hz, SWA) during a typical period of sleep, associated with a minor decrease in surface body temperature (left), and the dynamics of SWA during the entrance into a deep bout of hypothermia (right). SWA is plotted in 4 s epochs and is colour-coded according to the vigilance state (waking: green, NREM sleep: blue/dark blue, REM sleep: pink). The grey line at the top corresponds to surface body temperature. Note the drop in SWA in both cases, which is especially pronounced as the temperature decreases. b, Representative EEG traces of NREM sleep at the beginning of sleep periods when the surface body temperature remains high (as shown on Panel a) or subsequently declines (as on Panel b). Note that during this time EEG activity is virtually indistinguishable between the two states, suggesting that even the deepest hypothermia bouts start from NREM sleep. c,d, The time course of surface body temperature and the proportion of NREM sleep starting from the onset of euthermic and hypothermic NREM. Note the rapid increase in the amount of NREM

sleep at the beginning of a hypothermia bout in fasted animals and a greater proportion of NREM sleep later during the hypothermia bout. The bars at the bottom denote differences ($p < 0.05$, paired t-test). e, The time course of EEG SWA during NREM sleep from the onset of hypothermia bout in fed ad lib and fasted animals. Note that the values of SWA are initially high and show a progressive decrease in both cases. $n = 6$, mean values, SEM.

2.4 Discussion

2.4.1 Body temperature changes

A detailed investigation was performed of EEG/EMG defined states of vigilance during hypothermia and torpor induced by restricted feeding in mice. There were minor decreases of $T_{surface}$ during baseline, likely corresponding to episodes of sleep, but more profound bouts of hypothermia were common as fasting progressed. The observation that fasting in the laboratory mouse induces progressively deeper bouts of hypothermia tending towards T_a confirms the results of several previous studies.[76,79,117,123,126] Although it is well known that body temperature also decreases during sleep, previous studies suggest that the minimum T_b decreases to a greater extent during torpor than during sleep.[74,82,135] During hibernation, as discussed in 1.4.1, the set-point T_b is defended at a lower temperature , resulting in a T_b decrease that corresponds to net passive heat transfer to the surrounding environment (governed by basic thermodynamic principles).[136] In this study, T_a was relatively high (20 ± 1 °C), though T_b as low as 16 °C have previously been recorded in mice during torpor and pharmacologically-induced hypothermia where T_a was of a similar value.[137,138] However, in larger mammals such as the black bear, the influence of body size in determining T_b becomes more apparent. During torpor in the black bear, T_b typically does not drop below 30 °C. [85,139] Larger mammals, by simple geometry, have a smaller surface area:volume ratio than smaller mammals, and therefore they lose heat to the environment at a slower rate. However, it remains unclear and has not yet specifically been investigated whether or not there are other factors at play. For example, torpor may not be an all-or-nothing phenomenon, and, depending on the degree to which saving energy is required, T_b homeostasis could be partially (rather than fully) suppressed, leading to T_b that is much closer to euthermia than T_a. This could be explained by the notion that larger mammals such as the black bear are of much larger volume and therefore

capacity for storage of metabolic fuel, meaning there is not as much physiological need for the extreme energy-saving typical of torpor in the Arctic ground squirrel.[85,139]

2.4.2 EEG changes

Numerous studies have investigated the EEG changes that occur during torpor, and most of these have been in animals that undergo spontaneous torpor modulated primarily by circannual changes in photoperiod.[102,103,114–118] Relatively few studies have focused on EEG changes in animals that undergo torpor triggered by fasting.[109,122] My results confirm that fasting-induced torpor in laboratory mice bears key similarities to torpor seen in other species. For example, consistent with earlier work, EEG power decreases during hypothermia, especially during NREM-like sleep states, as previously seen in Djungarian hamsters.[108,131]

Previous studies have shed light on how temperature, both directly and indirectly, affects EEG power. For example, processes involved in generating synaptic and spiking activities, such as transmembrane ionic currents, synaptic vesicle release, and intracellular signalling cascades are expected to be inhibited at lower temperatures.[7,140–142] Most biochemical and physiological processes, with some important exceptions, such the circadian clock, which is characterised by "temperature-compensation", have a temperature coefficient (Q10) of 2–3, and the specific relationship between brain temperature and EEG power follows a Q10 of approximately 2.5.[74,112] Likely also contributing to this value are the structural changes in neurons that occur during hypothermia: several studies have demonstrated that both torpor in ground squirrels and pharmacologically-induced hypothermia in laboratory mice lead to the marked loss of synaptic contacts, i.e., retraction of dendrites, decrease in spine density and branching, and the dissociation of proteins from the cytoskeletal active zone – all of which occur in different cortical regions and reverse upon rewarming.[138,143–145] However, the decrease in the EEG

power during fasting-induced torpor in mice, may also be accounted for, at least in part, by changes not directly related to hypothermia. For example, a breakdown in network synchronisation or increased inhibition, such as can be observed in deep anaesthesia, coma or other pathological states, may lead to EEG changes similar to those observed in torpor.[146,147] The above changes may reflect decreased excitability of neurons, which would be consistent with the neuroprotective effects of hypothermia.

2.4.3 Vigilance state changes

Despite the marked decrease in EEG amplitude, distinctive EEG and EMG signatures of normothermic wakefulness and sleep were still ascertainable – an unsurprising finding since previous studies in mice suggest that the EEG only becomes truly isoelectric at T_b of below 10–14 °C.[102,148] This allowed scoring of vigilance states throughout hypothermic bouts.

The daily amount of NREM sleep increases as fasting progresses, consistent with previous studies.[102,103,114–116,122] There was also a marked decrease in REM sleep, both with successive days of fasting and with successively lower $T_{surface}$. The spectral peak of REM sleep EEG also shifted towards a slower frequency band, as was previously described in hamsters.[132] REM sleep was essentially abolished below a $T_{surface}$ of 25—26 °C. This is consistent with previous studies demonstrating the temperature dependence of REM sleep.[149–151] It has been shown previously that there is a linear correlation between the amount of REM sleep and brain temperature.[119] Furthermore, it has been shown in rats, which are strictly homeothermic, that REM sleep is sensitive even to changes in T_a alone: the amount of REM at 29 °C T_a is double that at 23 °C.[152] It has been postulated that, since during REM sleep there is a loss of thermoregulatory control, the absence of REM sleep during torpor allows for sustained and uninterrupted control of body and brain temperature.[119,153,154] While the underlying

neurophysiological mechanisms remain to be further clarified, it is possible that the lateral hypothalamic melanin-concentrating hormone (MCH) neurons are involved, as it has been recently demonstrated that their effects on REM sleep expression vary dynamically with T_a.[155]

Finally, the amount of wakefulness initially increases up to Day 3, before decreasing towards Day 5. The initial increase in waking possibly reflects the initial dominance in arousal and food-seeking behaviours. By Day 5, this has reversed and the need to save energy outweighs the benefits of staying awake to forage for food.[156] Thus, an intriguing contrast with hibernation is that an important trigger for entering fasting-induced torpor in mice is that the strong wake drive associated with hunger needs to be exceeded by the need for energy conservation. Interestingly, under a restricted feeding schedule, mice enter torpor predominantly in the dark phase, during which they are typically active in laboratory conditions, whereas the opposite is mostly true for torpor triggered by shortening of the photoperiod. This is consistent with previous studies of fasting-induced torpor in mice [79,123,157], but further work is necessary to disentangle the roles of the endogenous clock, the timing of feeding and the degree of energetic challenge in torpor initiation and its other characteristics.[158,159]

2.4.4 The transition into torpor

I observe that the time interval during which mice enter a bout of hypothermia is dominated by a state indistinguishable from NREM sleep, consistent with earlier studies.[106,109,160] Previous studies suggest that any detectable decrease in T_b at torpor onset occurs *after* the drop in metabolic rate.[86,161] This drop in T_b is facilitated by a decline in the set-point temperature of the thermoregulatory system, which is likely to decline initially upon the wake–NREM transition and decline even further as torpor progresses.[150,162] However, vigilance state transitions such as wake–NREM typically occur on a much faster time scale than any detectable

changes in T_b or metabolic rate. The precise timing of NREM sleep onset relative to changes in T_b and metabolic rate could be confirmed in future studies. It would also be interesting to investigate whether using sleep deprivation to prevent animals from entering sleep would also prevent hypometabolism; however, this possibility remains to be experimentally addressed. I would predict that, were metabolic rate also measured (e.g., in a metabolic chamber), hypometabolism would not be detected: the very process of sleep deprivation (e.g., via gentle handling and tapping on the cage) would increase activity levels and thus metabolic rate beyond what they would be without sleep deprivation.

Following on from normothermic NREM sleep, $T_{surface}$ decreases, accompanied by a progressive decrease in EEG power. This change is gradual and, like in previous studies, it is difficult to precisely define a time point at which the EEG no longer resembles typical normothermic NREM sleep.[116,160] For the shorter hypothermic bouts, there is a clear inflection point at which $T_{surface}$ reverses and increases back towards normothermia within a few hours. For the longer bouts, $T_{surface}$ eventually reaches a stable level at near T_a, which may last up to 10 hours in the most extreme of cases. This is still short when compared with bouts of hibernation e.g., in the Arctic ground squirrel, which can last for weeks at a time. As observed in this study, in fasting-induced torpor, there is substantial variability in bout duration, i.e., this likely reflects the wide range in severity of fasting.[123,163]

2.4.5 Post-emergence from torpor

The adenosine hypothesis of sleep pressure suggests that adenosine, a neurotransmitter that accumulates in the brain as a result of neural activity, plays a key role in regulating sleep-wake cycles. As extracellular adenosine levels increase during wakefulness, this increases sleep pressure. During sleep, increased activity of adenosine deaminase reduces extracellular

adenosine, which in turn reduces sleep pressure and promotes wakefulness upon waking.[164] Under the same hypothesis, EEG SWA, which, in both rodents and humans, has been found to increase as a function of prior waking duration and decrease as a function of sleep, is a marker of sleep pressure.[165,166]

Some of the earlier studies in hibernating animals reported they go into deep normothermic sleep shortly after emergence from a bout of hibernation.[103,107,108,167,168] Spectral EEG analysis revealed that cortical SWA is typically high at the beginning of normothermia and declines thereafter. These findings suggested that the preceding torpor bout does not restore sleep need, which may seem paradoxical as torpor is comprised predominantly of a state most similar to NREM sleep, as characterised by EEG.[168,169] However, the EEG is merely a window unto brain activity: just because torpor shares EEG similarities with NREM sleep does not mean that it *is* sleep; indeed, the EEG during anaesthesia appears similar to NREM sleep.[146,147]

This study suggests that, unlike hibernating animals, mice are generally awake post-emergence from fasting-induced torpor. Whether or not there is a similar build-up in sleep pressure could potentially be masked by another determining factor that is wake-promoting and acts in opposition to sleep pressure: hunger. Thus, it is possible that latency to sleep and its subsequent intensity are determined both by the level of hunger and/or metabolic state of the animals, and by the levels of homeostatic sleep drive. However, duration and depth of the preceding torpor bout are likely to affect sleep pressure. Since there is natural variability between animals with respect to these, further repeats of this experiment would be necessary to ensure reliable comparisons between the competing factors of sleep pressure and hunger. Future studies could employ a more controlled approach, standardising torpor duration and depth across subjects, perhaps through careful manipulation of T_a and fasting duration. Additionally, incorporating

measures of metabolic state and hunger levels, such as blood glucose monitoring, could help disentangle the competing influences of sleep pressure and hunger on post-torpor behaviour.[170]

An important question that remains to be resolved is whether the rates of build-up of sleep pressure during wakefulness and its dissipation during sleep are temperature-dependent, or whether they are related to specific patterns of brain activity. Sleep pressure, classically characterised by the accumulation of adenosine in the brain, serves as a key regulator of sleep-wake transitions.[164,171] Adenosine, a purine nucleoside, steadily builds up during wakefulness as a byproduct of metabolic processes.[164] When adenosine levels reach a critical threshold, its binding to A_1 adenosine receptors, likely in the ventrolateral preoptic area of the hypothalamus, promotes the transition from wakefulness to NREM sleep.[172] Whether adenosine levels fluctuate differently during torpor, and how this may influence post-torpor sleep pressure and timing remains unclear and represents an intriguing direction for future research.

Arguably, the minimal T_b at which torpor occurs can influence subsequent sleep regardless of changes in the EEG, and, on the other hand, just because the torpid EEG shares similarities with NREM sleep does not mean that the state is functionally the same. It remains to be determined why torpor may lead, under certain circumstances, to elevated sleep need, and it is still unclear whether this is the case for fasting-induced torpor. It has been shown that lower body and brain temperatures are associated with decreased EEG amplitude and left-shift in peak frequency – to levels far lower than those seen during normothermic NREM.[112,173,174] In Djungarian hamsters, at $T_b < 30$ °C the slow waves typical of normothermic NREM no longer dominate the EEG, and at $T_b < 27$ °C these waves are no longer seen in the EEG. Furthermore, other studies show that at T_b of below 10–14 °C the EEG becomes truly isoelectric.[102,148] Associated with these temperature-sensitive changes are substantial, but reversible, structural

and neurochemical transformations such as the loss of synaptic connectivity and sequestration of dendritic cytoskeletal proteins, the latter of which has been demonstrated in subcortical and multiple cortical regions.[138,143–145] It would be unsurprising if such drastic changes in synaptic structure and function have a significant impact on post-rewarming brain activity. Elucidating the precise sequence and time-course of these changes would be crucial to gaining further insight into the underlying neurophysiological mechanisms.

Finally, single unit recordings, previously performed *in vitro* and *in vivo* in posterior thalamic neurons from torpid ground squirrels, reveal that hypothermia prolongs action potentials, yet there is continued spontaneous firing down to T_b of 14 °C, below which firing ceases.[140,175] It remains to be determined how spontaneous neuronal activity in different cortical areas changes throughout torpor, given that sleep-wake related changes in cortical firing at normothermia can be highly localised.[176]

2.4.6 Concluding remarks

In this chapter, I tested the hypothesis that fasting-induced torpor in mice shares key electrophysiological characteristics with hibernation. My findings largely support this hypothesis. In summary, my study suggests that fasting-induced torpor in mice bears important electrophysiological similarities with hibernation, as well as highlights some important differences, such as the observation that mice spend considerable time awake post-torpor. My data are consistent with previous studies showing that electrophysiologically-defined NREM sleep is a predominant state of vigilance at the transition to hypothermia, and during torpor the animals spend most time in a NREM-like state with a low EEG amplitude. However, there are numerous aspects that remain open to further investigation. For example, although thermal imaging cameras allowed me to non-invasively and reliably detect torpor bouts, recording core

T_b using intraperitoneal probes would provide a more accurate readout of changes in T_b. Furthermore, in future studies, concurrent measurement of core T_b and metabolic rates would allow more precise determination of the relative timings of the drop in metabolism, drop in T_b, and associated EEG changes upon entrance into torpor, as well as during rewarming. Furthermore, future studies could provide more detailed analysis of specific EEG features during torpor. For example, examining the presence and characteristics of sleep spindles and K-complexes during the transition into torpor could reveal whether these NREM sleep hallmarks persist at lower temperatures, and how their morphology changes with declining temperature. Such analysis might identify unique EEG signatures of successful torpor induction and could provide additional insights into the relationship between torpor and NREM sleep states. Finally, further experiments, involving post-torpor sleep deprivation, would be required to gain insights into whether or not fasting-induced torpor is associated with the build-up of sleep need, and if sleep after torpor in mice is homeostatically regulated. Such experiments would involve inducing torpor in mice through fasting, then preventing sleep for varying durations post-emergence. EEG activity, sleep latency and slow-wave activity would be monitored in subsequent sleep periods. My hypothesis would be that being in the state of torpor does not fulfil sleep's restorative functions and instead leads to accumulation of sleep need and. Thus, longer post-torpor sleep deprivation would result in: 1) shorter sleep latency, 2) higher initial SWA, and 3) longer total sleep duration. This prediction stems from observations in hibernating animals, which often sleep extensively upon emerging from hibernation. [103,107,108,167,168] If supported, these findings would support the notion that torpor is indeed a sleep-depriving state.

Statement of Authorship for joint/multi-authored papers for PGR thesis

To appear at the end of each thesis chapter submitted as an article/paper

The statement shall describe the candidate's and co-authors' independent research contributions in the thesis publications. For each publication there should exist a complete statement that is to be filled out and signed by the candidate and supervisor **(only required where there isn't already a statement of contribution within the paper itself).**

Title of Paper	The relationship between fasting-induced torpor, sleep, and wakefulness in laboratory mice
Publication Status	X Published ☐ Accepted for Publication ☐Submitted for Publication ☐Unpublished and unsubmitted work written in a manuscript style
Publication Details	Huang YG, Flaherty SJ, Pothecary CA, Foster RG, Peirson SN, Vyazovskiy VV. The relationship between fasting-induced torpor, sleep, and wakefulness in laboratory mice. Sleep. 2021 Sep 13;44(9):zsab093. doi: 10.1093/sleep/zsab093.

Student Confirmation

Student Name:	Dr Yi-Ge Huang		
Contribution to the Paper	Conceptualization, methodology, data collection, performing analysis, manuscript writing (original draft preparation, reviewing and editing), funding acquisition. (Other co-authors' contributions: Conceptualization: VV (project supervisor) Methodology: VV, SP Data collection: (YH only) Performing analysis: VV, SF Manuscript writing (original draft preparation, reviewing and editing): VV Funding acquisition: VV, RF, SP)		
Signature 		Date	11/01/24

Supervisor Confirmation

By signing the Statement of Authorship, you are certifying that the candidate made a substantial contribution to the publication, and that the description described above is accurate.

Supervisor name and title: Prof. Alastair M. Buchan		
Supervisor comments		
Signature 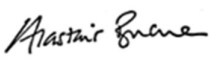	Date	12/01/24

This completed form should be included in the thesis, at the end of the relevant chapter.

3 Electrophysiological properties of pharmacological torpor

3.1 Introduction

As described in the Chapters 1 and 2, torpor is a regulated and reversible state of metabolic suppression used as a strategy by many animals to conserve energy.[71–73] However, until relatively recently, it was not known whether a torpor-like state could be induced pharmacologically. As mentioned in Section 1.3, it has now been demonstrated in several rodent species that activation of CNS A_1 adenosine receptors (A_1AR) is sufficient for entry into a reversible torpor-like hypothermic state.[86,89,177–179]

The A_1AR is one of four G-protein coupled receptors (GPCRs) for which the purine nucleotide adenosine is the endogenous ligand. The other known subtypes of adenosine receptor are A_{2A}, A_{2B} and A_3. A_{2A}AR are found mainly in the cortex and have roles in sleep initiation, motor control and potentially anti-inflammatory effects. A_{2B}AR and A_3AR are distributed more widely throughout the body and play roles in inflammation and vascular regulation. Although activation of A_{2A}AR, A_{2B}AR and A_3AR (in addition to A_1AR) by their specific agonists has been shown to trigger hypothermia, relatively few studies have confirmed this.[180,181] Thus, A_{2A}AR, A_{2B}AR and A_3AR will not be covered in further detail in this thesis. By way of contrast, multiple studies have demonstrated the involvement of A_1AR in inducing hypothermia and torpor.[86,89,177–179] A_1AR are found predominantly in the CNS, cardiac tissue (where activation

leads to decreased heart rate and cardiac output) and renal tissue (where activation leads to afferent arteriolar constriction).[182] A_1AR are expressed on both neurons and astrocytes and are found widespread throughout the CNS, with the CA1 hippocampus and the preoptic area of the hypothalamus being notable examples.[87,183] A_1AR is thought to have inhibitory effects within neurons: its activation leads to binding of the $G_{i/o}$ protein to the receptor, which inhibits adenylate cyclase and a decrease in cyclic adenosine monophosphate (cAMP). Downstream, this leads to activation of phospholipase C (PLC) and increase in inositol triphosphate (IP3) and diacylglycerol, both associated with decreased cellular activity, and thus neuronal excitability and firing.[182]

The physiological and neuroanatomical bases of thermoregulation are covered in the Introductions to Chapters 1 and 2. Briefly, CNS areas such as the lateral and median preoptic areas of the hypothalamus, raphe pallidus and paraventricular nucleus form key components of the central thermoregulatory control system.[65–68,82] Although the precise neuroanatomical pathways have not yet been fully elucidated, activation of A_1AR in neurons in these areas is thought to disrupt the normal thermogenic response to low T_b. Thus, body heat equilibrates with the surrounding environment and T_b decreases, tending towards T_a.[92,184]

The fact that several studies have shown that A_1AR agonists can be used to induce a torpor-like hypothermic state suggests that this may be a potential means by which therapeutic hypothermia can be induced as a neuroprotective treatment for acute stroke, justifying further study in this area. Notably, there is limited understanding of the impact of A_1AR agonist-induced torpor upon brain activity (e.g., as recorded by cortical EEG). Furthermore, comparing A_1AR agonist-induced torpor with natural (fasting-induced) torpor is both valid and intriguing from a comparative physiology point of view, not least because CNS A_1AR activation has been

shown to be not only sufficient but also *necessary* for natural torpor: in both the Arctic ground squirrel (AGS) and laboratory mouse, A_1AR antagonists (theophylline and 8-sulfophenyltheophylline, respectively) administrated i.p. in the middle of torpor led to sustained reversal of torpor.[86,185] This suggests that A_1AR-mediated torpor is a form of true torpor rather than another type of hypothermia that occurs via a different mechanistic pathway. Thus, in this study, the continuous changes in body temperature, EEG, EMG and vigilance states during pharmacological induction of a torpor-like state via i.p. administration of CHA in mice are investigated. At the time of writing, this would be the first time that chronic EEG has been recorded throughout pharmacological torpor in any animal. Where appropriate, the results from these experiments are compared and contrasted with those of natural (fasting-induced) torpor in laboratory mice (Chapter 2).

3.2 Materials and methods

Most of the methods used in this chapter have been covered in the previous chapter, including: Animals and recording conditions (2.2.1, also Figure 7a); Surgical procedure (2.2.2); Signal processing (2.2.4); Scoring of vigilance states (2.2.6); and Statistics (2.2.7). Instead of undergoing food restriction, mice were injected with CHA according to Section 3.2.1 (also illustrated in Figure 7b).

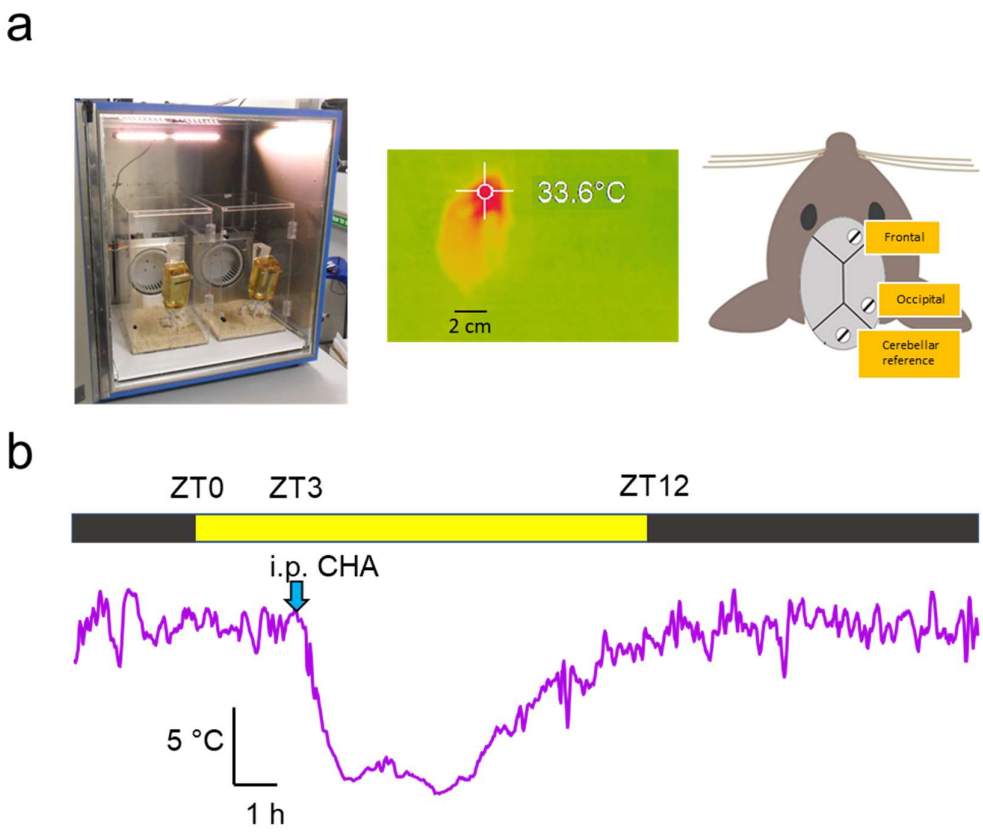

Figure 7. Experimental design. a, Left: photograph showing the recording chamber with two Plexiglas cages for individually housed mice. Middle: a representative thermal image of a mouse acquired with the camera. Right: schematic diagram showing the position of EEG electrodes. b, Surface body temperature trace (over 24 h) annotated with the time-point of i.p. cyclohexyladenosine injection and light-dark cycle.

3.2.1 Drug preparation and administration

CHA was dissolved in 8% DMSO (Sigma-Aldrich) and physiological saline. Based upon methods used in previous published studies, to induce a torpor-like hypothermic state, mice were given a single i.p. injection of CHA (0.5 mg/kg) at the same time (ZT3; Zeitgeber time; ZT0 = lights on, ZT12 = lights off) during the light-dark cycle. The dose used is based upon those used in similar previous studies in rodents.[66,88,92,118,179,186] Mice were allowed to return to normothermia unassisted. Approximately 8–10 hours were required for $T_{surface}$ to return to normothermia following injection of CHA.

Supervision and methodology for experiments was provided by Prof. Vladyslav V. Vyazovskiy and lab member Dr. Lukas Krone was involved in EEG probe implantation, i.p. injection and subsequent $T_{surface}$ and EEG recording.

3.3 Results

3.3.1 Body temperature

$T_{surface}$ was recorded throughout the experiment. Immediately following i.p. injection of 0.5 mg/kg CHA, mice underwent a bout of reversible hypothermia where $T_{surface}$ gradually tended towards T_a (20 ± 1 °C) which consisted of cooling, maintenance and rewarming phases. Cooling and rewarming rates were calculated as the slope of respective segments of the $T_{surface}$ trace, as indicated by Figure 8a. Cooling was faster in CHA-induced torpor when compared with fasting-induced torpor: –8.4 ± 0.6 and –5.8 ± 0.1 °C.h^{-1} respectively ($p = 0.003$). However, the opposite was true of rewarming, which was 2.20 ± 0.12 °C.h^{-1} in CHA-induced torpor and higher at 6.5 ± 0.6 °C.h^{-1} in fasting-induced torpor ($p < 0.001$) (Figure 8b). Next, the total cumulative durations of hypothermic episodes over 24 h during fasting-induced torpor (Day 5) and CHA-induced torpor were calculated. The former was more than double the latter (865.3 ± 58.0 and 371.8 ± 29.8 min respectively; $p < 0.001$). However, total cumulative (over 24 h) hypothermia indices (defined as the area between the temperature curve and a horizontal line representing euthermic core body temperature) were not different between fasting-induced torpor (Day 5) and CHA-induced torpor (1409.1 ± 352.2 and 1399.1 ± 220.4 °C.min respectively). When duration of hypothermia was taken into account, hypothermia indices per min of hypothermia CHA-induced torpor were greater than those of fasting-induced torpor (Day 5) (3.76 ± 0.59 and 1.63 ± 0.41 °C respectively).

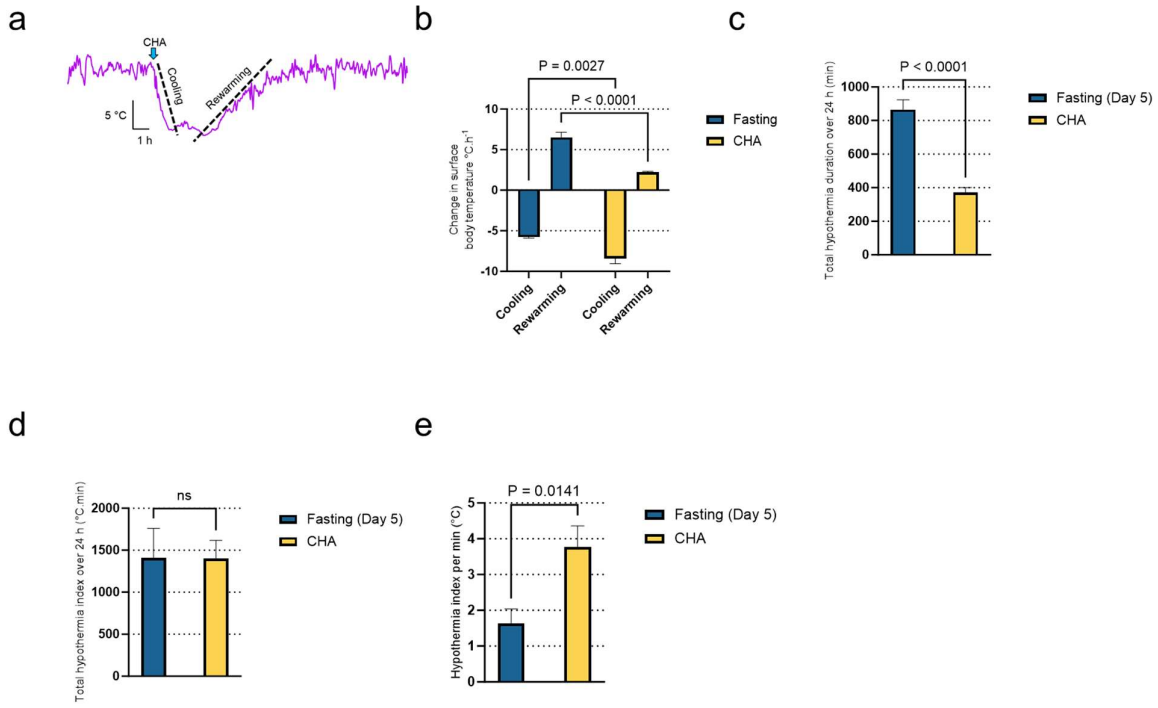

Figure 8. Comparisons of CHA-induced and fasting-induced hypothermia characteristics. a, Schematic with the surface body temperature trace of an individual mouse labelled with negative and positive slopes used to calculate cooling and rewarming rates respectively during a bout of CHA-induced hypothermia. b, Bar chart illustrating cooling and rewarming rates for fasting-induced and CHA-induced hypothermia. c, Bar chart showing the total cumulative duration of hypothermia over 24 h during fasting-induced torpor (Day 5) and CHA-induced torpor. d, Comparison of total cumulative hypothermia index (area between the temperature curve and a horizontal line representing euthermic core body temperature). e, Comparison of total cumulative hypothermia indices, corrected for total duration of hypothermia, for fasting-induced torpor (Day 5) and CHA-induced torpor. n = 6 per group, mean values, SEM.

3.3.2 Vigilance state changes during pharmacological torpor

The typical EEG and EMG signatures of wakefulness, NREM sleep and REM sleep were apparent throughout the duration of CHA-induced hypothermic torpor. This allowed vigilance state annotation throughout the recording period (Figure 9). The amount of wakefulness as

expressed as a percentage of 24 h was higher for CHA-induced torpor than for fasting-induced torpor during the cooling phase (33.6 ± 9.0% compared with 6.9 ± 1.1% respectively; $p = 0.0142$). There were no corresponding differences for the maintenance and rewarming phases. Conversely, the percentage of NREM sleep was lower for CHA-induced torpor than for fasting-induced torpor during the cooling phase (64.5 ± 8.4% compared with 92.0 ± 1.8% respectively; $p = 0.0107$). Similar to wakefulness, the percentages of NREM sleep and REM sleep for the maintenance and rewarming phases were not different between CHA-induced and fasting-induced torpor. N.B., there were negligible amounts of REM sleep in both maintenance and rewarming phases, which meant that statistical comparisons were not possible in these instances.

Upon visual inspection of the EEG, while there were clear differences in morphology in all three vigilance states between euthermia and both types of hypothermia (CHA and fasting-induced), there were no clearly discernible differences between hypothermia induced by fasting versus by CHA. Both hypothermic conditions showed similar alterations in EEG patterns across vigilance states compared to euthermia, characterised by generally reduced amplitude and frequency. Spectral analysis of EEG is performed in Section 3.3.4, which reveals specific frequency-dependent alterations across vigilance states.

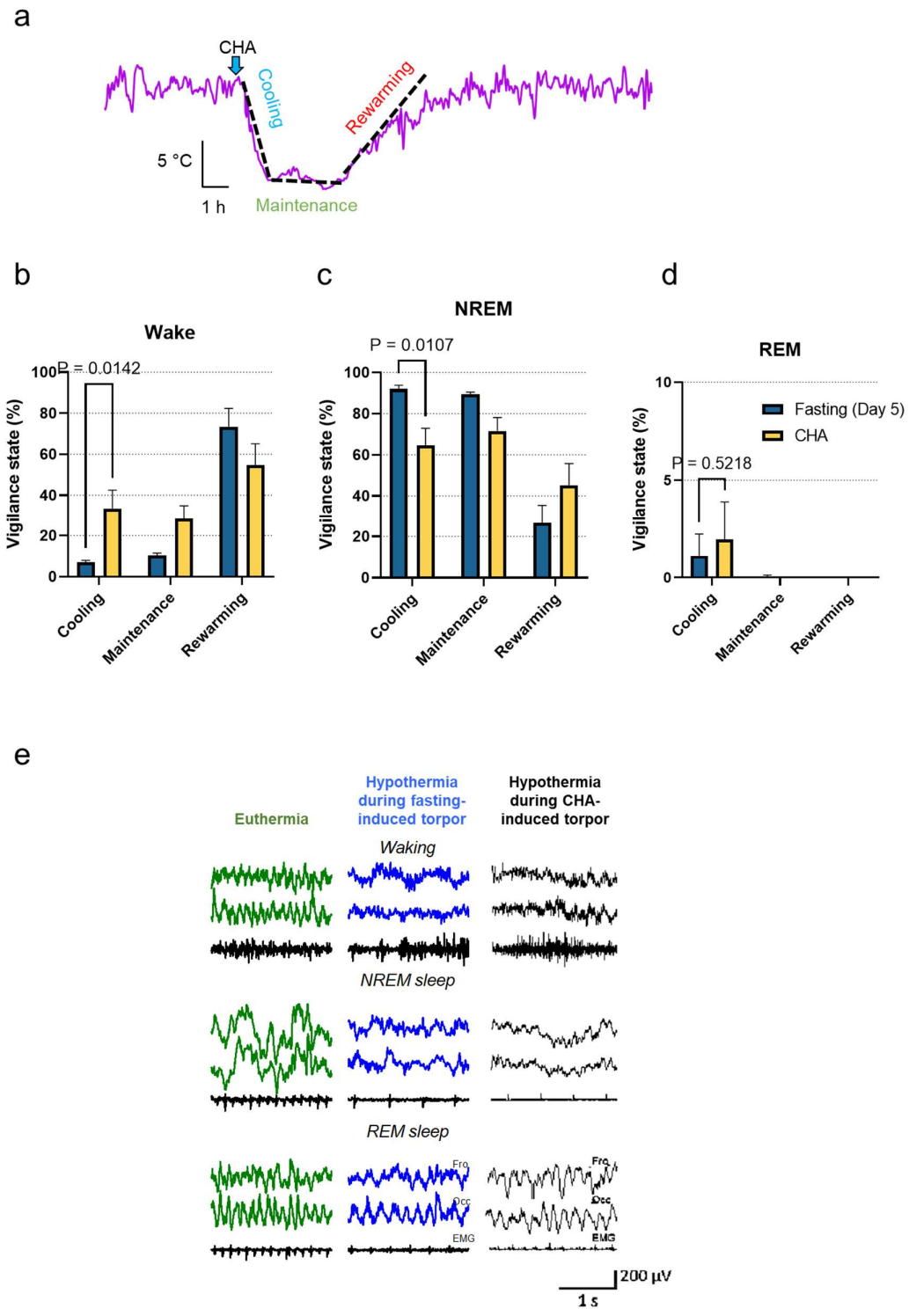

Figure 9. Comparisons of vigilance state characteristics between fasting-induced and CHA-induced torpor. a, Schematic with the surface body temperature trace of an individual mouse labelled with the cooling, maintenance and rewarming phases during a bout of CHA-induced hypothermia. Amounts of b, Wakefulness, c, NREM sleep and

d, REM sleep during cooling, maintenance and rewarming phases expressed as percentages of the total duration of each phase. n = 6 per group, mean values, SEM. e, Representative EEG and EMG traces taken from wakefulness, NREM sleep and REM sleep during euthermic conditions (surface body temperature > 36 °C) and during hypothermia (< 24 °C) during fasting-induced and CHA-induced torpor. EEG and EMG traces labelled as: Fro (frontal EEG); Occ (occipital EEG); EMG.

3.3.3 Vigilance state changes post-pharmacological torpor

Vigilance states during the first hour post-rewarming from pharmacological torpor were analysed (Figure 10). Mice were in NREM sleep for 78.4 ± 4.0% of this period and were awake for only 16.0 ± 4.2%. This contrasts with the post-rewarming period for fasting-induced torpor, where 16.3 ± 7.9% was spent in NREM sleep and 80.3 ± 10.2% was spent awake. The p-values for the comparisons of CHA-induced versus fasting-induced torpor were $p < 0.001$ and $p < 0.001$ for NREM sleep and wakefulness respectively. There were no corresponding differences in REM sleep.

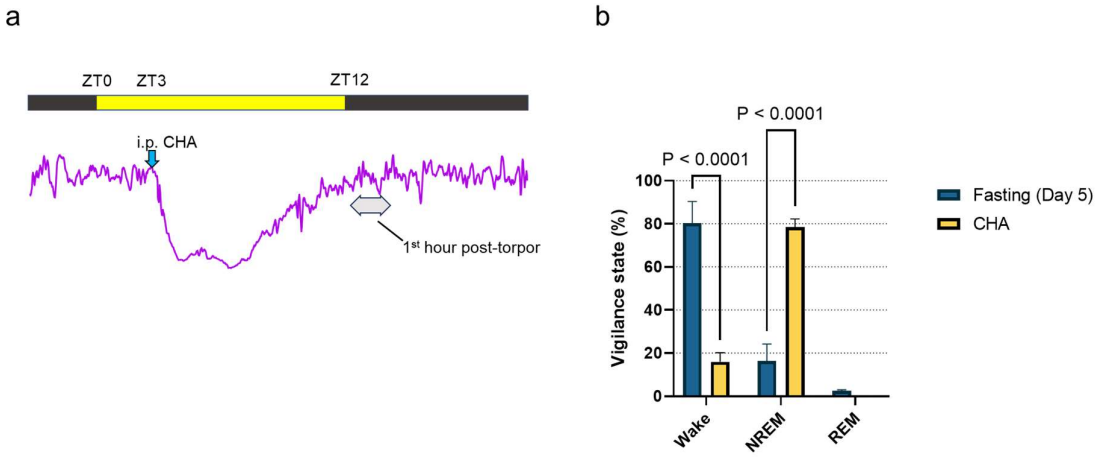

Figure 10. Vigilance state changes post-pharmacological torpor. a, Schematic with a surface body temperature trace of an individual mouse during a bout of CHA-induced hypothermia, labelled with the time-point of CHA injection and the 1 h time-period post-torpor. b, Durations of Wakefulness, NREM sleep and REM sleep expressed as

percentages of the total 1 h period following a hypothermic bout, for fasting-induced (Day 5) and CHA-induced hypothermia. n = 6, mean values, SEM.

3.3.4 EEG spectral analysis

The effects of CHA-induced hypothermic torpor on vigilance state-specific EEG spectral power were investigated (Figure 11). EEG power spectra were calculated separately for waking, NREM sleep and REM sleep states for CHA-induced torpor, as well as for fasting-induced torpor and baseline when the animals were fed *ad libitum* (for the purpose of comparison). Across all three vigilance states, EEG peak frequency was lower during CHA-induced torpor and fasting-induced torpor, with the decrease being more noticeable for the former. For the *ad lib* feeding condition, the EEG peak frequencies were 7.50, 1.25 and 7.25 Hz for waking, NREM and REM, respectively. For fasting-induced torpor (Day 5), they were 7.00, 2.75 and 1.75 Hz, respectively. For CHA-induced torpor, they were 1.50, 1.25 and 1.50 Hz, respectively. The decreases in EEG peak frequencies associated with fasting and CHA induced torpor during REM sleep were somewhat more pronounced than during NREM sleep or waking, but caution is warranted with interpreting this result as the total amount of REM sleep was substantially lower during torpor.

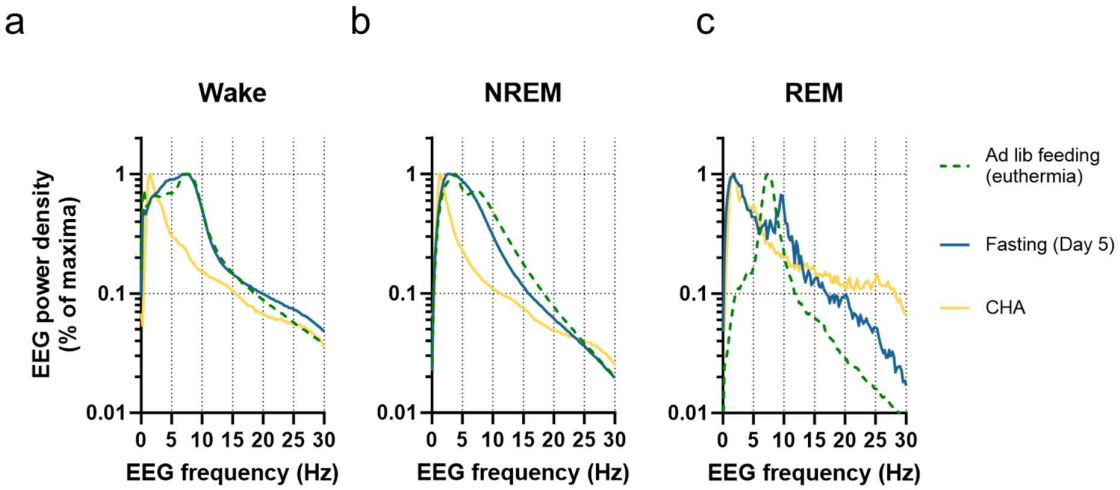

Figure 11. Changes in vigilance state-specific EEG power spectra during CHA-induced torpor, as compared with fasting-induced torpor (Day 5) and ad lib feeding at euthermia, expressed as a percentage of maximal power. Note the left-shift (slowing) of peak EEG frequency in all 3 vigilance states for CHA-induced torpor versus this occurring in only NREM and REM-scored epochs for fasting-induced torpor. n = 6 per group, mean values, SEM.

3.4 Discussion

3.4.1 Cyclohexyladenosine induces a hypothermic torpor-like state

Consistent with previous studies in mice, rats and ground squirrels,[66,88,92,118,179,186] i.p. administration of the A_1AR agonist CHA (0.5 mg/kg) in mice results in a reversible bout of hypothermia lasting 8–10 hours. This bout consists of an entrance phase (where $T_{surface}$ decreases), maintenance phase (where $T_{surface}$ remains relatively constant at near T_a) and a rewarming phase (where $T_{surface}$ increases back to normothermia). These three phases also occur during fasting-induced torpor.

Analyses of rates of change of $T_{surface}$ during entrance into and exit from CHA-induced torpor demonstrate that the rate of cooling is faster than that of rewarming (and also faster than equivalent cooling phase during fasting-induced torpor). This is in contrast with fasting-induced torpor, where cooling and rewarming occur at similar rates. During fasting-induced torpor, endogenous adenosine is the sole ligand for the A_1AR receptor. It is thought that fasting results in a change in the balance of AMP:adenosine.[187] As a result, there is net accumulation of extracellular adenosine in the preoptic area of the hypothalamus, which results in net activation of A_1AR and initiation of torpor.[87,188] The faster cooling rate of CHA-induced torpor could merely be a factor of the dose used (0.5 mg/kg), resulting in a higher maximum extracellular concentration of A_1AR-specific ligand than that of endogenous adenosine and/or a faster increase in agonist available to bind to A_1AR, given that a bolus dose is given rather than an infusion that gradually increases in rate.

However, this would not explain why the rewarming rate for CHA-induced torpor is slower than that of fasting-induced torpor. Adenosine has a very short half-life in plasma (15 s) and

therefore the level of A_1AR activation (and thus rate of thermogenesis) responds more rapidly and more sensitively to changes in the AMP:adenosine ratio. By contrast, CHA, which acts as the primary A_1AR ligand in CHA-induced torpor, has a much longer half-life (approximately 2 h).[66,189] The shallower gradient of rewarming in CHA-induced torpor may be due to CHA's slower rate of elimination compared with adenosine (and thus slower change in the net level of A_1AR activation). These findings may have practical implications for pharmacologically-induced therapeutic hypothermia, e.g., the ideal A_1AR agonist should have a half-life that is long enough to allow stable hypothermia, but short-enough to allow fine control of the duration of hypothermia. Also, BBB-permeable A_1AR antagonists may have a role in reversing pharmacological torpor. To date, A_1AR antagonists have mainly been used in 2 contexts: 1) to reverse natural torpor in Arctic ground squirrels; 2) a BBB-impermeable A_1AR antagonist (8-p-sulfophenyl-theophylline) given concomitantly with CHA (which is BBB-permeable) in rats to induce hypothermia with a net reduction in systemic/cardiac (but not CNS) A_1AR activation.[66,186]

As with fasting-induced torpor (Chapter 2), further analyses are performed on the $T_{surface}$ data from mice undergoing CHA-induced hypothermia, to take into account not only duration but also depth of hypothermia. The total cumulative duration of hypothermic episodes over 24 h during CHA-induced hypothermia were approximately double that of fasting-induced torpor (Day 5), which is explained simply due to the fact that the timing of CHA-induced torpor was artificial and dependent upon the dose of the fixed bolus of CHA. Important to note is that, whereas CHA-induced hypothermia was a single long bout, fasting-induced torpor (Day 5, and prior days) often consisted of more than one bout: the mice warmed back up and cooled back down again without entering any prolonged periods of hypothermia until feeding time. These changes in T_b may be due to the competing needs to warm up and forage for food versus cool

down and conserve energy. Interestingly, there was no difference between the two states in total daily cumulative hypothermia indices (defined as the area between the temperature curve and a horizontal line representing euthermic core body temperature), suggesting that despite CHA-induced hypothermia being shorter in total duration, this was compensated for by higher depth of hypothermia. Indeed, when duration of hypothermia was taken into account (by dividing cumulative hypothermia index by cumulative hypothermia duration), CHA-induced hypothermia had a much higher hypothermia index *per unit of time* compared with fasting fasting-induced torpor. These findings are consistent with the previous finding that the rate of cooling (i.e., deeper hypothermia is reached more quickly) during the former is faster compared with the latter.

3.4.2 EEG changes

Numerous studies have investigated the EEG changes that occur during natural torpor – of both hibernation and fasting-induced types.[102,103,109,114–118,122,190] However, chronic EEG has never (at the time of writing) been recorded from any animal undergoing pharmacologically-induced torpor. My results confirm that CHA-induced torpor in laboratory mice bears electrophysiological resemblance to fasting-induced torpor. In particular, EEG power decreases during hypothermia, especially during NREM-like sleep states. However, the decrease is more profound than for fasting-induced torpor, as demonstrated by a much more marked left-shift in the power spectrum.

As discussed in detail in Chapter 2, temperature both directly and indirectly affects EEG power, with the relationship between brain temperature and EEG power following a Q_{10} of approximately 2.5.[74,112] For example, processes involved in generating synaptic and spiking activities, such as transmembrane ionic currents, synaptic vesicle release, and intracellular

signalling cascades are expected to be inhibited at lower temperatures.[7,140–142] In addition, there is a decrease in synaptic connectivity, as detected by neuroanatomical studies in both rodents undergoing natural torpor and in rodents undergoing pharmacological torpor.[138,143–145]

Despite differences in cooling and rewarming rates, CHA-induced torpor follows a largely similar $T_{surface}$ profile to fasting-induced torpor. However, their EEG power spectra are different, which suggests that CHA-specific pharmacodynamic factors completely unrelated to temperature are at least partly responsible for this. Specifically, A_1AR are expressed throughout the cortex; binding of CHA dampens firing activity of *all* neurons – not only those in the preoptic area that are responsible for thermoregulation.[191] This is likely to affect the EEG profile and spectra of CHA-induced torpor, for example, by dampening of neuronal firing further to that already caused by the lower brain temperature. These factors may have additional importance from a clinical point of view since it is unknown what the effects of CHA would be on other parts of the cortex, in the context of an already-hypothermic brain. This would be especially important considering CHA's much longer half-life and potentially higher maximum extracellular concentration than physiological endogenous adenosine.[189]

3.4.3 Changes in vigilance states during cyclohexyladenosine-induced torpor

The question of whether torpor represents a unique vigilance state or can be interpreted within traditional sleep-wake frameworks is central to understanding both natural and pharmacologically-induced torpor. Several lines of evidence support interpreting torpor using traditional vigilance states rather than as a distinct state. Despite reduced amplitude and

frequency, the fundamental EEG patterns characteristic of NREM sleep (delta waves), REM sleep (theta rhythm), and wakefulness remain discernible during both natural and CHA-induced torpor.[116,168,192] Whilst these patterns are attenuated, their relative relationships and temporal organisation remain consistent with normal vigilance states. The behavioural manifestations during torpor align with traditional vigilance states, though with important distinctions. During NREM-like periods, animals maintain sleep-like postures and show reduced responsiveness to stimuli, but with notably tighter huddling, minimal postural adjustments, and markedly higher arousal thresholds compared to normal sleep.[193] Furthermore, the involvement of adenosine signalling in both natural sleep and torpor (particularly evident in CHA-induced torpor) is more suggestive of shared underlying mechanisms rather than distinct physiological states. Thus, while torpor can be usefully interpreted using traditional vigilance state criteria, it may represent a specialised adaptation of these states rather than a completely distinct state.

Table 2: Comparative analysis of EEG characteristics, behavioural signs and physiological markers across normal sleep, natural torpor and CHA-induced torpor. The table highlights both shared features that support interpretation using traditional vigilance states and key differences that reflect adaptation to hypothermia.

Characteristic	Normal Sleep	Natural Torpor	CHA-Induced Torpor
EEG Patterns			
- NREM	High delta (0.5–4 Hz), sleep spindles (12–14 Hz)	Reduced amplitude delta	Reduced amplitude delta
- REM	Theta-dominated (4–7 Hz)	Rare, if present shows attenuated theta	Rare, minimal theta activity
- Wake	High frequency (>7 Hz)	Reduced amplitude and frequency	Reduced amplitude and frequency

Behavioural Signs			
- Posture	Curled sleeping position	Tight balling	Similar to natural torpor
- Movement	Periodic repositioning	Minimal, mostly during arousal	Very minimal throughout
- Arousal Threshold	Normal, varies by stage	High, but can respond to strong stimuli	Very high, reduced responsiveness
Neurological Signs			
- Muscle Tone	Variable by state	Reduced but maintained	Markedly reduced
- Temperature	Normal (36–37°C)	Reduced (20–25°C)	Reduced (20–25°C)
- Metabolic Rate	Normal	Significantly reduced	Significantly reduced
Sleep Architecture			
- State Transitions	Regular cycling	Mainly NREM-like	Mainly NREM-like
- Bout Duration	Regular 10–20 min cycles	Extended NREM-like periods	Extended NREM-like periods
- Post-State Behavior	Normal activity	Immediate foraging	Euthermic NREM sleep

Consequently, despite the marked decrease in EEG power, distinctive EEG signatures seen in normothermic wakefulness and sleep are still ascertainable, which facilitates the scoring of vigilance states throughout CHA-induced torpor. Similar to fasting-induced torpor, during cooling and maintenance phases, there are higher percentages of NREM sleep, and lower percentages of wakefulness and REM sleep when compared with normothermic baseline. This is consistent with previous studies of natural torpor, where EEGs were shown to predominantly be SWA resembling NREM sleep.[102,103,114–116,122]

However, for CHA-induced torpor, these differences are less pronounced than those for fasting-induced torpor: specifically, there is a slightly greater amount of wakefulness and slightly less NREM sleep.[190] Shivering thermogenesis during torpor, detected as periods of sustained and intense EMG activity, are scored as waking epochs, according to traditional

vigilance state scoring criteria. One might presume that the increased wakefulness during cooling and maintenance phases were due to shivering, which is an autonomically controlled reflex. However, in another study by Bailey and colleagues, during i.p. CHA-induced cooling in rats there was no evidence of thermogenesis during cooling as measured by oxygen consumption.[66] This is also consistent with cooling during CHA-induced torpor being much more rapid than during fasting-induced torpor, perhaps suggesting greater suppression of thermogenesis and shivering. The other possibility is that the increased epochs scored as wake during CHA-induced torpor reflect true wakefulness (as per euthermia) or a different type of brain activity pattern. This activity, while meeting the criteria for wakefulness according to traditional EEG scoring methods, may not be associated with the same physiological or behavioural characteristics of normal wakefulness. Though outside of the scope of this thesis, future studies could involve more in-depth analysis of the EEG during the cooling and maintenance phases of CHA-induced torpor, to determine if there are patterns of activity distinct from euthermic wakefulness. Furthermore, correlation with simultaneous recordings of other physiological parameters such as heart rate, respiratory rate, and oxygen consumption (as a proxy for metabolic rate), could provide a more comprehensive picture.

Conversely, during the rewarming phase, there is a higher percentage of NREM sleep and lower percentage of wakefulness in CHA-induced torpor when compared with fasting-induced torpor. This indicates that less shivering occurs during the rewarming phase of CHA-induced torpor, which can be more readily explained through current understanding of shivering thermogenesis:[194] due to the likely higher average extracellular concentration of CHA compared with endogenous adenosine, suppression of shivering thermogenesis persists even during the rewarming phase. This is also in keeping with the slower rewarming rate observed

3.4.4 Changes in vigilance states post-cyclohexyladenosine-induced torpor

As discussed in detail in Chapter 2, previous studies in animals capable of hibernation reported that animals go into deep euthermic sleep very shortly after emergence from a bout of torpor, characterised by high SWA (a marker of sleep need, discussed in '2.4.5 Post-emergence from torpor'). These findings suggested that torpor, despite appearing similar to NREM sleep on EEG, paradoxically does not restore sleep need.[103,107,108,167,168].[168,169] On the other hand, mice emerging from fasting-induced torpor (described in Chapter 2, Discussion) did not immediately go to sleep after torpor, suggesting either that sleep pressure does not build up significantly during fasting-induced torpor, or that the need to sleep is outweighed by the need to stay awake and forage for food (Chapter 2, Discussion).

By way of contrast, analysis of vigilance states in the one hour post-emergence from CHA-induced hypothermia reveals that, unlike for fasting-induced torpor, mice that undergo CHA-induced hypothermia afterwards spend a substantial proportion of this time in normothermic NREM sleep. This suggests that, unlike fasting-induced torpor, CHA-induced hypothermia *is* a sleep-depriving state. At first glance, this finding seems paradoxical: according to the adenosine hypothesis of sleep (described in Section 2.4.5), administering an A_1AR agonist such as CHA should promote sleep, via its action on A_1AR in sleep-promoting centres (such as the ventrolateral preoptic area of the hypothalamus), and thus dissipate sleep pressure. That the opposite is found could be explained by the presence of excess CHA altering the balance of endogenous adenosine:AMP such that extracellular adenosine actually *decreases* during the hypothermic bout, leading to an increase in sleep pressure by the end of the hypothermic bout, which would be consistent with the adenosine hypothesis. Another explanation may be that, unlike fasting-induced torpor, CHA-induced hypothermia would not lead to mice being energy-deprived to the same extent, meaning that they would *not* need to stay awake in order to forage

for food. In future studies, food intake could be measured to confirm that there is no unusual increase in food consumption following torpor or post-torpor sleep.

As discussed in Section 2.4.5, an important question to answer for both natural and pharmacologically-induced torpor is whether or not the rate of build-up of sleep pressure is temperature-dependent. Lower body and brain temperatures are associated with markedly decreased EEG amplitude and left-shift in peak frequency – to levels far lower than those seen during euthermic NREM.[112,173,174] It seems plausible that this stark contrast in EEG morphology could account for the observation that torpor does not function as sleep and therefore does not have the same effect on sleep pressure. To address this possibility, as a possible future experiment, T_b could be artificially maintained at 36–37 °C (e.g., via a thermostatically-controlled heating element) within the recording chamber. Under such a setup, after CHA-injection, one could hypothesise that 1) the EEG would more closely resemble normothermic NREM sleep, and 2) such a state may *not* be sleep-depriving, unlike its hypothermic equivalent. However, if even under normothermic conditions, CHA-induced torpor is still sleep-depriving, then this would suggest a more complex relationship between adenosine signalling and sleep homeostasis. If CHA-induced NREM at normothermia led to rebound NREM sleep, it would argue that A_1AR activation alone may not be sufficient to mediate the full restorative benefits of sleep, although it might be adequate to induce sleep-like states. This outcome would indicate that while A_1AR activation can trigger sleep, additional factors may be involved in fulfilling all the restorative functions of natural sleep. Such a finding would not necessarily invalidate the adenosine hypothesis of sleep, but rather suggest that the mechanisms underlying sleep pressure and restoration involve additional complexities beyond A_1AR activation.

3.4.5 Concluding remarks

This chapter tested the hypothesis that CHA-induced torpor produces a state electrophysiologically similar to natural fasting-induced torpor. My results partially support this hypothesis. Firstly, it is evident that CHA-induced torpor shares several similarities with fasting-induced torpor. Both exhibit phases of hypothermia, maintenance, and rewarming, with CHA's induction leading to a more rapid cooling rate. This may be attributed to the higher extracellular concentration of A_1AR-specific ligand induced by the bolus dose of CHA. The slower rewarming rate in CHA-induced torpor, likely due to CHA's longer half-life, may have implications for therapeutic hypothermia strategies, necessitating a careful balance between stability and control. Furthermore, the depth of hypothermia during CHA-induced torpor is notably greater than in fasting-induced torpor when considering the duration. This emphasises the significance of the rate of cooling, which correlates with deeper hypothermia. EEG changes during CHA-induced torpor are similar to those during fasting-induced torpor, although the degree of left-shift in peak frequency is more pronounced. Factors unrelated to temperature, such as CHA's action on A_1AR receptors throughout the cortex, may be responsible. Vigilance state analysis during CHA-induced torpor reveals overall similarity to fasting-induced torpor. Intriguingly, unlike after fasting-induced torpor, after CHA-induced hypothermia mice enter normothermic NREM sleep. On the one hand, this seems to contradict the expected sleep-promoting effect of A_1AR agonists like CHA. On the other, this could be explained by the absence of the wake-promoting effect of fasting. Overall, the insights gained from this study provide further insights into effects of CHA-induced torpor on body temperature, EEG and the temporal dynamics of vigilance states. The results prompt further investigations into the temperature-dependence of sleep pressure as well as how CHA-induced hypothermia could be applied in a clinically-relevant scenario such as acute stroke.

4 Neuroprotective properties of pharmacological torpor *in vitro*

4.1 Introduction

Having established the electrophysiological characteristics of both natural and pharmacologically-induced torpor in Chapters 2 and 3, this chapter investigates the potential neuroprotective effects of CHA-induced torpor in an *in vitro* model of ischaemia. As discussed in Chapter 1, stroke is a leading cause of adult disability and mortality globally. Whilst recanalisation therapies have revolutionised acute stroke treatment, their limited therapeutic window necessitates the development of additional neuroprotective strategies. Therapeutic hypothermia has emerged as a promising approach, with preclinical studies consistently demonstrating its potent neuroprotective effects in both global and focal ischaemia models.[49] However, as previously noted in Chapter 1, the clinical translation of therapeutic hypothermia has faced significant challenges. The homeothermic nature of humans means that physical cooling triggers compensatory thermogenic responses, potentially negating the neuroprotective benefits. This physiological obstacle has spurred research into alternative methods of inducing hypothermia, particularly those that might suppress the body's thermogenic response.[50 195]

One such approach, as introduced in Chapter 1, involves the pharmacological activation of CNS A_1AR agonists such as CHA. These have been shown to induce a torpor-like state characterised by profound hypothermia in several species, which mimics natural torpor, a state of regulated metabolic suppression observed in some mammals in response to food scarcity or

seasonal cues. As explained in Chapter 1, hypothermia slows the rates of all processes involved in neuronal injury: it reduces CMR and demand for oxygen, glucose and ATP;[196,197] it enables maintenance of the physiologic ionic gradients in neurons despite ischaemic conditions, and thus delays or prevents processes such as excessive calcium influx and excitotoxic release of neurotransmitters such as glutamate;[198,199] and it suppresses generation of reactive oxygen species (ROS), generation of proinflammatory cytokines, and apoptosis (via caspase inhibition and reduction in mitochondrial damage).[57,199–201]

However, other studies demonstrate that A_1AR specific agonists can directly decrease neuronal death *at normothermia*, i.e., independently of temperature.[189,202–205] This is thought be achieved through activation of A_1AR on all cortical neurons leading to cellular changes that reduce neuronal excitability and susceptibility to ischaemia-related injury. Many of the neuroprotective mechanisms of A_1AR signalling overlap with those of hypothermia (described above): suppression of calcium influx and glutamate release via direct activation of hyperpolarising potassium channels and suppression of voltage-gated calcium channels;[206,207] suppression of proinflammatory cytokine release, free-radical formation and apoptosis. Additionally, activation of A_1AR on cerebrovascular smooth muscle cells leads to their hyperpolarisation (via activation of potassium channels and inhibition of voltage-gated calcium channels), and thus smooth muscle relaxation and vasodilation.[92,208,209]

Despite hypothermia-mediated neuroprotection and A_1AR mediated neuroprotection being relatively well-studied individually, their effects have very seldom been compared within the same model and study. *In vivo* rodent studies have previously been conducted in which A_1AR agonists have been found to be neuroprotective in global and focal models of ischaemia.[204,205,210,211] However, it is often unclear as to what extent and for what duration of

the experiment T_b is artificially maintained at normothermia. If T_b were not tightly controlled, it is possible for these A_1AR agonists to inadvertently cause transitory hypothermia, which would contribute to the observed neuroprotection. This applies not only to A_1AR agonists but also to other purported neuroprotectants that induce hypothermia. For example, Buchan and Pulsinelli and others have demonstrated that MK-801-induced hypothermia, but not direct action of MK-801 upon cortical neurons, is responsible for its neuroprotective effect.[38,212] It is a possibility that the same could be true of A_1AR agonists. It is also possible that both components contribute to neuroprotection, in which case it may be possible to determine their relative contributions. Finally, in addition to providing mechanistic insights, comparing the temperature-dependent and independent neuroprotective effects of A_1AR agonists would have clinical importance: hypothermia induction could be challenging in clinical practice, due to side effects, for example, associated with immunosuppression;[213,214] normothermic administration of A_1AR potentially offers a viable alternative.

Thus, these topics are investigated in this thesis, in both *in vitro* (this chapter) and *in vivo* (Chapter 5) models of ischaemia. In this chapter, the effects of mild hypothermia, CHA, and both together upon markers of neuronal viability are investigated in SH-SY5Y human neuroblastoma cell cultures undergoing oxygen glucose deprivation (OGD) – a readily reproducible neuronal model of ischaemia that mimics acute stroke and is well-established for investigating putative neuroprotective agents.[215–217] SH-SY5Y cells, being human, are clinically relevant and, crucially, are known to express adenosine receptors, including A_1AR.[218–220] The degree of hypothermia used in this is 33 °C, which is a level used in previous studies, both *in vitro* and *in vivo*, and is a level that is not only neuroprotective but also more neuroprotective than 36 °C hypothermia.[48,61,221]

4.2 Materials and methods

4.2.1 Neuronal culture

SH-SY5Y human neuroblastoma cells (passage no. 20–30) were cultured in Dulbecco modified Eagle's medium (DMEM) supplemented with 10% fetal bovine serum, penicillin and streptomycin (100 µg/mL), and maintained at 37 °C in 95% air, 5% CO_2 in a humidified incubator. Experiments were performed next day after seeding at 80% confluence.

4.2.2 Oxygen glucose deprivation

The *in vitro* model of ischemia comprised of 8 h of OGD followed by 24 h of normoxic conditions. Briefly, OGD medium (154 NaCl, 5.4 KCl, 0.8 $MgSO_4$, 1 $NaHPO_4$, 1.8 $CaCl_2$, 26.2 $NaHCO_3$, in mM) was left overnight to gas-equilibrate in an anoxic chamber (95% N_2, 5% CO_2; Coy Laboratory Products, Michigan, USA). Inside the anoxic chamber, SH-SY5Y neuroblastoma cells were washed once with this medium and incubated in it at 37 or 33 °C for 8 h. Then, the OGD medium was replaced with the normal culture medium described in the previous section and incubated at normal conditions for 24 h of recovery. Control cells were incubated with the culture medium in culture conditions as described in the previous section.

4.2.3 Treatment groups and outcome measures

For assessment of the effect of 33 °C hypothermia and/or CHA upon cell death following OGD, stable cultures were randomly assigned to the following groups: normoxia, 8 h OGD at 37 °C and 8 h OGD at 33 °C. Within each group, wells were randomly assigned to either 1 µM CHA (a dose of A_1AR agonist previously found to be neuroprotective in similar *in vitro* OGD studies)[222–224] or vehicle containing medium. N_6-cyclohexyladenosine (Sigma-Aldrich, UK)

was dissolved in absolute ethanol and used at a concentration of 1 μM (1:1000 dilution of ethanol). Absolute ethanol was used (1:1000 in media) as the vehicle control where indicated.

Cell death was assessed by flow cytometry (Cytek Aurora 4-laser 58-channel flow cytometer, Cytek Biosciences, Fremont, CA), following staining with cell viability and apoptosis detection dyes (Biolegend Zombie Red and CellEvent Caspase 3/7 respectively). Zombie Red is a reliable marker of cell necrosis, and caspases 3/7 were chosen as markers as they are downstream executioner-type caspases specific to apoptosis. Briefly, neurons were detached using EDTA, washed twice with flow cytometry buffer (PBS with 10% FBS and 0.1% sodium azide), with an approximate cell count of 1 x 10^6 per sample. The sample was incubated with Zombie Red (15 min, room temperature, in the dark, 1:1500 dilution) and then Caspase 3/7 (30 min, 37 °C, in the dark, 1:500 dilution). The sample was washed twice in flow cytometry buffer after each staining.

Subsequently, the effects of hypothermia and CHA on expression of intracellular cold-shock proteins was assessed using flow cytometry. Neurons were fixed and permeabilised (BD Cytofix/Cytoperm Plus kit with Golgistop, BD Bioscience, UK; as instructed by the manufacturer) and stained with rabbit anti-human RBM3 and CIRP antibodies (primary) and AlexaFluor 488-labelled goat anti-rabbit antibodies (secondary) (Abcam, 1:1000, Cambridge, UK).

4.2.4 Data analysis

Analysis of flow cytometry data was performed using FlowJo v. 10 (Oregon, USA). Firstly, forward scatter (FSC) vs. side scatter (SSC) and FSC height vs. FSC area dot-plots allowed visual identification and gating of the neuronal population, whilst excluding debris and doublet

cells respectively (examples shown in Figure 12a upper four panels). Then, for assessing cell viability, Caspase 3/7 versus Zombie Red fluorescence dot-plots were used to gate and identify subpopulations of non-necrotic/non-apoptotic, apoptotic, necrotic/non-apoptotic neurons (examples shown in Figure 12a lower four panels). For the assessment of cold-shock protein expression, after gating for singlet neurons (as for above), levels of AlexaFluor 488 fluorescence were measured which corresponded to the expression of either RBM3 or CIRP. One-way and two-way ANOVA were used as appropriate to compare the effects of different treatments, using $p < 0.05$ to test for significance using GraphPad Prism (GraphPad Software, La Jolla, CA, USA).

4.3 Results

4.3.1 Neuronal death is correlated with duration of oxygen glucose deprivation

A time kinetics study was performed whereby SH-SY5Y neurons were subjected to different durations of OGD (0, 4, 8 and 16 h) (Figure 12). There was a linear decrease ($R^2 = 0.90$; $p = 0.049$) in the percentage of necrosis and apoptosis (Zombie Red and Caspase 3/7 respectively) double-negative neurons from 0 h (82.3 ± 2.1%) to 16 h OGD (17.5 ± 5.4%). There was a corresponding linear increase ($R^2 = 0.91$; $p = 0.041$) in necrotic neurons from 0 h (5.7 ± 2.1%) to 16 h OGD (80.2 ± 6.4%). However, the decrease of apoptotic non-necrotic neurons (from 12.0 ± 4.2% to 2.3 ± 1.0%) was not correlated with OGD duration. The duration of OGD chosen for subsequent experiments was 8 h: at this duration, the percentage of double-negative neurons at this level was 36.1 ± 5.3%, which allows for any treatment effect to be detectable.

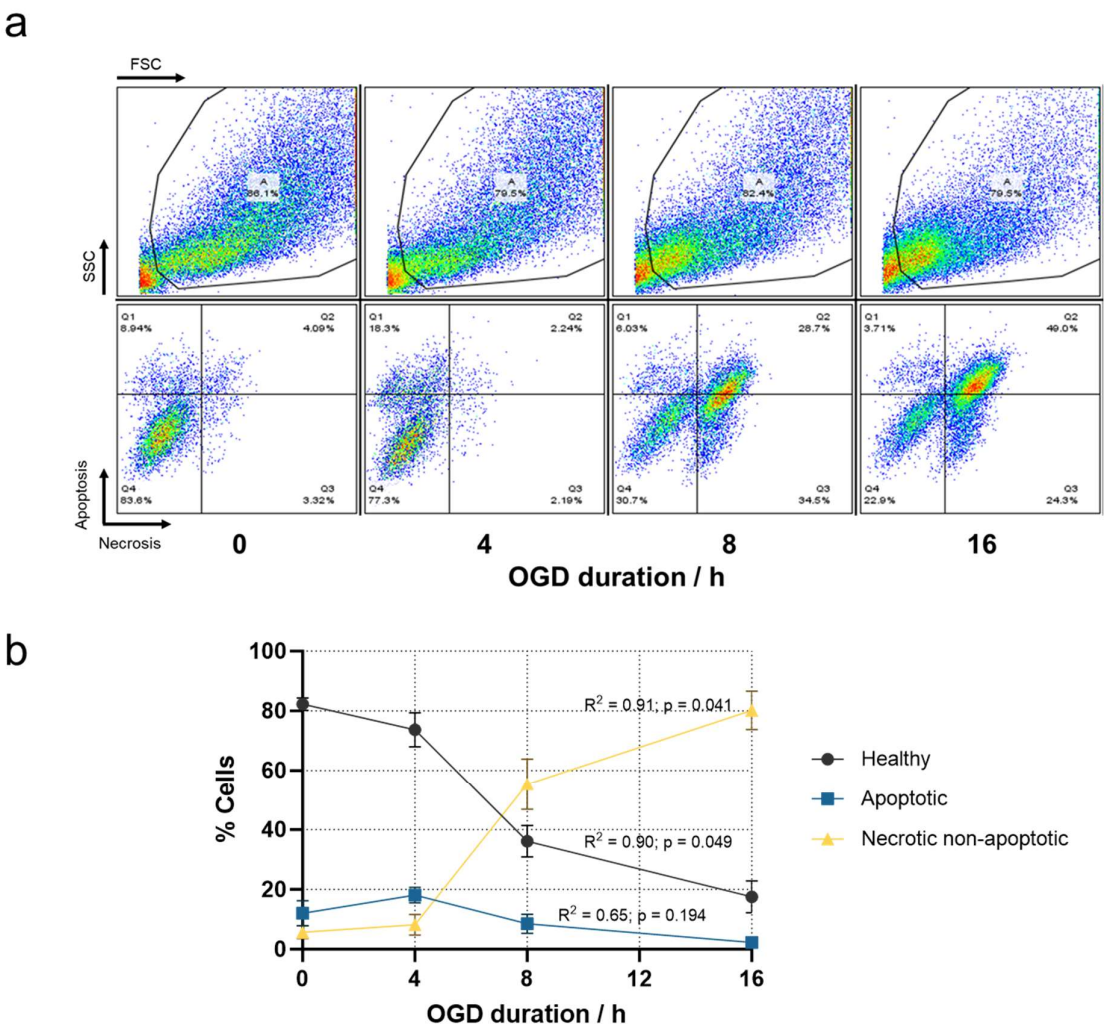

Figure 12. A time kinetics study whereby SH-SY5Y neurons were subjected to different durations of oxygen glucose deprivation (OGD) (0, 4, 8 and 16 h). a) Flow cytometry dot-plot panels showing forward scatter versus side scatter (upper four panels) and apoptosis versus necrosis (lower four panels). b) A line chart showing the percentages of healthy, apoptotic and necrotic non-apoptotic neurons. n = 3, mean values, SEM.

4.3.2 Hypothermia rescues neurons from oxygen glucose deprivation

SH-SY5Y neurons that underwent 8 h OGD under 33 °C hypothermia were protected compared with the normothermic 37 °C OGD control (79.5 ± 4.0% double-negative neurons versus 46.0 ± 1.2% respectively; p = 0.001) (Figure 13). The percentage of apoptotic neurons was reduced under OGD at 33 °C compared with OGD at 37 °C (17.7 ± 0.7% and 42.5 ± 0.3% respectively; p = 0.001). However, the percentages of necrotic non-apoptotic cells under the respective conditions were not different (19.7 ± 4.6% and 11.5 ± 1.0% respectively).

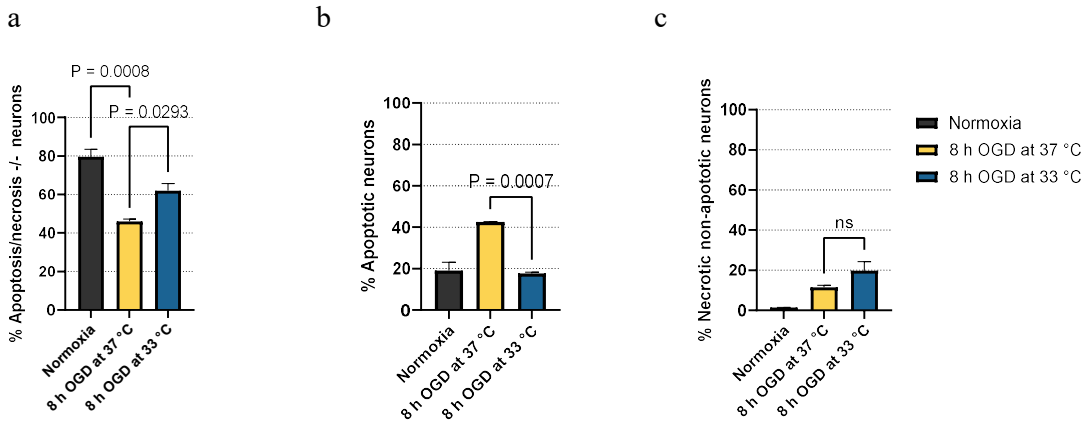

Figure 13. Bar charts showing percentages of a) apoptosis/necrosis double-negative ("healthy"), b) apoptotic and c) necrotic non-apoptotic neurons at normoxia, 8 h oxygen glucose deprivation (OGD) at normothermia and 8 h OGD at 33 °C. n = 3, mean values, SEM.

4.3.3 Cyclohexyladenosine confers additional protection at both 37 and 33 °C

CHA (1 μM) administered during normoxic normothermic conditions was associated with no change in the percentage of apoptosis/necrosis double-negative ("healthy") neurons, nor changes in the percentages of apoptotic or necrotic non-apoptotic neurons. However, CHA (1

μM) administered during OGD at 37 °C was associated with an increased percentage of double-negative neurons when compared with vehicle only (54.9 ± 2.4% versus 45.3 ± 1.4% respectively; p = 0.0254) (Figure 14). However, unlike with the effect of hypothermia, there were no changes in the percentages of apoptotic neurons when CHA was administered (37.1 ± 2.5 % with CHA c.f. 44.6 ± 3.9% with vehicle only; p = 0.0997). There was also no change in the percentage of necrotic non-apoptotic neurons (9.4 ± 3.4% with CHA c.f. 11.0 ± 1.0% with vehicle only; p = 0.8619).

Similarly, when administered during OGD together with 33 °C hypothermia, CHA was associated with an increased percentage of double-negative neurons compared with hypothermia alone (72.4 ± 2.6% double-negative neurons versus 61.0 ± 2.5%; p = 0.0105). There were no changes in the percentages of apoptotic neurons when CHA was administered, (19.1 ± 4.0% with CHA c.f. 42.5 ± 0.3% with vehicle only; p = 0.1038). There was no difference in terms of decrease in the percentage of necrotic neurons (9.4 ± 3.4% with CHA c.f. 11.0 ± 1.0% with vehicle only; p = 0.8619).

Finally, when comparing the effects of CHA alone versus hypothermia alone, there was no difference between these two conditions in terms of percentage of double-negative neurons (54.9 ± 2.4% with CHA at 37 °C c.f. 61.0 ± 2.5% with 33 °C hypothermia and vehicle only; p = 0.1309).

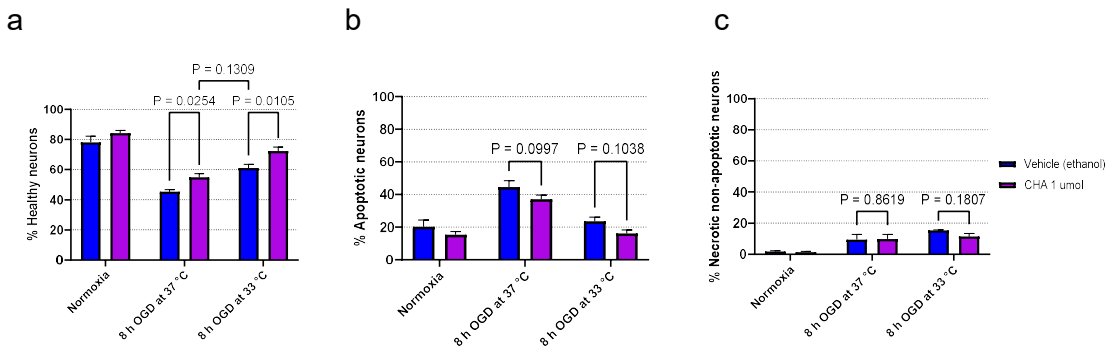

Figure 14. Bar charts showing percentages of a) apoptosis/necrosis double-negative, b) apoptotic and c) necrotic neurons at normoxia, 8 h oxygen glucose deprivation (OGD) at normothermia and 8 h OGD at 33 °C, and for both with and without CHA treatment. n = 3, mean values, SEM.

4.3.4 Hypothermia but not cyclohexyladenosine increases expression of cold-shock protein RBM3 and CIRP

Select parameters of neurons undergoing hypothermia at 33 °C and neurons exposed to CHA are investigated using flow cytometry. These include forward scatter (FSC) and side scatter (SSC), which correspond to neuronal size and granularity respectively, as well as expression of known cold-shock proteins RNA-binding motif 3 (RBM3) and cold-inducible RNA-binding protein (CIRP). Neither treatment with hypothermia nor with CHA leads to changes in FSC or SSC. However, treatment with hypothermia (but not CHA) was associated with increased expression of both RBM3 and CIRP. Hypothermia leads to an increase in RBM3 from a baseline relative peak expression level of 9868 ± 404 to 14391 ± 1009 fluorescence intensity units ($p < 0.05$) and an increase in CIRP from a baseline level of 17649 ± 951 to 25778 ± 1440 fluorescence intensity units ($p < 0.05$) (Figure 15).

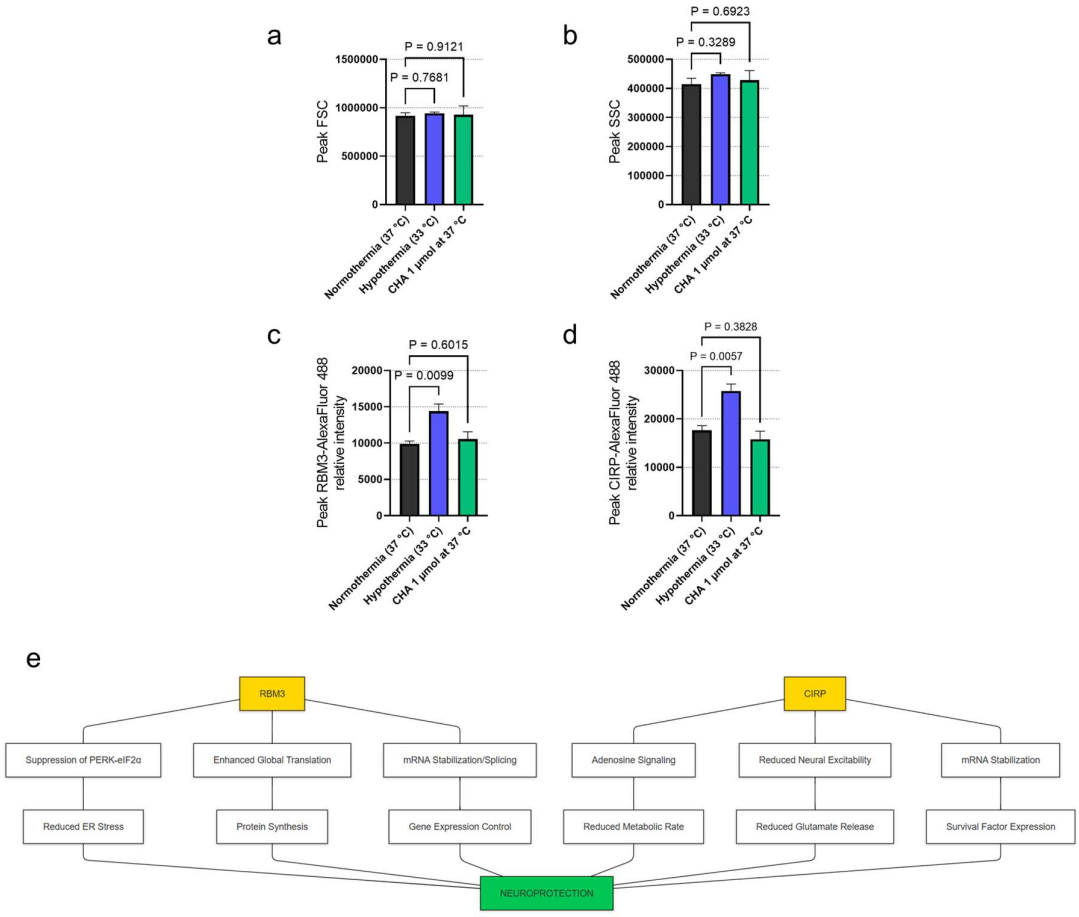

Figure 15. Bar charts showing the differences in peak a) forward scatter, b) side scatter, c) RBM3 expression and d) CIRP expression, of SH-SY5Y neurons at normothermia, 33 °C hypothermia and with 1 µmol CHA at normothermia. n = 3, mean values, SEM. e) Schematic overview of RBM3 and CIRP-mediated neuroprotective pathways. The two cold-shock proteins (yellow) act through distinct molecular mechanisms (white) that converge on neuroprotection (green). RBM3 primarily operates through protein synthesis regulation and stress response pathways, while CIRP functions through adenosine signalling and neural activity modulation.

4.4 Discussion

4.4.1 Effects of hypothermia and CHA on neuronal viability

Previously, *in vitro* and *in vivo* studies have repeatedly, but in separate experiments, demonstrated that both hypothermia and normothermic effects of A_1AR agonists can confer neuroprotection against cerebral ischaemia.[189,202–205] In this study, for the first time, the temperature-dependent and independent neuroprotective effects of A_1AR agonists are directly compared within the same experimental setup, in an SH-SY5Y model of OGD. The main findings are that, both 33 °C hypothermia and CHA (at normothermia) increase neuronal viability, which are consistent with previous studies.[61,202,222,224,225] Furthermore, CHA administered during 33 °C hypothermia results in increased neuronal viability exceeding that of either hypothermia or CHA alone. This suggests that neuroprotection via A_1AR agonists and via hypothermia could potentially be additive or synergistic, at least at the level of hypothermia and dose of CHA used in this study.

As mentioned in the Introduction to this chapter, hypothermia-mediated and A_1AR-mediated neuroprotection are thought to at least partially overlap in terms of mechanism: briefly, both decrease cellular metabolic rate, excitotoxic release of neurotransmitters, proinflammatory cytokine production, and free radical generation.[57,198–201,206,207] However, unlike hypothermia, which has a simultaneous and global effect on multiple processes involved in neuronal injury, the upstream origin of all neuroprotective effects of A_1AR agonists is at the point of ligand-receptor binding. Furthermore, whilst hypothermia *directly* influences metabolic rate by reducing the rates of all biochemical reactions, A_1AR activation *indirectly* decreases metabolic rate in neurons by suppressing neuronal firing, which in turn reduces neuronal metabolic demand.[206,207]

Regardless of how much overlap there is mechanistically, the potentially additive nature of CHA and hypothermia could be explained in functional terms: since hypothermia at 33 °C may not be at a low enough temperature to result in "maximal" neuroprotection, there exists capacity for CHA to further increase the level of neuroprotection. To investigate whether or not the above is true, future studies could compare the effects of different doses of CHA and different levels of hypothermia (e.g., 31 °C, 33 °C, and 35 °C ; for example, there could be a level of hypothermia that induces maximal protection, which could mean addition of CHA would confer no further protection.

That hypothermia itself may interact with and influence A_1AR signalling is a possibility that needs to be taken into account. Hypothermia is thought to increase endogenous extracellular adenosine via inhibition of dipyridamole-sensitive nucleoside reuptake transporters.[225] The increased extracellular adenosine, together with the CHA, together increase ligand-A_1AR binding, potentially further reducing neuronal excitability. On the other hand, hypothermia is thought to affect the pharmacodynamics of cell surface receptors, including high-affinity insulin receptors.[226] It is possible that hypothermia itself may affect CHA-A_1AR pharmacodynamics, such that the ratio of surface membrane:internalised receptors is altered, leading to a change in magnitude to the overall response to CHA. Both possibilities could be investigated via radioligand-binding and/or cell surface expression/internalisation experiments using fluorescence microscopy or flow cytometry.

4.4.2 Effects on other properties of neurons

The use of flow cytometry to collect information on cell death enabled a brief supplementary exploration of a few select neuronal properties with potential to be associated with the

neuroprotective effects of hypothermia and/or CHA. Firstly, forward scatter (FSC) and side scatter (SCC) (corresponding to size and granularity respectively) of neurons treated with 33 °C hypothermia or CHA, were analysed. Based upon previous studies which observed that neuronal dendritic spines contract and become fewer in number following hypothermia, one possible outcome was that neurons treated with hypothermia would have lower FSC.[138,227–229] However, the results in this study suggest that neither hypothermia nor CHA leads to changes in FSC or SSC. The neurons in the previous studies were in ground squirrel brains subjected to much lower temperatures (below freezing), rather than the milder 33 °C used in this study, which may account for the discrepancy. Also, although overall size of the neuronal body may change during hypothermia, neuronal dendrites themselves are much smaller and more difficult to differentiate in terms of overall number in the flow cytometer. Thus, change in FSC may not be a true representation of the shrinkage of dendrites. That no change in SSC was detected suggests that neuronal granularity as detected by flow cytometry (usually reflective of a cell undergoing apoptosis), remains constant despite treatment with hypothermia or CHA. This tentatively suggests that, under the experimental parameters used, there is no evidence either 33 °C hypothermia or CHA exacerbate cell death.

In addition to FSC and SSC, markers of hypothermia and hypothermia-associated neuroprotection are quantified using antibody staining and flow cytometry. RBM3 and CIRP are cold-shock transcription factors whose expression are elevated during hypothermia, and are two of the most well-studied in this context.[138,230–232] The molecular mechanisms by which these proteins confer neuroprotection are complex and involve multiple parallel pathways (Figure 15e). RBM3 acts primarily through suppression of PERK-eIF2α signalling, enhancement of global protein translation, and regulation of gene expression via mRNA stabilisation. CIRP operates through distinct but complementary pathways including adenosine

signalling and reduction of neural excitability.[230] Importantly, RBM3 is overexpressed in mice undergoing pharmacological hypothermia and associated with neuroprotection in *in vitro* and rodent models of neurodegeneration. In fact, in these models, lentiviral mediated over-expression of RBM3 in neurons leads to neuroprotection *under normothermia*, whereas siRNA knock-down of RBM3 accelerated neurodegeneration and abolished any neuroprotective effect of hypothermia, suggesting that RBM3 is responsible for this effect.[138] Similarly, hypothermia-induced CIRP expression has been associated with neuroprotection in several *in vitro* and *in vivo* studies.[232–235] Thus, one possibility considered was that CHA-mediated neuroprotection, which overlaps with hypothermic neuroprotection in terms of mechanisms (as described above), may also be associated with raised RBM3 and CIRP expression. In this study, consistent with previous studies, RBM3 and CIRP are over-expressed in neurons that underwent 33 °C hypothermia. However, neuronal RBM3 and CIRP levels did not change after exposure to CHA, which indicates that neuroprotection via CHA is unlikely to be mediated by RBM3 or CIRP, though this does not rule out the possibility of overlap(s) between their respective downstream pathways.

4.4.3 Concluding remarks

In this chapter, I tested the hypothesis that both hypothermia and CHA provide neuroprotection against oxygen-glucose deprivation in vitro, with potentially additive effects when combined. My findings support this hypothesis. Key results include: (1) both hypothermia and CHA individually provided significant neuroprotection against OGD, (2) the combination of hypothermia and CHA resulted in additive protective effects, and (3) CHA demonstrated neuroprotective effects at normothermia, suggesting mechanisms independent of hypothermia. These outcomes provide strong support for the potential of combining hypothermia and CHA

as a neuroprotective strategy and highlight the need for further investigation into the mechanisms of CHA-mediated neuroprotection.

A more detailed exploration of molecular mechanisms of hypothermia and CHA induced torpor was outside the scope of this particular study. Future studies could further investigate the mechanisms and downstream molecular pathways via which hypothermia (including the roles of RBM3 and CIRP) and A_1AR agonists (such as CHA) induce neuroprotection. In particular, larger scale gene expression and protein assays for components of molecular pathways commonly associated with neuroprotection in the context of OGD could be conducted. These may reveal candidates that are upregulated by both hypothermia *and* CHA, potentially providing further insight into any mechanistic overlaps between the two treatments.

Additionally, although this study adopted a simplistic system to study protection of neurons specifically, future *in vitro* studies could investigate how other components of the neurovascular unit (e.g., astrocytes, microglia and vascular endothelial and smooth muscle cells), both individually and in interaction with one another, respond to hypothermia compared with CHA under OGD. It is already known that hypothermia has differential effects on components of the neurovascular unit undergoing OGD.[61] On the other hand, it is also known that adenosine receptor (including A_1AR) agonists are associated with protection of astrocytes and microglia against OGD *in vitro*.[236–239] However, like with neurons, no study has compared hypothermia with A_1AR agonists in these contexts. Astrocytes express multiple adenosine receptor subtypes, with A_1AR activation reducing glutamate release and inflammatory mediator production.[240,241] Similarly, microglial A_1AR activation promotes an anti-inflammatory phenotype through reduced pro-inflammatory cytokine production.[237] Furthermore, vascular endothelial cells respond distinctly to hypothermia and adenosine

signalling – hypothermia stabilises the BBB, while A_1AR activation causes vasodilation and increases BBB permeability.[61,242] Such cellular interactions become particularly relevant during OGD, where coordinated responses determine tissue survival. Understanding these mechanisms could guide development of therapeutic approaches targeting multiple components of the neurovascular unit. Finally, with the view to adopting a stroke model that more closely mimics the pathophysiological complexities of human stroke, the next study in this thesis (Chapter 5) compares the effects of 33 °C hypothermia and CHA in a well-established rat model of focal ischaemia.

5 Neuroprotective properties of pharmacological torpor *in vivo*

5.1 Introduction

Building upon the insights gained from my *in vitro* studies discussed in Chapter 4, this chapter investigates the neuroprotective potential of CHA-induced torpor in an *in vivo* model of focal cerebral ischemia. As discussed in Chapter 1, therapeutic hypothermia (TH) has been widely studied as a treatment for global and focal ischaemic stroke. Meta-analyses of preclinical data demonstrate high efficacy of TH as a treatment for focal ischaemia.[49] This is particularly true of intra-ischaemic TH (as opposed to post-ischaemic TH) and where vessel occlusion is temporary rather than permanent where, on average, there are ~40–45% reduction and ~30–45% improvement in lesion volume and neurobehavioral scores respectively.[49,243] Clinically, TH is applied within a mild to moderate range, with ~33 °C being a common target temperature.[244–246] Phase II trials have demonstrated that TH with target temperatures of 33–35°C for 12–24 h is overall feasible and safe in ischaemic stroke patients.[53,63,247]

However, there have been challenges related to efficacy of TH. Many current TH induction methods (e.g., surface cooling) require several hours for target core body temperature (T_b) to be reached, with the delay resulting in lower efficacy and increased likelihood of complications.[248,249] Likely due to its immunosuppressive effects, TH also increases rates of infection, with pneumonia being a complication seen in several clinical trials.[53,63,250] Arguably

the most important stumbling block is physiological: the fact that humans, like most mammals, are homeotherms means that any displacement of core body temperature (T_b) away from set-point of 36–37 °C T_b provokes compensatory thermogenesis, leading to shivering and potentially reducing efficacy.[195]

With the goal of successfully translating therapeutic hypothermia into a neuroprotective treatment, several alternative protocols and co-therapies have been developed as attempts to mitigate the above problems. For example, anti-shivering treatments can reduce the shivering thermogenic response, which is unpleasant for patients. However, such treatments have the unwanted effect of respiratory suppression, increasing the risk of pneumonia.[251,252] Prophylactic antibiotics may have an important role in reducing this risk.[64] Other studies have investigated, both in rodents and in humans, the effectiveness of local cooling (e.g., cooling helmets, or intra-arterial chilled saline infusions).[253,254] Notably, some methods of local cooling have trade-offs, e.g., although intra-arterial cold saline infusions allow rapid TH induction speeds, hypothermia cannot be maintained without additional methods.[255] Cooling helmets allow more sustained TH, but there is often a temperature gradient: deep brain structures may not be cooled as much as surface ones.[256] Finally, TH can be induced using drugs.[66,257,258] There are eight classes of pharmacological agents with hypothermic effects, including cannabinoid, opioid, dopamine, transient receptor potential vanilloid 1 (TRPV1), thyroxine derivatives, neurotensin and adenosine derivatives.[258] Of all of these agents, adenosine derivatives are the only class that have been consistently shown to not only cause hypothermia but also alter the temperature set-point of the thermoregulatory control system in the CNS.[90,179,184]

As discussed in Chapters 1 and 4, A_1 adenosine receptors (A_1AR) are G-protein coupled receptors located on neurons throughout the CNS, as well as on microglia, astrocytes and

oligodendrocytes.[182] Pharmacological agonism of CNS A_1AR has been shown to induce torpor-like deep hypothermia in several species[86,92,179,180,259] while neuroanatomical studies, including localisation experiments involving A_1AR agonist microinjections, have determined that A_1AR on neurons in CNS regions associated with thermoregulation, such as the MnPO, DMH, raphe pallidus and nucleus of the solitary tract, are specifically responsible for inducing hypothermia.[82,87,91–93]

At the time of writing, whether CHA-induced hypothermia lessens injury after *focal* cerebral ischaemia has not been studied. However, several studies in rats demonstrated that CHA-induced hypothermia reduced mortality and ameliorates neurological deficits post-*global* ischaemia.[90] Importantly, during and following ischaemia, increased extracellular adenosine levels form an endogenous neuroprotective response.[260] The possible mechanisms of such a response, which are overall thought to reduce neuronal excitability, are discussed in the Introductions to Chapters 1 and 4. Thus, A_1AR agonists like CHA can potentially have "dual" neuroprotective effects: via hypothermia and via directly reduced neuronal excitability. Outside of the hypothalamic thermoregulatory control centre, activation of A_1AR expressed on neurons in the rest of the cortex reduces neuronal excitability independently of temperature.[172,261–264] There have been other studies carried out with the intention of studying the *normothermic* neuroprotective effects of A_1AR agonists such as cyclopentyladenosine and R-PIA post- middle cerebral artery occlusion (MCAO) in rodents. Apparent from these studies was the authors' unawareness that the drugs they were using were capable of causing hypothermia, a major neuroprotectant. A failure to document control of body temperature post-drug administration means it is difficult to discern the extent to which any neuroprotection is due to hypothermia versus due to temperature-independent effects. Nevertheless, these studies overall demonstrated protective effects in global and focal cerebral ischaemia models.[204,262,265–

[268] Similarly, it is unclear whether or not T_b was recorded continuously throughout drug administration in a non-human primate study in which AST-004, an adenosine A_1 and A_3 receptor agonist, was given intravenously and reduced cerebral infarction.[269]

The potential of CHA to induce rapid hypothermia suggests that it is a promising potential pharmacological TH agent (e.g., ~ –1 °C/h to –1.75 °C/h at a T_a of 16 °C).[90] Based upon the findings from the aforementioned studies, the overarching hypothesis of this study is that CHA-induced hypothermia lessens injury following focal cerebral ischaemia. Thus, this study evaluates the neuroprotective effects of CHA given post-endovascular suture occlusion of the middle cerebral artery, a stroke model that provides heterogeneity in the degree of injury consistent with the gold standard STAIR criteria of translational stroke research.[33,270] The primary endpoint is infarct volume and secondary endpoint is behavioural deficit measured using a neurological deficit scale (NDS). Next, this study investigates whether any neuroprotective effect of CHA would be due to hypothermia or due to temperature-independent effects. To do this, the experimental groups form a 2-by-2 factorial design, including: 1) normothermia with a saline control; 2) CHA given, allowing 33 °C hypothermia; 3) CHA given, but artificially maintaining normothermia; 4) 33 °C physical hypothermia (based upon a systemic TH protocol with proven efficacy post-focal ischaemic stroke.[221]) The hypotheses here are that, CHA plus 33 °C hypothermia is protective similar to 33 °C physical TH,[221,271] and that CHA plus normothermia is protective, but to a lesser degree.

5.2 Materials and methods

5.2.1 Animals

Adult, male Sprague-Dawley rats were used in this study (n = 97 (see 5.3.3 for group sizes); aged 12 weeks; Charles River). Rats were individually housed in a room with temperature maintained at 20 ± 1 °C and 12 h light-dark cycles, post-telemetry implantation surgery and for the remainder of the experiment. Animals were given food and water *ad libitum* before and during the study. Post-MCAO, all rats were given a soft diet to help mitigate weight loss.

5.2.2 Surgical procedures

All surgical procedures were conducted using aseptic technique during the light phase of the light-dark cycle. Prior to incision, surgical sites were shaved, and sterilised with Betadine. Rats were anaesthetised with 4% isoflurane and maintained at 2% during all procedures (60% N_2O/O_2). Body temperature was maintained at approximately 37 °C using a negative feedback system temperature control system consisting of a rectal temperature probe and heat mat. Post-operative analgesia was given to all rats (bupivacaine 0.5 mg/kg s.c.; SteriMax, Oakville, CA).

5.2.3 Telemetry implantation and recording

Sterilised and pre-calibrated telemetry probes (Model TA10TA-F40, Data Sciences International, St. Paul, MN, USA) were implanted into the abdominal cavity.[272] The probes were inserted more than 3 days prior to MCAO (the range was 3–7 days, though for most animals this was 3–4 days). Baseline data were collected for at least 24 h before MCAO. The sampling frequency was per 30 s and this was averaged into hourly bins. In addition to body temperature, the probes used also record relative whole-body movement. Probes were inserted

abdominally; abdominal and skin layers were closed using sterile suture (absorbable Vicryl® suture for the muscle layer; silk 5-0 suture for the skin layer; Ethicon Inc., Raritan, New Jersey). Bupivacaine was given (0.5 mg/kg, as above) and then Meloxicam (0.2 mg S.C.; Boehringer Ingelheim Ltd.) was given for additional post-operative analgesia.

5.2.4 Endovascular suture occlusion model

As per the method of Longa and colleagues, the neck was shaved and sterilised with Betadine.[273] An incision was made on the midline of the neck and the common, external and internal carotid arteries were isolated. Then, a silicone rubber-coated 4-0 suture (total length 30 mm, coated length 2–3 mm; Doccol Corporation, Sharon, MA, USA) was inserted 20–22 mm into the internal carotid artery via the external carotid. The occluding suture was secured in place using 5-0 silk suture and the rats were allowed to awaken from the anaesthesia. Rats were later re-anaesthetised 115 minutes after ictus, with the occluding suture being removed to establish reperfusion. The external carotid artery stump was fastened off and the neck incision was closed using wound clips.

5.2.5 CHA administration

CHA was dissolved in 8% DMSO (Sigma-Aldrich) in physiological saline.[90] To induce a torpor-like hypothermic state, an induction dose of CHA was administered 10 minutes post-reperfusion (1.5 mg/kg i.p.) and 3 additional maintenance doses of CHA every 6 h (1.0 mg/kg i.p.) were given in order to maintain hypothermia for ~24 h.

5.2.6 Clamping of core body temperature and treatment groups

Figure 16 summarises the experimental timeline and all treatment groups.

CHA-HYPOTHERMIA: Since CHA is expected to reduce the body temperature of the rat to near to ambient (room) temperature (20–22 °C),[89,186] a lower T_b boundary of 33 °C was maintained in the CHA-HYPOTHERMIA rats using servo-controlled 175 W infrared heat lamps (positioned ~30 cm above the animal) for 36 h post-MCAO.[274] This was in order to reduce the risk of potential complications related to deep hypothermia (e.g., cardiac bradyarrhythmias) and to maintain a lower T_b boundary consistent with current clinical TH practice.[275]

PHYSICAL HYPOTHERMIA: The physical TH protocol was designed to closely mimic the T_b profile of 6 CHA-treated rats (i.e., cooled to 33 °C post-CHA injection as per above). Instead of i.p. CHA, i.p. vehicle (8% DMSO in physiological saline) was injected. The parameters were: TH duration of ~24 h, 0.8 °C/h induction rate, depth of ~33 °C and 0.36 °C/h rewarming rate. Physical TH was achieved using a servo-regulation system that reduced T_b via a water mist spray coupled with an overhead cooling fan, and increased T_b via overhead 175 W infrared heating lamps (to avoid over-cooling and to assist with re-warming).[274] This system typically clamps the animal T_b to within 0.5 °C of the target T_b. The PHYSICAL HYPOTHERMIA protocol is based upon ones previously used in preclinical models of global and focal ischaemia.[276,277]

CHA-NORMOTHERMIA and NORMOTHERMIA (control): Both CHA-NORMOTHERMIA and NORMOTHERMIA animals had their T_b clamped at < 36.5 °C through the servo-regulation system mentioned in the previous paragraph. This is ~ 0.5–1 °C

lower than baseline so as to reduce the risks of stress and overheating. The T_b clamp is crucial particularly for the CHA-NORMOTHERMIA group, as these animals' T_b are likely to fall well below 36.5 °C without any external heating.

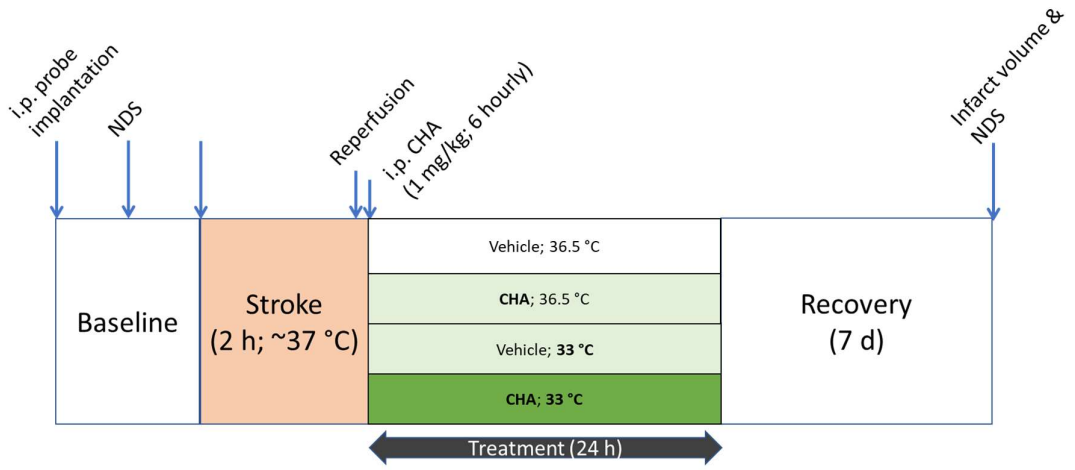

Figure 16. Male Sprague-Dawley rats (total n = 97) were implanted with wireless core body temperature / activity telemetry probes and underwent baseline testing for neurological disability score (NDS). Middle cerebral artery stroke was induced using the intraluminal filament methods. Reperfusion occurred after 2 h, at which point one of 4 treatments was applied for ~24 h. 7 days was allowed for recover prior to NDS testing and culling for histological analyses.

5.2.7 Behavioural Assessment: Neurological Deficit Score (NDS)

All rats underwent two handling sessions each lasting 10 min and a familiarisation session to reduce potential confounds of testing-related stress during baseline and subsequent analyses. They were assessed two days before MCAO (baseline) and on Day 7 post-MCAO. NDS was scored as described by MacLellan and colleagues.[278] Briefly, each rat was scored from 0 (no deficits) to 14 (severe deficits) on performance on 5 sub-tests: spontaneous circling (graded from 0 (no circling) to 3 (continuous circling)); contralateral hindlimb retraction (0 = immediate retraction when displaced, 3 = no retraction); bilateral forepaw grasp (0 = normal

grasp of a bar, 3 = rat unable to grasp bar); beam walking ability (0 = readily crosses beam, 3 = rat unable to cross or stay on beam for more than 10 s); contralateral forelimb flexion (0 = uniform forelimb extension, 2 = shoulder adduction and wrist flexion).

5.2.8 Infarct volume quantification

On Day 7 post-MCAO (after behavioural testing), rats were overdosed with sodium pentobarbital (100 mg/kg i.p.; Bimeda-MTC, Lavaltrie, Canada) and transcardially-perfused with 0.9% saline and 10% neutral-buffered formalin. Brain tissue was vibratome-sectioned at 100 μm intervals, stained with Thionin and analysed using ImageJ (v. 1.51; NIH). Tissue loss was measured as per MacLellan et al.[278]

5.2.9 Ethics Statement

All experiments had approval from the Animal Care and Use Committee of the University of Alberta and Canadian Council on Animal Care Guidelines, and complied with the United Kingdom Animals (Scientific Procedures) Act of 1986 and the University of Oxford Policy on the Use of Animals in Scientific Research. *a priori* sample size calculations were performed using G-Power (v. 3.1) and appropriate group sizes were used to ensure sufficient statistical power. These were also based upon results of previously published studies carried out in the same laboratory, e.g., assuming a standard deviation of ~30 mm^3, at least 17 animals per group were required in order to detect a 25–30% reduction in infarct volume with 80% statistical power.[221] Rats were randomly allocated to groups using an online tool (https://www.randomlists.com/team-generator). The surgeon was blinded to the group allocation during MCAO induction; histological analyses were also blinded.

5.2.10 Statistical Analysis

Data were analysed and graphed using GraphPad Prism 9 (GraphPad Software Inc., San Diego, CA, USA). Analyses were performed via ANOVA, except for ordinal data (i.e., NDS scores), which were analysed using nonparametric techniques (e.g., Mann-Whitney U Test). Data are expressed either as mean ± 95% confidence intervals or medians with interquartile ranges. The alpha-value threshold was set at 0.05 to correspond to statistical significance.

5.3 Results

5.3.1 Intraoperative Variables

Intraoperative temperature and pulse oximetry data were recorded throughout the MCAO surgery (Table 3).

Table 3: Intraoperative Physiological Variables

Group	Temperature °C (SD)	O_2 Saturation % (SD)	Heart Rate BPM (SD)
CHA-HYPOTHERMIA	36.52 (0.46)	98.03 (0.51)	372.7 (6.68)
CHA-NORMOTHERMIA	36.46 (0.75)	97.79 (0.64)	366.5 (7.00)
HYPOTHERMIA	36.48 (0.56)	97.46 (0.71)	366.6 (4.97)
NORMOTHERMIA	36.49 (0.46)	97.78 (0.91)	375.9 (5.11)

5.3.2 Pilot Experiment

A pilot experiment was performed to test the feasibility of the CHA-HYPOTHERMIA protocol post-MCAO. Temperature and activity data were collected post-MCAO in 6 rats, and their temperature profiles were used to inform the design of the physical hypothermia paradigm, so that parameters, e.g., hypothermia duration and depth, and rates of cooling and rewarming were closely modelled. Figure 17 shows the temperature profile of the rats used in the pilot experiment. One animal died, likely due to subarachnoid haemorrhage.

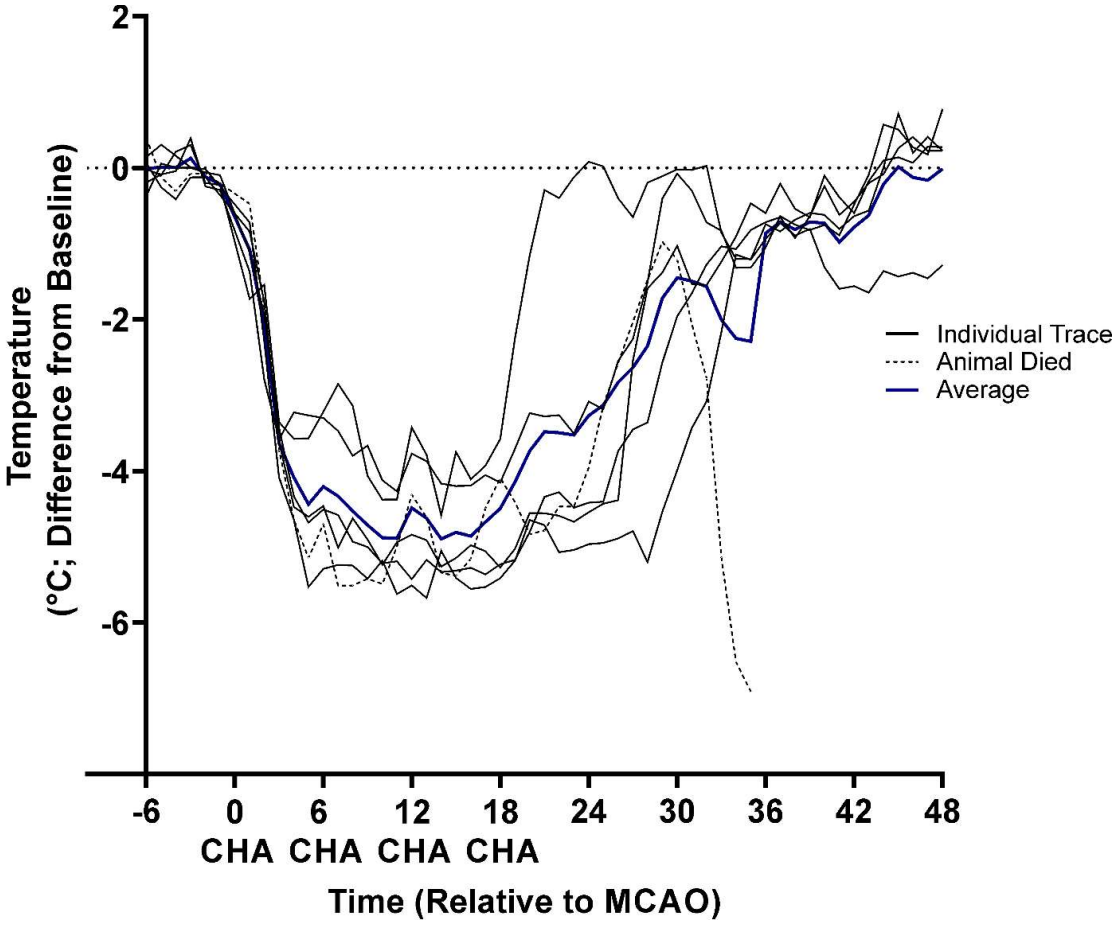

Figure 17. Core body temperature measured in 6 CHA-HYPOTHERMIA animals following a 2-h MCAO. CHA was administered at 0, 6, 12, and 18 hours post-MCAO. One animal died at ~ 30 h post-MCAO and is represented using a dashed line. Average temperature profile is denoted by a blue line.

5.3.3 Mortality and Exclusions

There were 23 animals excluded in this study, including those in the pilot experiment: 18 animals died: 2 of these died before treatment; 11 had evidence of subarachnoid haemorrhage; 5 died without evidence of intracranial haemorrhage. 2 were prematurely euthanised (due to > 30% loss of body weight), 2 were excluded due to surgical error and 1 was excluded due to technical difficulties. Of the animals that died, 7 were in the CHA-HYPOTHERMIA group, 6 were in the CHA-NORMOTHERMIA group, 1 was in the PHYSICAL-HYPOTHERMIA

group, and 4 were in the NORMOTHERMIA group. Mortality was not different between groups as analysed by chi-squared test ($p = 0.220$). After exclusions, the group sizes were: 21 in the CHA-HYPOTHERMIA group, 15 in the CHA-NORMOTHERMIA group, 19 in the PHYSICAL-HYPOTHERMIA group and 19 in the NORMOTHERMIA group.

5.3.4 Post-operative Temperature

Two-way ANOVA of post-operative T_b data showed that time under treatment, treatment type and interaction factors were all different between groups ($p < 0.0001$; Figure 18). Simple effects post-hoc analyses were conducted to further explore differences in temperature between select groups. When CHA-HYPOTHERMIA was compared with PHYSICAL HYPOTHERMIA, animals subject to the former were cooler at 2 h and 3 h post-MCAO, but there was no difference between 4–24 h (as per the intended experimental design). During the rewarming period, CHA-HYPOTHERMIA animals were overall warmer than PHYSICAL-HYPOTHERMIA animals until T_b approached baseline ($p \leq 0.03$ for comparisons between 25–40 h post-MCAO; range of differences = 0.9 °C to 2.9 °C). CHA-NORMOTHERMIA rats were colder (by ~ 1–2 °C) than NORMOTHERMIA animals until 35 h post-MCAO.

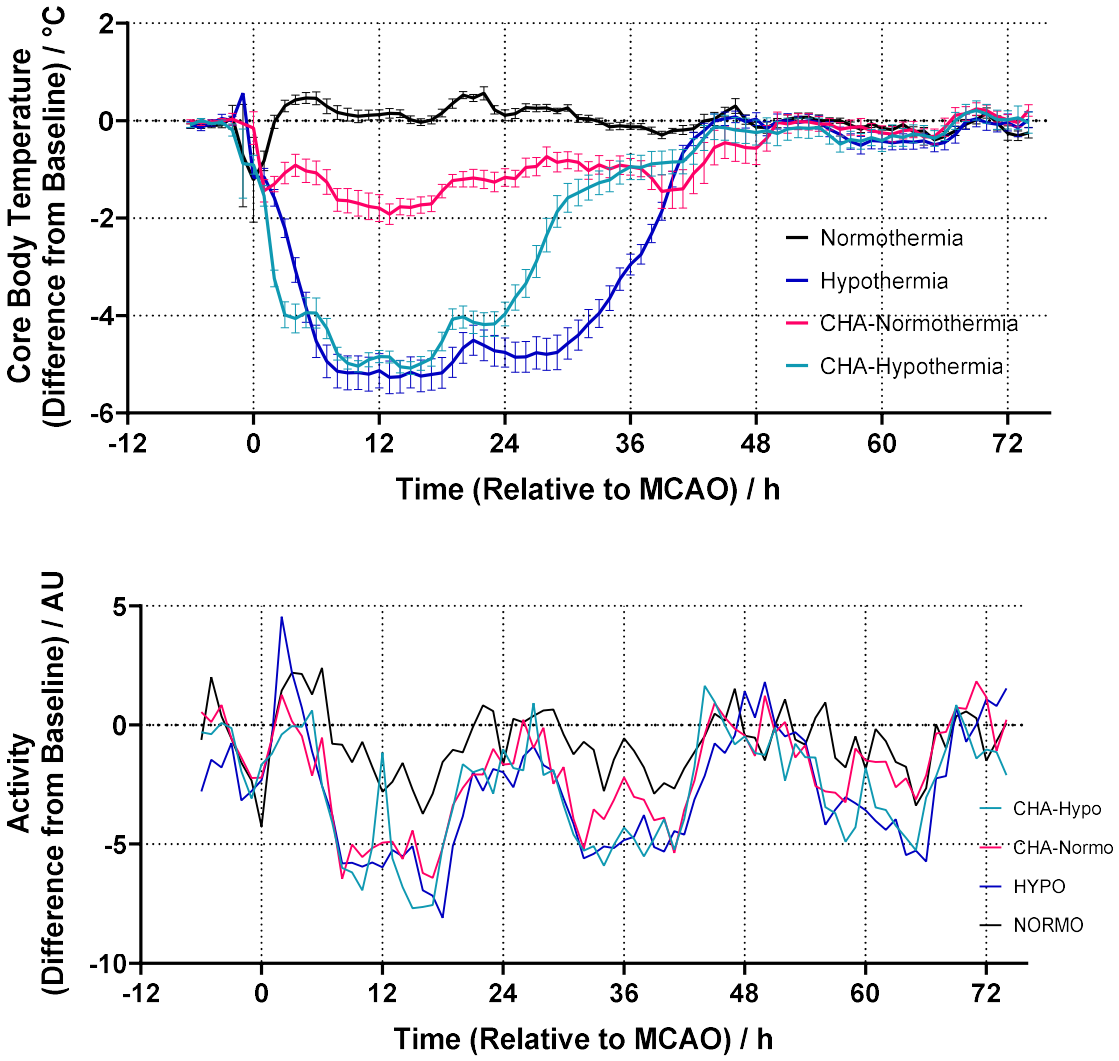

Figure 18. Core temperature and relative activity data collected using abdominal telemetry probes. Lines represent means for each group. Upper panel: Body temperature profiles collected for 3 days post-MCAO. Data were circadian corrected using baseline data. Lower panel: Relative activity profiles collected simultaneously with temperature profiles, data were circadian corrected using baseline data. CHA-HYPOTHERMIA n = 21, CHA-NORMOTHERMIA n = 15, PHYSICAL-HYPOTHERMIA n = 19, NORMOTHERMIA n = 19.

5.3.5 Post-operative Activity

Two-way ANOVA of post-op activity data showed that time under treatment, treatment type and interaction factors are all different between groups ($P < 0.001$; Figure 18). For the first 24

h, simple effects analyses show that PHYSICAL-HYPOTHERMIA animals were less active than NORMOTHERMIA animals at 6, 12, 14, 18, 20, 21, 23 and 24 h post-MCAO. At 24–48 h: PHYSICAL-HYPOTHERMIA rats were less active between 29–33, 35 and 36 h post-MCAO. When the activity of CHA-HYPOTHERMIA rats and NORMOTHERMIA rats were compared, the former were less active ($p \leq 0.05$) at 6–9, 14–15, 19–22, 27, 29–32, 34–35 and 37 h post-MCAO. There were no differences in activity between CHA-HYPOTHERMIA and CHA-NORMOTHERMIA rats in the first 48 h post-MCAO. In summary, both CHA treatments and PHYSICAL-HYPOTHERMIA treatment seemed to reduce animal activity, compared with NORMOTHERMIA animals.

5.3.6 PHYSICAL-HYPOTHERMIA, but not CHA-HYPOTHERMIA, reduced histological tissue loss

Comparison of PHYSICAL-HYPOTHERMIA and NORMOTHERMIA (control) animals showed that the former had a 39% reduction in tissue loss (mean difference = 36.8 mm^3; Cohen's d = 0.75; Figure 19a) compared with the latter ($p = 0.021$). However, CHA-HYPOTHERMIA and NORMOTHERMIA were not different ($p = 0.420$), nor were CHA-HYPOTHERMIA and CHA-NORMOTHERMIA ($p = 0.631$). Post-hoc comparison of all 36 CHA-treated animals compared with 19 NORMO-treated animals revealed no difference in tissue loss ($p = 0.250$). In summary, physical cooling was neuroprotective, but neither CHA group were. The stroke model resulted in injury ranging from frontal brain regions (e.g., 3 mm anterior to Bregma) to the hippocampus (e.g., 5.5 mm posterior to Bregma). Subcortical injury was mostly in the striatum and cortical injury extended anterior and posterior to the striatum. Representative histological imaging for animals in the PHYSICAL-HYPOTHERMIA and NORMOTHERMIA groups are in Figure 19b.

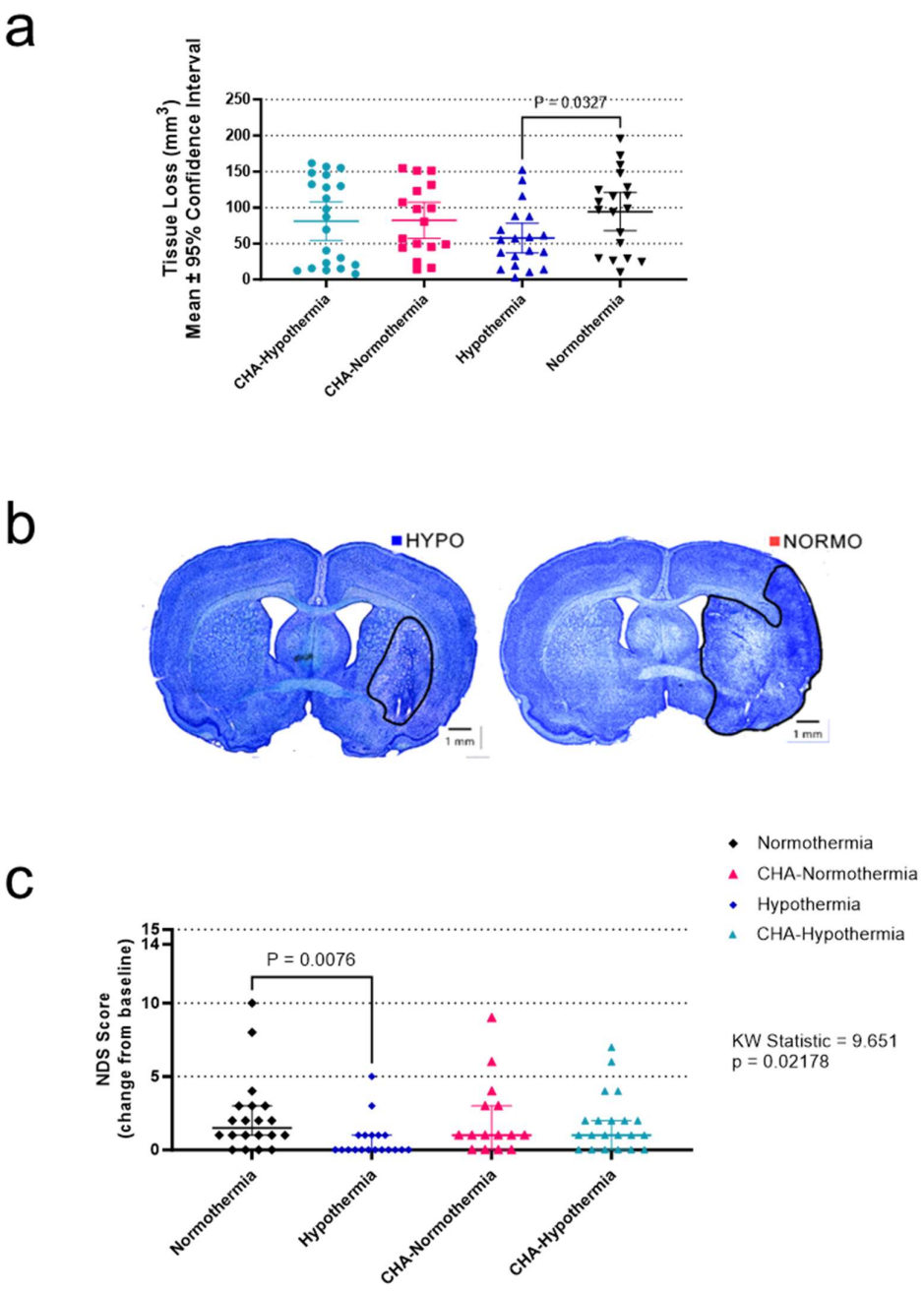

Figure 19. Biological and behavioural endpoints, data were collected on day 7 post-MCAO. a, PHYSICAL-HYPOTHERMIA treatment reduced infarction volume by 39% compared to NORMO-treated animals ($p = 0.021$). Tissue loss is a tissue-level assessment which represents the subtraction of remaining tissue in the infarcted hemisphere from the unaffected hemisphere. Data are presented as means ± 95% confidence interval. Arrows point to representative PHYSICAL-HYPOTHERMIA and NORMOTHERMIA animals that are depicted in panel b. b, Representative histological

images taken from animals in PHYSICAL-HYPOTHERMIA and NORMOTHERMIA groups. Histological images demonstrate neuroprotection primarily in cortical regions in the PHYSICAL-HYPOTHERMIA group (left photograph), with NORMOTHERMIA animals demonstrating cortical and subcortical injury (right photograph). c, Post-MCAO behavioural assessment, PHYSICAL-HYPOTHERMIA treatment reduced behavioural impairment compared to NORMOTHERMIA animals ($p = 0.014$). We used a neurological deficit scale which is a global functional assessment that includes circling behaviour, paw placement, beam walking, and fore- and hindlimb assessments. Scores range from 0 (no deficits) to 14 (maximum deficits). Data are presented as medians ± interquartile range. CHA-HYPOTHERMIA n = 21, CHA-NORMOTHERMIA n = 15, PHYSICAL-HYPOTHERMIA n = 19, NORMOTHERMIA n = 19.

5.3.7 PHYSICAL-HYPOTHERMIA, but not CHA-HYPOTHERMIA, improved behavioural outcomes

MCAO resulted in worsened NDS scores 7 days post-stroke (baseline median = 0, Day 7 median = 1; $p < 0.0001$; Figure 19c). Across groups, there was an effect detected ($p = 0.014$), which was due to difference between the PHYSICAL-HYPOTHERMIA and NORMOTHERMIA groups (PHYSICAL-HYPOTHERMIA median = 0; NORMOTHERMIA median = 2; $p = 0.008$). PHYSICAL-HYPOTHERMIA rats appeared to perform better than CHA-HYPOTHERMIA rats, but this did not reach significance ($p = 0.085$). No other post-MCAO behavioural comparisons were different ($p > 0.9999$). A post-hoc comparison of all CHA-treated rats and NORMOTHERMIA animals revealed no differences between groups ($p = 0.49$). There were no baseline differences between animals ($p = 0.78$). Therefore, as with the histology, although physical cooling was beneficial, there was no evidence for either CHA group affecting NDS score.

5.4 Discussion

Previous studies using similar protocols have demonstrated neuroprotective effects of both physical hypothermia and A_1AR agonists in established *in vivo* models of (mainly global) cerebral ischaemia.[204,262,265–268] However, in this study, only physical cooling was neuroprotective. CHA administration (comprising of 1.5 mg/kg loading dose of CHA, and 3 additional 1.0 mg/kg maintenance doses following 2 h of MCAO) – with T_b artificially maintained at either normothermia or 33 °C hypothermia – did not reduce post-MCAO injury or neurological impairment. This is true of both histological and behavioural endpoints. These findings are particularly striking since a major component of CHA-HYPOTHERMIA is hypothermia (32–33 °C; 21–24 h), which has repeatedly been shown (including in this study) to induce effective neuroprotection, even in permanent occlusion models.[221,271,279] Thus, at least with this experimental setup and parameters, CHA was ineffective at inducing neuroprotection. It is possible that CHA used in this context has detrimental effects that negated the neuroprotective effects of pure hypothermia.

There are several factors that may account for the above discrepancy. The first to be highlighted is with regard to potential off-target effects of CHA. A_1AR are present not only on neurons and glia but also on cardiac myocytes. A_1AR agonists like adenosine and CHA are well-known in terms of their effects of reducing cardiac output and causing bradyarrhythmias, potentially resulting in further impaired cerebral perfusion beyond that associated with MCAO. A more clinically-relevant approach would be, as two groups have adopted in the context of *global* ischaemia, to systemically administer an A_1AR antagonist that does not cross the BBB concurrently with the BBB-permeable A_1AR agonist, which counteracts these systemic side effects.[90,205] However, such an approach was deliberately not used for this particularly study

since its main aim was to answer basic questions about whether or not CHA-induced hypothermia is neuroprotective in a model of *focal* ischaemia, and whether CHA together with artificially maintained normothermia would also be neuroprotective. Aside from non-efficacy of CHA observed in this study, relating possibly to its systemic off-target effects, it may be considered to be safe in the context of MCAO: infarct sizes were not larger in either CHA treated group, nor were there any worse behavioural abnormalities or weight recovery differences at 1-week post-MCAO. However, further studies would be needed to investigate in more depth the precise reasons for non-efficacy of CHA in this experimental setup. For example, if bradycardia and reduced perfusion were indeed contributing factors, these effects could be detected using a more advanced telemetry probe that records both heart-rate and blood pressure, in addition to T_b and activity. Another future study would involve using the aforementioned A_1AR agonist/BBB-impermeable A_1AR-antagonist combination therapy (in place of monotherapy), which has been used in the context of global ischaemia but not *focal* cerebral ischaemia; it may be that, once potential systemic side effects have been adequately mitigated, CHA could possibly demonstrate neuroprotective efficacy on par with physical hypothermia.

Although factors associated with CHA itself most likely account for its non-efficacy, another factor to be addressed is whether or not CHA-HYPOTHERMIA and PHYSICAL HYPOTHERMIA are adequately analogous, particularly in terms of their T_b profile. The physical TH protocol was designed to as closely as possible match the T_b profile generated from a pilot study of the CHA-HYPOTHERMIA protocol involving 6 animals. Despite this profile matching, the final data showed that the T_b profile for physical hypothermia protocol was slightly longer in duration (~ 6 h longer time spent at the target temperature of ~33 °C). This meant slightly different temperature profiles between CHA-HYPOTHERMIA and

PHYSICAL-HYPOTHERMIA animals between 25 and 40 h post-MCAO. This may be due to variation between individual rats in terms of CHA pharmacokinetics, possibly contributing to greater variability in terms of time at target T_b and depth of hypothermia compared with PHYSICAL-HYPOTHERMIA rats. Although this heterogeneity is beneficial in terms of being more clinically relevant, it may have contributed added variability to an already-variable stroke model.[61]

During the period of active maintenance of T_b, T_b of animals in the CHA-NORMOTHERMIA group was ~ 1 °C lower than animals in the NORMOTHERMIA group. CHA-NORMOTHERMIA animals were maintained at 36.5 °C (as opposed to 37–37.5 °C at baseline) in order to prevent stress and potential overheating.[280] There were small (i.e., fever was not apparent), transient increases in T_b that had circadian rhythmicity in the NORMOTHERMIA group. Although such increases were not apparent in the CHA-NORMOTHERMIA group (due to the cooling effect of CHA), this did not affect treatment efficacy.

Several methodological considerations warrant detailed discussion regarding our negative findings. Our a priori power analysis suggested 17 animals per group would detect a 25–30% reduction in infarct volume with 80% power, based on previous studies showing standard deviations of ~30 mm^3 in this model. Whilst our final group sizes (15–21 animals) largely met this requirement, we observed much smaller effect sizes than anticipated. The complete absence of trend toward protection in either CHA group suggests increasing group sizes would be unlikely to reveal meaningful therapeutic effects.

The rat MCAO model used here offers several advantages for studying stroke therapeutics, particularly its ability to produce consistent infarcts with controlled occlusion duration, as well

as the fact that rats, like humans, do not naturally undergo torpor. However, important translational considerations include differences in brain size and white:grey matter ratio compared to humans. Additionally, anatomical variations in collateral circulation between individual rats contribute to variability in infarct size, despite standardised surgical technique. This variability, evident in our data, could potentially mask subtle therapeutic effects. However, the model was sufficiently sensitive to detect the neuroprotective effects of physical hypothermia, suggesting adequate ability to identify therapeutically meaningful effects.

The strength of previous evidence supporting CHA's neuroprotective effects deserves careful scrutiny. For instance, whilst Jinka and colleagues showed promising trends in a global ischaemia model, their small sample size (n = 3 per group) limited robust statistical analysis.[90] Moreover, many previous studies focused on global rather than focal ischaemia models, which have fundamentally different pathophysiology. Global ischaemia produces more uniform injury patterns and may be more amenable to metabolic suppression strategies. In contrast, focal ischaemia produces complex patterns of injury with varying degrees of hypoperfusion in different regions, potentially making it more challenging to protect with metabolic suppression alone.

5.4.1 Concluding remarks

This chapter tested the hypothesis that CHA-induced torpor provides neuroprotection in a rat model of focal cerebral ischaemia, comparable to the effects of physical hypothermia. Contrary to my expectations, our my do not support this hypothesis. Pharmacologically-induced hypothermia through i.p. administration of the A_1AR agonist CHA was ineffective in treating a 2-hour focal ischaemic stroke in rats whereas physical cooling of a matching profile reduced infarct volume and NDS deficit. The comparison between rats in the NORMOTHERMIA and

PHYSICAL-HYPOTHERMIA groups contribute further data to comparable existing data from previous studied, which may aid future meta-analyses of the efficacy of physically-induced therapeutic hypothermia. Future studies may investigate whether concomitantly administering an A_1AR antagonist that does not cross the BBB improves efficacy (e.g., by preventing bradyarrhythmias and hypoperfusion), or whether increasing the duration or depth of CHA-induced hypothermia is neuroprotective. Also, future studies could investigate whether CHA can be used synergistically with physical hypothermia methods, e.g., using CHA to speed up the induction phase of targeted temperature management, which is often time consuming and difficult.[281,282]

Statement of Authorship for joint/multi-authored papers for PGR thesis

To appear at the end of each thesis chapter submitted as an article/paper

The statement shall describe the candidate's and co-authors' independent research contributions in the thesis publications. For each publication there should exist a complete statement that is to be filled out and signed by the candidate and supervisor **(only required where there isn't already a statement of contribution within the paper itself).**

Title of Paper	An Assessment of Physical and N6-Cyclohexyladenosine-Induced Hypothermia in Rodent Distal Focal Ischemic Stroke
Publication Status	X Published ◻ Accepted for Publication ◻Submitted for Publication ◻Unpublished and unsubmitted work written in a manuscript style
Publication Details	Liddle LJ, Huang YG, Kung TFC, Mergenthaler P, Colbourne F, Buchan AM. An Assessment of Physical and N6-Cyclohexyladenosine-Induced Hypothermia in Rodent Distal Focal Ischemic Stroke. Ther Hypothermia Temp Manag. 2023 Jun 20. doi: 10.1089/ther.2023.0025. Epub ahead of print.

Student Confirmation

Student Name:	Dr Yi-Ge Huang		
Contribution to the Paper	Statement not required (as per instructions above): statement of contribution is within the paper itself.		
Signature		Date	

Supervisor Confirmation

By signing the Statement of Authorship, you are certifying that the candidate made a substantial contribution to the publication, and that the description described above is accurate.

Supervisor name and title:		
Supervisor comments		
Signature	Date	

This completed form should be included in the thesis, at the end of the relevant chapter.

6 Final discussion

The work presented in this thesis used different approaches to investigate several key questions pertinent to the translation of torpor to a neuroprotective treatment for acute stroke. Firstly, I sought to elucidate the cortical electrophysiological properties of natural (fasting-induced) torpor in laboratory mice, comparing them with those of pharmacological (CHA-induced) torpor. Then, I addressed whether or not CHA-induced torpor was protective in both *in vitro* and *in vivo* models of ischaemia. As a reminder, the principal findings of each chapter of this thesis could be briefly summarised as:

- Both fasting-induced and CHA-induced torpor in laboratory mice are characterised by reversible hypothermia and by SWA on EEG that resembles NREM sleep; this reflects decreased net neuronal firing which may reflect decreased potential for an excitotoxic response to an ischaemic insult (Chapters 2 & 3).
- Both 33 °C hypothermia and CHA provide neuroprotection against oxygen glucose deprivation in *in vitro* SH-SY5Y neuronal cultures. Further protection is achieved by combining 33 °C hypothermia and CHA with one another (Chapter 4).
- *in vivo*, although physically-induced 33 °C hypothermia was neuroprotective in a 2 h middle cerebral artery occlusion model of stroke, neither CHA-induced 33 °C hypothermia nor CHA given at normothermia were protective (Chapter 5).

The results of the individual chapters are examined altogether in this Chapter, whose purpose is to bring together and expand on the key findings and discussions from the individual studies.

6.1 Comparing natural and pharmacologically-induced torpor

Torpor, which is defined as regulated and reversible reduction of body temperature, naturally occurs in some mammals in response to low food availability or intake.[78] A_1AR signalling has been shown through different studies to be necessary for entering torpor, since administration of an A_1AR antagonist brings animals out of torpor.[86] Conversely, administration of A_1AR agonists has been shown to be sufficient for induction of a hypothermic torpor-like state in several mammalian species, including the laboratory rat, which does not naturally undergo torpor.[90,92] In this thesis (Chapters 2 & 3), natural (fasting-induced) torpor and pharmacologically (CHA)-induced torpor in the laboratory mouse are compared in terms of T_b and EEG. Notably, as of the time of writing, the EEGs of natural and pharmacological torpor have not previously been directly compared within the same species and within analogous experimental setups.

As discussed in Chapter 3, fasting-induced and CHA-induced torpor in the laboratory mouse have key similarities and differences in terms of T_b dynamics. In both, there is a drop in T_b towards T_a, which is followed by a stable trough (often lasting several hours) and subsequently an increase in T_b back towards normothermia. Interestingly, there are differences between the two types of torpor in terms of rates of change of T_b during cooling and rewarming: in CHA-induced torpor, the animals are quicker to cool down during the entrance phase, but slower to warm up during the emergence phase. This may be accounted for by pharmacodynamic factors, e.g., different extracellular concentrations of A_1AR ligand (adenosine and CHA for fasting-induced and pharmacological torpor, respectively) in the hypothalamic preoptic area responsible for central control of thermoregulation.[283] Also, the fact that CHA has a much longer half-life than pure adenosine may impact the levels of A_1AR signalling over time.[189] As a general consideration, the upstream drivers of changes in adenosine levels for natural torpor

are likely to be complex, including the energetic (i.e., fasted versus fed) state of the animal – this would be in stark contrast with torpor induced via CHA, which is administered as a single bolus in the study described in Chapter 3.[180,190] Though technically difficult, direct measurement of adenosine and CHA levels from the hypothalamic preoptic area (POA) via neurochemical methods (e.g., *in vivo* microdialysis), may be one method of confirming the precise extracellular concentrations and temporal dynamics of each ligand, which would provide data that may provide further clarity to this issue.[164] Subsequently, one could explore the effects of different doses and dosing regimens of CHA, as well as a more direct route of administration, i.e., intracerebroventricular infusion, via appropriate implanted cannulae.

In terms of cortical electrophysiological properties, both fasting-induced and CHA-induced torpor are characterised predominantly by slow-wave (low frequency, high amplitude) EEGs. The normothermic EEG state that bears closest resemblance is NREM sleep.[119,190] However, the EEGs of both fasting-induced and CHA-induced torpor are different from NREM sleep in that their power (= amplitude x frequency) reduces as a function of T_b, which is a finding consistent with similar previous studies (and which is discussed in-depth in Chapter 3, Discussion).[103,190] Analyses of EEG power spectra suggest that, even at similar T_b, the EEG during CHA-induced torpor is further left-shifted in terms of peak frequency. This finding may be consistent with the observation that, as discussed in the Introduction sections of Chapters 4 & 5, CHA can directly modulate neuronal firing independently of temperature. Alternatively, as mentioned above, pharmacodynamic factors, namely, differences in adenosine and CHA concentrations and temporal dynamics (between fasting-induced and pharmacologically-induced torpor respectively), may account for differences in neuronal firing behaviour, which may be detected by cortical EEG.[283] Future studies could use intracortical microelectrode

arrays to record local field potentials (LFP) and gain better understanding of how single units behave in terms of firing during fasting-induced and CHA-induced torpor.[176]

An important set of experiments to be conducted in future studies would involve recording both EEG and metabolic rates (for example, in a metabolic chamber) of mice undergoing fasting-induced and CHA-induced torpor at different T_b, to include comparisons between normothermia and various degrees of hypothermia. Due to basic principles of thermodynamics and heat transfer, probably the most reliable method of changing T_b during torpor would be to change the T_a either via a thermostatically controlled and thermally-insulated chamber or simply via changing the air temperature of the experiment room. The first question to answer would be if, at different T_a, torpor still occurs in response to fasting or CHA. Since, torpor is not expected to change T_b at normothermic T_a, the only way of detecting torpor would be a decrease in metabolic rate. If torpor were detected, then the second question would be regarding how the EEG might be different, e.g., at normothermic T_b. As mentioned above, since EEG power is a function of T_b, one could hypothesise that the EEGs of both types of torpor, under normothermic conditions, are predominantly of SWA similar to NREM sleep, but that there is not the reduction in EEG power that is seen with hypothermic torpor. Such a study could subsequently be repeated with the same microelectrode array setup (mentioned in the previous paragraph) to investigate if there are corresponding changes in LFPs single unit activity.

However, the above experiments alone are insufficient for yielding insight into how fasting-induced and CHA-induced torpor are initiated and controlled from mechanistic and neuroanatomical perspectives. The EEG can be thought as merely a window unto neuronal activity: though it measures summed activity, it provides little information about the relative activities of different brain regions, including those purported to be involved in regulating

torpor, such as the hypothalamic POA.[192] Although, as mentioned previously, studies have shown that CNS A_1AR signalling is necessary and sufficient for torpor induction, the precise neuroanatomical circuits involved in natural and CHA torpor induction are still unconfirmed.[82,86,92,284] Amongst different methods that can be used to explore this, those that allow top-down investigation of these circuits may be most helpful in providing initial insight into this (e.g., c-Fos immunohistochemistry, lesioning experiments, and LFP recording (via implanted microelectrode arrays) of the POA and surrounding areas). This is because, whilst bottom-up approaches such as optogenetics could potentially uncover circuits responsible for similar phenotypes (e.g., hypothermia), it is difficult to be sure that such phenotypes are precisely the same as those seen in fasting-induced or CHA-induced torpor.

The above points of comparison between fasting-induced and pharmacologically-induced torpor are important in highlighting that, though the two phenomena are very similar, they are not identical. As such, it could be argued that pharmacologically-induced torpor should be termed "torpor-like" state to make a point of this distinction. From a translational perspective, however, there is sufficient electrophysiological evidence from this study and previous studies to suggest that the overall firing rates of neurons decrease during both types of torpor. This would theoretically align with torpor potentially possessing neuroprotective properties, and is consistent with hypothermia – itself a key component of torpor – being strongly associated with neuroprotection.

6.2 The translational relevance of torpor: towards optimisation of the pharmacologically-induced torpor protocol

After establishing that fasting-induced and CHA-induced torpor share key similarities in terms of changes in T_b and EEG, I next evaluated the neuroprotective potential of CHA-induced torpor against *in vitro* and *in vivo* models of ischaemia. Several preclinical studies have demonstrated hypothermia to be highly protective against focal cerebral ischaemia.[49] Although CHA-induced hypothermia was observed to be protective in a rat model of global ischaemia, until recently this has not been investigated in an equivalent model of focal ischaemia, which was the primary aim of study described in Chapter 5.[90] On the other hand, results from other *in vitro* and *in vivo* studies have suggested that A_1AR agonists like CHA protect neurons, possibly even at normothermia.[260] Thus, the secondary aim of Chapter 5 was to investigate to what extent temperature-dependent and temperature-independent effects of CHA each contribute to any neuroprotective effect seen.

In the two studies carried out in Chapters 4 & 5, measures of neuroprotective efficacy of hypothermia versus CHA alone versus hypothermia and CHA combined were compared *in vitro* and *in vivo*. Whilst CHA, hypothermia and CHA combined with hypothermia were all protective *in vitro*, only physical hypothermia was protective *in vivo*. The finding that, *in vivo*, only physical hypothermia (and not CHA-induced hypothermia or CHA at normothermia) was associated with neuroprotection could be due to a variety of reasons, the key ones of which are explained in Chapter 5, Discussion. These reasons are further expanded upon in this section, which places the discussion in a wider context and takes into account the *in vitro* findings from Chapter 4.

Firstly, the *in vitro* and *in vivo* studies were inherently different from one another, not just in the traditional sense, but also in that the *in vitro* study used only neurons in order to focus solely on neuroprotection, which (as discussed in Chapter 4) is not representative of the entire neurovascular unit *in vivo*, which also comprises of other cells which play crucial roles in its normal functioning, such as astrocytes, microglia and endothelial cells.[5,61] (Intriguingly, on this note, a recent study of CHA-induced torpor in mice observed reduced apoptotic signalling and several markers of inflammation in the context of lipopolysaccharide-induced neuroinflammation; though whether these effects were attributed to temperature-dependent or independent effects of CHA is unclear.[285]) Furthermore, although the duration of OGD and dose of CHA used *in vitro* were selected due to the necessity of being able to detect treatment effects, these do not precisely match those of *in vivo* study. However, key parameters, such as depth of hypothermia (33 °C) were consistent between the two studies, as well as the experimental groups having a 2 x 2 factorial design to investigate all four possible combinations of treatments (CHA versus vehicle; hypothermia versus normothermia).

The *in vitro* versus *in vivo* conundrum explained above cannot fully explain the outcomes of the *in vivo* study, particularly given that other previous *in vivo* studies have observed that: 1) CHA-induced hypothermia is neuroprotective in a rat model of global ischaemia, and 2) other A_1AR agonists, presumably used at normothermia (see Introductions to Chapters 4 & 5) are neuroprotective in both focal and global models of ischaemia.[90,204,205,269] Thus, it is possible that the discrepancies between the designs of these studies and of my study could explain the different outcomes. The Discussion section of Chapter 5 elaborates on how these could potentially be explained by systemic side effects of CHA (e.g., bradycardia and reduced cardiac output resulting in decreased cerebral perfusion), as well as the durations of PHYSICAL-HYPOTHERMIA and CHA-HYPOTHERMIA not precisely matching one another.

Chapter 5 also suggests specific future experiments that could be performed to address these issues, e.g., concurrently administering an A_1AR antagonist that does *not* cross the BBB to counteract the systemic effects of CHA whilst preserving its CNS effects. This approach has been adopted by Drew and colleagues in the context of global ischaemia, where it was found to be protective.[90,205] Incidentally, they also adopted a lower temperature of hypothermia (mean T_b ~ 29.7 °C) than in my studies, which is another possible explanation for the discrepancy seen. As previously mentioned, in Chapters 4 and 5, a T_b of 33 °C was selected due to previous physical hypothermia studies observing neuroprotective effect at such a temperature. It is possible that, instead of defending the lower T_b boundary of 33 °C, allowing the animals to go into a deeper hypothermia would increase the level of neuroprotection such that it would counteract any deleterious effect of CHA, e.g., through bradycardia and hypoperfusion. It is possible that hypothermia may itself influence extracellular adenosine levels (as mentioned in the Discussion of Chapter 4) which may enhance A_1AR signalling.[225] Finally, Drew and colleagues adopted a shorter total duration of ischaemia (albeit global rather than focal), which may also be a factor. However, the duration of hypothermia (24 h) they (and others, instead using physical hypothermia) used led to protection being observed.[90] Thus, future experiments comparing the outcomes of different depths and durations of hypothermia, as well as different doses and dosing regimens of CHA (in combination with co-administered A_1AR antagonists) could provide insight into the factors that are key to achieving successful neuroprotection.

Only once the parameters for pharmacologically-induced torpor have been optimised for treatment of focal ischaemia in rodents, can such a treatment be advanced along the translational pathway. This would typically involve investigating safety and efficacy in further studies in larger mammals and/or non-human primates, before first-in-human trials can be

planned. Since torpor is a phenomenon that relatively few mammals undergo naturally, it is important to consider the likelihood of *pharmacologically*-induced torpor potentially being inducible in humans before Phase 1 trials are designed and approved. First of all, it has been demonstrated in this and prior studies that CHA-induced torpor is possible in laboratory rats, which, like humans, do not naturally undergo torpor.[92,186] Secondly, human neurons are known to express A_1AR, which confirms that there are valid targets for CHA. Finally, as mentioned in Chapter 5, an IV administered A_1AR/A_3AR agonist, AST-004, was found to be safe and efficacious in a non-human primate (NHP) model of focal ischaemia and has recently undergone Phase 1 trials in healthy volunteers [data not yet published]. Notably, there was no chronic T_b recording in the NHP study.[269] Another Phase 1 trial demonstrated the safety of intrathecally administered adenosine, used as a spinal anaesthetic.[286] Thus, once the factor(s) that led to non-efficacy in my study have been addressed, it is possible that A_1AR agonists may be administered in a way that is safe and efficacious in patients. In terms of inducing hypothermia, however, humans are unlike rodents as their lower surface area:volume ratio results in slower rates of cooling and rewarming, with a higher equilibrium T_b due to relatively slower heat transfer.[70,287] This is also demonstrated in black bears that undergo torpor, whose T_b often does not drop below 30 °C.[85] Clinically, however, this may not be a disadvantage as lower T_b is associated with greater risk of infections, e.g., pneumonia.[250] In summary, whilst the studies described in thesis failed to demonstrate protective effect of CHA-induced hypothermia, reasons for this have been discussed. Nevertheless, the findings have provided further evidence that physical hypothermia is protective. Exploring pharmacological methods of inducing hypothermia may eventually yield neuroprotective strategies that will be beneficial in acute stroke.

6.3 Further methodological refinements and extensions of experimental approaches

The findings presented in this thesis point to several essential methodological refinements that could enhance understanding of both natural and pharmacologically-induced torpor. Traditional sleep scoring, whilst providing valuable insights and justifiable as a utilisable framework, may not fully capture torpor's unique characteristics. While my work demonstrated that both natural and CHA-induced torpor share EEG features with NREM sleep, more sophisticated analyses combining high-density EEG recordings with continuous video monitoring could reveal crucial distinctions.[192] The addition of detailed behavioural analysis would allow correlation between specific EEG patterns and behaviours such as posture, movement patterns, and arousal responses. This integrated approach would be particularly valuable during periods currently scored as "NREM-like", where traditional criteria may miss torpor-specific signatures. Examining the presence and characteristics of sleep spindles and K-complexes during the transition into torpor could reveal whether these NREM sleep hallmarks persist at lower temperatures and how their morphology changes with declining temperature. Furthermore, automated assessment of spectral power changes across different temperature ranges could help identify unique EEG signatures that distinguish torpor from conventional sleep states, particularly during the crucial transition periods into and out of torpor. These analyses could be enhanced by simultaneous recording of LFPs across multiple cortical regions to understand region-specific responses to temperature changes and CHA administration.[176]

The electrophysiological changes during MCAO in rats undergoing CHA-induced torpor warrant thorough investigation, particularly given CHA's lack of neuroprotection despite promising *in vitro* results. Continuous EEG recording during stroke evolution, with strategic

electrode placement targeting both core and penumbral regions, could reveal how CHA affects phenomena such as peri-infarct depolarisations and seizure activity.[288] Real-time laser Doppler flowmetry would strengthen the model by verifying occlusion success and monitoring reperfusion dynamics, particularly important given concerns about CHA's cardiovascular effects potentially compromising cerebral perfusion.[289] The cellular mechanisms underlying hypothermia and CHA's effects deserve deeper investigation through enhanced *in vitro* approaches. While the SH-SY5Y model proved valuable for isolating neuronal responses, mixed culture systems incorporating astrocytes, microglia and endothelial cells would better reflect neurovascular unit complexity.[61,290] This approach becomes particularly relevant given my observation that CHA and hypothermia showed additive protection in isolated neurons but not *in vivo*. The differential expression of cold-shock proteins RBM3 and CIRP between hypothermia and CHA treatment suggests distinct molecular pathways that warrant investigation through studies of inflammatory mediators and cell survival signalling.[230] Time-course analyses examining the temporal relationship between temperature changes, inflammatory responses, and cell death could help identify critical therapeutic windows.

Beyond acute outcomes, extended behavioural assessment beyond 7 days post-stroke using more sophisticated testing paradigms could reveal subtle functional deficits masked by basic neurological scoring. Weekly testing using standardised tasks including ladder walking, skilled reaching, and cognitive assessment could capture delayed effects on recovery and better reflect the spectrum of post-stroke deficits seen clinically.[291] Integration of advanced physiological monitoring including continuous blood pressure recording and blood gas analysis would help maintain strict parameter control, potentially reducing outcome variability.[292] These methodological refinements would address key questions raised by my findings while strengthening their translational relevance.

6.4 Concluding remarks

In this thesis, I have made several novel observations regarding the electrophysiological properties of fasting-induced and CHA-induced torpor, as well as the latter's neuroprotective effects. First, I demonstrated that fasting-induced and CHA-induced torpor in the laboratory mouse in terms of EEG both consist predominantly of SWA similar to NREM sleep. Then I showed that post-torpor, whereas in fasting-induced torpor mice stay awake for a prolonged period (presumably in order to feed or seek food), in CHA-induced torpor mice enter sleep almost immediately post-torpor. I demonstrated that both hypothermia at 33 C and CHA were protective in neuronal cultures undergoing oxygen glucose deprivation. I then showed that combining CHA and hypothermic treatments led to additional protective effect. Finally, I observed that neither CHA-induced hypothermia nor CHA given at normothermia is protective against focal cerebral ischaemia in a rat MCAO model.

Whilst further work is needed to investigate aspects such as (1) the EEG of mice undergoing CHA-induced torpor at near normothermia and (2) the reasons why CHA was not protective *in vivo*, this thesis nonetheless highlights the potential for torpor-like states, such as that induced by CHA, to be translated into a hypothermic neuroprotective therapy in humans for clinical scenarios such as acute ischaemic stroke. Ultimately, the aim of acute stroke therapeutics is to reduce infarct size and improve both short-term and long-term clinical outcome. Although recanalisation would still be required in the vast majority of cases, simultaneously applying an effective neuroprotective therapy as early as possible could buy precious time for this to happen.

7 References

1. World Health Organization (WHO). WHO reveals leading causes of death and disability worldwide: 2000-2019. *World Heal. Organ.* (2020).

2. Feigin, V. L. *et al.* Global and regional burden of stroke during 1990–2010: findings from the Global Burden of Disease Study 2010. *Lancet* **383**, 245–255 (2014).

3. Mozaffarian, D. *et al.* Heart Disease and Stroke Statistics—2016 Update. *Circulation* **133**, (2016).

4. Hackett, M. L., Köhler, S., O'Brien, J. T. & Mead, G. E. Neuropsychiatric outcomes of stroke. *Lancet Neurol.* **13**, 525–534 (2014).

5. Iadecola, C. The Neurovascular Unit Coming of Age: A Journey through Neurovascular Coupling in Health and Disease. *Neuron* **96**, 17–42 (2017).

6. Einenkel, A. & Salameh, A. Selective vulnerability of hippocampal CA1 and CA3 pyramidal cells: What are possible pathomechanisms and should more attention be paid to the CA3 region in future studies? *J. Neurosci. Res.* **102**, (2024).

7. Thompson, S. M., Masukawa, L. M. & Prince, D. A. Temperature dependence of intrinsic membrane properties and synaptic potentials in hippocampal CA1 neurons in vitro. *J. Neurosci.* (1985) doi:10.1523/jneurosci.05-03-00817.1985.

8. Liu, L. & Yenari, M. A. Therapeutic hypothermia: Neuroprotective mechanisms. *Front. Biosci.* **12**, 816–825 (2007).

9. Soundarapandian, M. M., Tu, W. H., Peng, P. L., Zervos, A. S. & Lu, Y. AMPA Receptor Subunit GluR2 Gates Injurious Signals in Ischemic Stroke. *Mol. Neurobiol.*

32, 145–156 (2005).

10. Iadecola, C. & Anrather, J. Stroke research at a crossroad: Asking the brain for directions. *Nat. Neurosci.* **14**, 1363–1368 (2011).

11. Jin, R., Yang, G. & Li, G. Inflammatory mechanisms in ischemic stroke: role of inflammatory cells. *J. Leukoc. Biol.* **87**, 779–789 (2010).

12. Dirnagl, U., Iadecola, C. & Moskowitz, M. A. Pathobiology of ischaemic stroke: an integrated view. *Trends Neurosci.* **22**, 391–397 (1999).

13. Lipton, P. Ischemic Cell Death in Brain Neurons. *Physiol. Rev.* **79**, 1431–1568 (1999).

14. Mergenthaler, P., Dirnagl, U. & Meisel, A. Pathophysiology of Stroke: Lessons from Animal Models. *Metab. Brain Dis.* **19**, 151–167 (2004).

15. Chen, H. *et al.* Oxidative Stress in Ischemic Brain Damage: Mechanisms of Cell Death and Potential Molecular Targets for Neuroprotection. *Antioxid. Redox Signal.* **14**, 1505–1517 (2011).

16. Sims, N. R. & Muyderman, H. Mitochondria, oxidative metabolism and cell death in stroke. *Biochim. Biophys. Acta - Mol. Basis Dis.* **1802**, 80–91 (2010).

17. Rosenberg, G. A. Neurological Diseases in Relation to the Blood–Brain Barrier. *J. Cereb. Blood Flow Metab.* **32**, 1139–1151 (2012).

18. Chamorro, Á., Dirnagl, U., Urra, X. & Planas, A. M. Neuroprotection in acute stroke: Targeting excitotoxicity, oxidative and nitrosative stress, and inflammation. *Lancet Neurol.* **15**, 869–881 (2016).

19. Sandoval, K. E. & Witt, K. A. Blood-brain barrier tight junction permeability and ischemic stroke. *Neurobiol. Dis.* **32**, 200–219 (2008).

20. Murphy, M. P. How mitochondria produce reactive oxygen species. *Biochem. J.* **417**, 1–13 (2009).

21. Ayala, A., Muñoz, M. F. & Argüelles, S. Lipid Peroxidation: Production, Metabolism, and Signaling Mechanisms of Malondialdehyde and 4-Hydroxy-2-Nonenal. *Oxid. Med. Cell. Longev.* **2014**, 1–31 (2014).

22. Cooke, M. S., Evans, M. D., Dizdaroglu, M. & Lunec, J. Oxidative DNA damage: mechanisms, mutation, and disease. *FASEB J.* **17**, 1195–1214 (2003).

23. Lambertsen, K. L., Finsen, B. & Clausen, B. H. Post-stroke inflammation—target or tool for therapy? *Acta Neuropathologica* at https://doi.org/10.1007/s00401-018-1930-z (2019).

24. Barone, F. C. & Feuerstein, G. Z. Inflammatory mediators and stroke: New opportunities for novel therapeutics. *Journal of Cerebral Blood Flow and Metabolism* at https://doi.org/10.1097/00004647-199908000-00001 (1999).

25. Fisher, M. & Brott, T. G. Emerging therapies for acute ischemic stroke: New therapies on trial. *Stroke* **34**, 359–361 (2003).

26. Goyal, M. *et al.* Endovascular thrombectomy after large-vessel ischaemic stroke: A meta-analysis of individual patient data from five randomised trials. *Lancet* **387**, 1723–1731 (2016).

27. Neuhaus, A. A., Couch, Y., Hadley, G., Buchan, A. M. & Buchan, A. M. Neuroprotection in stroke: T he importance of collaboration and reproducibility. *Brain* **140**, 2079–2092 (2017).

28. Astrup, J., Siesjö, B. K. & Symon, L. Thresholds in cerebral ischemia - the ischemic penumbra. *Stroke* **12**, 723–725 (1981).

29. Del Zoppo, G. J., Sharp, F. R., Heiss, W. D. & Albers, G. W. Heterogeneity in the penumbra. *Journal of Cerebral Blood Flow and Metabolism* at https://doi.org/10.1038/jcbfm.2011.93 (2011).

30. Heiss, W.-D. *et al.* Dynamic Penumbra Demonstrated by Sequential Multitracer PET after Middle Cerebral Artery Occlusion in Cats. *J. Cereb. Blood Flow Metab.* **14**, 892–902 (1994).

31. Balami, J. S. *et al.* A Systematic Review and Meta-Analysis of Randomized Controlled Trials of Endovascular Thrombectomy Compared with Best Medical Treatment for Acute Ischemic Stroke. *Int. J. Stroke* **10**, 1168–1178 (2015).

32. Wardlaw, J. M. *et al.* Recombinant tissue plasminogen activator for acute ischaemic stroke: an updated systematic review and meta-analysis. *Lancet* **379**, 2364–2372 (2012).

33. Fisher, M. *et al.* Update of the stroke therapy academic industry roundtable preclinical recommendations. *Stroke* **40**, 2244–2250 (2009).

34. Liebeskind, D. S., Derdeyn, C. P. & Wechsler, L. R. Emerging considerations in developing and evaluating new stroke therapies. *Stroke* **49**, 2241–2247 (2018).

35. Fisher, M. Recommendations for standards regarding preclinical neuroprotective and restorative drug development. *Stroke* **30**, 2752–2758 (1999).

36. Hoyte, L., Barber, P., Buchan, A. & Hill, M. The Rise and Fall of NMDA Antagonists for Ischemic Stroke. *Curr. Mol. Med.* **4**, 131–136 (2005).

37. Gill, R., Foster, A. C. & Woodruff, G. N. MK-801 is neuroprotective in gerbils when administered during the post-ischaemic period. *Neuroscience* **25**, 847–855 (1988).

38. Buchan, A. & Pulsinelli, W. A. Hypothermia but not the N-methyl-D-aspartate antagonist, MK-801, attenuates neuronal damage in gerbils subjected to transient global

ischemia. *J. Neurosci.* **10**, 311–316 (1990).

39. Buchan, A., Li, H. & Pulsinelli, W. A. The N-methyl-D-aspartate antagonist, MK-801, fails to protect against neuronal damage caused by transient, severe forebrain ischemia in adult rats. *J. Neurosci.* **11**, 1049–1056 (1991).

40. Diemer, N. H., Jørgensen, M. B., Johansen, F. F., Sheardown, M. & Honoré, T. Protection against ischemic hippocampal CAI damage in the rat with a new non-NMDA antagonist, NBQX. *Acta Neurol. Scand.* **86**, 45–49 (1992).

41. Cook, D. J., Teves, L. & Tymianski, M. Treatment of stroke with a PSD-95 inhibitor in the gyrencephalic primate brain. *Nature* **483**, 213–217 (2012).

42. Hill, M. D. *et al.* Efficacy and safety of nerinetide for the treatment of acute ischaemic stroke (ESCAPE-NA1): a multicentre, double-blind, randomised controlled trial. *Lancet* **395**, 878–887 (2020).

43. J. Christenson, M. Hill, R. Swartz, D. Harris, A. Tkach, D. Selchen, L. Casaubon, G. Medvedev, M. Mehdiratta, Y. Perez, O. Benavente, L. Morrison, R. Verbeek, S. Cheskes, J. Tallon1, W. Dick, S. Jenneson, S. Pennington, M. Leroux, C. Harris, K. Heard, D., M. T. A randomized controlled trial of nerinetide initiated by paramedics in the field for acute stroke within three hours of symptom onset (FRONTIER trial). in *15th World Stroke Congress (WSC)* (2023).

44. Hill, M. & E.-N.T. Investigators. ESCAPE-NEXT trial (Presentation). in *15th World Stroke Congress (WSC)* (2023).

45. Shuaib, A. *et al.* NXY-059 for the treatment of acute ischemic stroke. *N. Engl. J. Med.* **357**, 562–571 (2007).

46. Tisherman, S. A., Rodriguez, A. & Safar, P. Therapeutic hypothermia in traumatology.

Surg. Clin. North Am. (1999) doi:10.1016/S0039-6109(05)70077-3.

47. Lyden, P. D., Krieger, D., Yenari, M. & Dietrich, W. D. Therapeutic hypothermia for acute stroke. *Int. J. Stroke* **1**, 9–19 (2006).

48. Kollmar, R., Blank, T., Han, J. L., Georgiadis, D. & Schwab, S. Different degrees of hypothermia after experimental stroke: Short- and long-term outcome. *Stroke* **38**, 1585–1589 (2007).

49. Dumitrascu, O. M., Lamb, J. & Lyden, P. D. Still cooling after all these years: Meta-analysis of pre-clinical trials of therapeutic hypothermia for acute ischemic stroke. *J. Cereb. Blood Flow Metab.* **36**, 1157–1164 (2016).

50. Lundbye, J., Badjatia, N., Polderman, K. H. & Lyden, P. Current Advances in the Use of Therapeutic Hypothermia. *Ther. Hypothermia Temp. Manag.* **10**, 2–5 (2020).

51. Krieger, D. W. & Yenari, M. A. Therapeutic hypothermia for acute ischemic stroke: What do laboratory studies teach us? *Stroke* at https://doi.org/10.1161/01.STR.0000126118.44249.5c (2004).

52. Hägerdal, M., Harp, J., Nilsson, L. & Siesjöu, B. K. THE EFFECT OF INDUCED HYPOTHERMIA UPON OXYGEN CONSUMPTION IN THE RAT BRAIN. *J. Neurochem.* **24**, 311–316 (1975).

53. Hallenbeck, J. M. & Frerichs, K. U. Stroke Therapy: It May be Time for an Integrated Approach. *Arch. Neurol.* (1993) doi:10.1001/archneur.1993.00540070080020.

54. Han, H. S., Qiao, Y., Karabiyikoglu, M., Giffard, R. G. & Yenari, M. A. Influence of Mild Hypothermia on Inducible Nitric Oxide Synthase Expression and Reactive Nitrogen Production in Experimental Stroke and Inflammation. *J. Neurosci.* (2002) doi:10.1523/jneurosci.22-10-03921.2002.

55. Inamasu, J. *et al.* Post-ischemic hypothermia delayed neutrophil accumulation and microglial activation following transient focal ischemia in rats. *J. Neuroimmunol.* (2000) doi:10.1016/S0165-5728(00)00211-3.

56. Zhang, Z., Sobel, R. A., Cheng, D., Steinberg, G. K. & Yenari, M. A. Mild hypothermia increases Bcl-2 protein expression following global cerebral ischemia. *Mol. Brain Res.* (2001) doi:10.1016/S0169-328X(01)00247-9.

57. Xu, L., Yenari, M. A., Steinberg, G. K. & Giffard, R. G. Mild hypothermia reduces apoptosis of mouse neurons in vitro early in the cascade. *J. Cereb. Blood Flow Metab.* (2002) doi:10.1097/00004647-200201000-00003.

58. Maier, C. M. *et al.* Optimal depth and duration of mild hypothermia in a focal model of transient cerebral ischemia: Effects on neurologic outcome, infarct size, apoptosis, and inflammation. *Stroke* (1998) doi:10.1161/01.STR.29.10.2171.

59. Dietrich, W. D., Busto, R., Halley, M. & Valdes, I. The importance of brain temperature in alterations of the blood-brain barrier following cerebral ischemia. *J. Neuropathol. Exp. Neurol.* (1990) doi:10.1097/00005072-199009000-00004.

60. Yenari, M. A. & Hemmen, T. M. Therapeutic hypothermia for brain ischemia: Where have we come and where do we go? *Stroke* **41**, 72–75 (2010).

61. Lyden, P. D. *et al.* Differential effects of hypothermia on neurovascular unit determine protective or toxic results: Toward optimized therapeutic hypothermia. *J. Cereb. Blood Flow Metab.* **39**, 1693–1709 (2019).

62. Lyden, P., Ernstrom, K. & Raman, on Behalf of the ICTuS-L Inv, R. Determinants of Pneumonia Risk During Endovascular Hypothermia. *Ther. Hypothermia Temp. Manag.* **3**, 24–27 (2013).

63. Lyden, P. *et al.* Results of the ICTuS 2 Trial (Intravascular Cooling in the Treatment of Stroke 2). *Stroke* **47**, 2888–2895 (2016).

64. Polderman, K. H. Mechanisms of action, physiological effects, and complications of hypothermia. *Crit. Care Med.* **37**, (2009).

65. Nakamura, K. Cold-defense neural pathway drives stress-induced hyperthermia. *Auton. Neurosci.* **192**, 1 (2015).

66. Bailey, I. R. *et al.* Optimization of thermolytic response to a1 adenosine receptor agonists in rats. *J. Pharmacol. Exp. Ther.* **362**, 424–430 (2017).

67. Nakamura, K. & Morrison, S. F. Central efferent pathways for cold-defensive and febrile shivering. *J. Physiol.* **589**, 3641–3658 (2011).

68. Morrison, S. F. F. & Nakamura, K. Central Mechanisms for Thermoregulation. *Annu. Rev. Physiol.* **81**, 285–308 (2019).

69. Saper, C. B. & Machado, N. L. S. News & views Flipping the switch on the thermoregulatory system.

70. Geiser, F. Evolution of daily torpor and hibernation in birds and mammals: Importance op body size. *Clin. Exp. Pharmacol. Physiol.* **25**, 736–740 (1998).

71. Jastroch, M. *et al.* Seasonal Control of Mammalian Energy Balance: Recent Advances in the Understanding of Daily Torpor and Hibernation. *J. Neuroendocrinol.* **28**, (2016).

72. Melvin, R. G. & Andrews, M. T. Torpor induction in mammals: recent discoveries fueling new ideas. *Trends Endocrinol. Metab.* **20**, 490–498 (2009).

73. Adamantidis, A. R., Gutierrez Herrera, C. & Gent, T. C. Oscillating circuitries in the sleeping brain. *Nature Reviews Neuroscience* vol. 20 746–762 at

https://doi.org/10.1038/s41583-019-0223-4 (2019).

74. Geiser, F. Metabolic Rate and Body Temperature Reduction During Hibernation and Daily Torpor. *Annu. Rev. Physiol.* **66**, 239–274 (2004).

75. Ruf, T. & Geiser, F. Daily torpor and hibernation in birds and mammals. *Biol. Rev.* **90**, 891–926 (2015).

76. Jensen, T. L., Kiersgaard, M. K., Sørensen, D. B. & Mikkelsen, L. F. Fasting of mice: A review. *Lab. Anim.* **47**, 225–240 (2013).

77. Swoap, S. J. & Gutilla, M. J. Cardiovascular changes during daily torpor in the laboratory mouse. *Am. J. Physiol. - Regul. Integr. Comp. Physiol.* **297**, R769–R774 (2009).

78. Staples, J. F. Metabolic flexibility: Hibernation, torpor, and estivation. *Compr. Physiol.* **6**, 737–771 (2016).

79. Oelkrug, R., Heldmaier, G. & Meyer, C. W. Torpor patterns, arousal rates, and temporal organization of torpor entry in wildtype and UCP1-ablated mice. *J. Comp. Physiol. B Biochem. Syst. Environ. Physiol.* **181**, 137–145 (2011).

80. Tan, C. L. & Knight, Z. A. Regulation of Body Temperature by the Nervous System. *Neuron* **98**, 31–48 (2018).

81. Haase, C. G. *et al.* Bats are not squirrels: Revisiting the cost of cooling in hibernating mammals. *J. Therm. Biol.* **81**, 185–193 (2019).

82. Hrvatin, S. *et al.* Neurons that regulate mouse torpor. *Nature* **583**, 115–121 (2020).

83. Weiss, B. & Laties, V. G. Behavioral thermoregulation: Behavior is a remarkably sensitive mechanism in the regulation of body temperature. *Science (80-.).* **133**, 1338–

1344 (1961).

84. Geiser, F. Reduction of metabolism during hibernation and daily torpor in mammals and birds: temperature effect or physiological inhibition? *J. Comp. Physiol. B* **158**, 25–37 (1988).

85. Tøien, Ø. *et al.* Hibernation in Black Bears: Independence of Metabolic Suppression from Body Temperature. *Science (80-.).* **331**, 906 LP – 909 (2011).

86. Jinka, T. R., Tøien, O. & Drew, K. L. Season primes the brain in an arctic hibernator to facilitate entrance into torpor mediated by adenosine A1 receptors. *J. Neurosci.* **31**, 10752–10758 (2011).

87. Ticho, S. R. & Radulovacki, M. Role of adenosine in sleep and temperature regulation in the preoptic area of rats. *Pharmacol. Biochem. Behav.* **40**, 33–40 (1991).

88. Anderson, R., Sheehan, M. J. & Strong, P. Characterization of the adenosine receptors mediating hypothermia in the conscious mouse. *Br. J. Pharmacol.* **113**, 1386–1390 (1994).

89. Tupone, D., Madden, C. J. & Morrison, S. F. Central Activation of the A1 Adenosine Receptor (A1AR) Induces a Hypothermic, Torpor-Like State in the Rat. *J. Neurosci.* **33**, 14512–14525 (2013).

90. Jinka, T. R., Combs, V. M. & Drew, K. L. Translating Drug-Induced Hibernation to Therapeutic Hypothermia. *ACS Chem. Neurosci.* **6**, 899–904 (2015).

91. Frare, C., Jenkins, M. E., McClure, K. M. & Drew, K. L. Seasonal decrease in thermogenesis and increase in vasoconstriction explain seasonal response to N6-cyclohexyladenosine-induced hibernation in the Arctic ground squirrel (Urocitellus parryii). *J. Neurochem.* **151**, 316–335 (2019).

92. Tupone, D., Madden, C. J. & Morrison, S. F. Central activation of the A1 adenosine receptor (A1AR) induces a hypothermic, torpor-like state in the rat. *J. Neurosci.* **33**, 14512–14525 (2013).

93. Shintani, M., Tamura, Y., Monden, M. & Shiomi, H. Characterization of N6-cyclohexyladenosine-induced hypothermia in Syrian hamsters. *J. Pharmacol. Sci.* **97**, 451–454 (2005).

94. Seebacher, F. Responses to temperature variation: Integration of thermoregulation and metabolism in vertebrates. *J. Exp. Biol.* **212**, 2885–2891 (2009).

95. Lee, C. C. Is Human Hibernation Possible? *Annu. Rev. Med.* **59**, 177–186 (2008).

96. Choukèr, A., Bereiter-Hahn, J., Singer, D. & Heldmaier, G. Hibernating astronauts—science or fiction? *Pflugers Arch. Eur. J. Physiol.* **471**, 819–828 (2019).

97. Bouma, H. R. *et al.* Induction of torpor: Mimicking natural metabolic suppression for biomedical applications. *J. Cell. Physiol.* **227**, 1285–1290 (2012).

98. Zhou, F. *et al.* Hibernation, a model of neuroprotection. *Am. J. Pathol.* **158**, 2145–2151 (2001).

99. Levy, W. J. Quantitative Analysis of EEG Changes during Hypothermia. *Anesthesiology* **60**, 291–297 (1984).

100. Callaghan, J. C., McQueen, D. A., Scott, J. W. & Bigelow, W. G. Cerebral effects of experimental hypothermia. *A.M.A Arch. Surg.* **68**, 208–215 (1954).

101. Weinstein, W., Kendig, J. H., Goldring, S., O'leary, J. L. & Lourie, H. Hypothermia and Electrical Activity of Cerebral Cortex. *Arch. Neurol.* **4**, 441–448 (1961).

102. Walker, J. M., Glotzbach, S. F., Berger, R. J. & Heller, H. C. Sleep and hibernation in

ground squirrels (Citellus spp): electrophysiological observations. *Am. J. Physiol. - Regul. Integr. Comp. Physiol.* **2**, (1977).

103. Daan, S., Barnes, B. M. & Strijkstra, A. M. Warming up for sleep? - Ground squirrels sleep during arousals from hibernation. *Neurosci. Lett.* **128**, 265–268 (1991).

104. Florant, G. L., Turner, B. M. & Heller, H. C. Temperature regulation during wakefulness, sleep, and hibernation in marmots. *Am. J. Physiol. - Regul. Integr. Comp. Physiol.* **4**, (1978).

105. Toutain, P. L. & Ruckebusch, Y. Arousal as a cyclic phenomenon during sleep and hibernation in the Hedgehog (Erinaceus europeanus). *Experientia* **31**, 312–314 (1975).

106. Blanco, M. B. *et al.* Hibernation in a primate: Does sleep occur? *R. Soc. Open Sci.* **3**, (2016).

107. Deboer, T. & Tobler, I. Sleep EEG after daily torpor in the Djungarian hamster: similarity to the effects of sleep deprivation. *Neurosci. Lett.* **166**, 35–38 (1994).

108. Vyazovskiy, V. V., Palchykova, S., Achermann, P., Tobler, I. & Deboer, T. Different Effects of Sleep Deprivation and Torpor on EEG Slow-Wave Characteristics in Djungarian Hamsters. *Cereb. Cortex* **27**, 950–961 (2017).

109. Walker, J., Garber, A., Berger, R. & Heller, H. Sleep and estivation (shallow torpor): continuous processes of energy conservation. *Science (80-.).* **204**, 1098–1100 (1979).

110. Neske, G. T. The Slow Oscillation in Cortical and Thalamic Networks: Mechanisms and Functions. *Front. Neural Circuits* **9**, (2016).

111. Vyazovskiy, V. V., Riedner, B. A., Cirelli, C. & Tononi, G. Sleep homeostasis and cortical synchronization: II. A local field potential study of sleep slow waves in the rat. *Sleep* **30**, 1631–1642 (2007).

112. Deboer, T. & Tobler, I. Temperature dependence of EEG frequencies during natural hypothermia. *Brain Res.* **670**, 153–156 (1995).

113. Franken, P., Dijk, D. J., Tobler, I. & Borbely, A. A. Sleep deprivation in rats: Effects on EEG power spectra, vigilance states, and cortical temperature. *Am. J. Physiol. - Regul. Integr. Comp. Physiol.* (1991) doi:10.1152/ajpregu.1991.261.1.r198.

114. Heller, H. C. Hibernation: neural aspects. *Annu. Rev. Physiol.* **41**, 305–321 (1979).

115. Strijkstra, A. M. & Daan, S. Dissimilarity of slow-wave activity enhancement by torpor and sleep deprivation in a hibernator. *Am. J. Physiol. - Regul. Integr. Comp. Physiol.* **275**, (1998).

116. Kilduff, T. S., Krilowicz, B., Milsom, W. K., Trachsel, L. & Wang, L. C. H. Sleep and mammalian hibernation: Homologous adaptations and homologous processes? *Sleep* **16**, 372–386 (1993).

117. Swoap, S. J., Gutilla, M. J., Liles, L. C., Smith, R. O. & Weinshenker, D. The full expression of fasting-induced torpor requires β3-adrenergic receptor signaling. *J. Neurosci.* **26**, 241–245 (2006).

118. Vicent, M. A., Borre, E. D. & Swoap, S. J. Central activation of the A1 adenosine receptor in fed mice recapitulates only some of the attributes of daily torpor. *J. Comp. Physiol. B Biochem. Syst. Environ. Physiol.* **187**, 835–845 (2017).

119. Berger, R. J. Slow wave sleep, shallow torpor and hibernation: Homologous states of diminished metabolism and body temperature. *Biol. Psychol.* **19**, 305–326 (1984).

120. Cerri, M. *et al.* Enhanced slow-wave EEG activity and thermoregulatory impairment following the inhibition of the lateral hypothalamus in the rat. *PLoS One* **9**, (2014).

121. Heller, H. C., Graf, R. & Rautenberg, W. Circadian and arousal state influences on

thermoregulation in the pigeon. *Am. J. Physiol. - Regul. Integr. Comp. Physiol.* **14**, (1983).

122. Lo Martire, V. *et al.* The physiological signature of daily torpor is not orexin dependent. *J. Comp. Physiol. B Biochem. Syst. Environ. Physiol.* (2020) doi:10.1007/s00360-020-01281-6.

123. Hudson, J. W. & Scott, I. M. Daily Torpor in the Laboratory Mouse, Mus musculus Var. Albino. *Physiol. Zool.* **52**, 205–218 (1979).

124. Guillaumin, M. C. C. *et al.* Cortical region-specific sleep homeostasis in mice: Effects of time of day and waking experience. *Sleep* (2018) doi:10.1093/sleep/zsy079.

125. Fisher, S. P. *et al.* Stereotypic wheel running decreases cortical activity in mice. *Nat. Commun.* **7**, (2016).

126. Northeast, R. C. *et al.* Sleep homeostasis during daytime food entrainment in mice. *Sleep* **42**, 1–13 (2019).

127. van der Vinne, V. *et al.* Continuous and non-invasive thermography of mouse skin accurately describes core body temperature patterns, but not absolute core temperature. *Sci. Rep.* (2020) doi:10.1038/s41598-020-77786-5.

128. Baud, M. O., Magistretti, P. J. & Petit, J. M. Sustained sleep fragmentation affects brain temperature, food intake and glucose tolerance in mice. *J. Sleep Res.* (2013) doi:10.1111/j.1365-2869.2012.01029.x.

129. Deboer, T., Franken, P. & Tobler, L. Sleep and cortical temperature in the Djungarian hamster under baseline conditions and after sleep deprivation. *J. Comp. Physiol. A* (1994) doi:10.1007/BF00193782.

130. Vyazovskiy, V. V. *et al.* Sleep EEG in mice that are deficient in the potassium channel

subunit K.v.3.2. *Brain Res.* **947**, 204–211 (2002).

131. Deboer, T. & Tobler, I. Natural hypothermia and sleep deprivation: Common effects on recovery sleep in the Djungarian hamster. *Am. J. Physiol. - Regul. Integr. Comp. Physiol.* **271**, (1996).

132. Deboer, T. Electroencephalogram theta frequency changes in parallel with euthermic brain temperature. *Brain Res.* **930**, 212–215 (2002).

133. Tobler, I., Deboer, T. & Fischer, M. Sleep and sleep regulation in normal and prion protein-deficient mice. *J. Neurosci.* (1997) doi:10.1523/jneurosci.17-05-01869.1997.

134. Hoekstra, M. M. B., Emmenegger, Y., Hubbard, J. & Franken, P. Cold-inducible RNA-binding protein (CIRBP) adjusts clock-gene expression and REM-sleep recovery following sleep deprivation. *Elife* (2019) doi:10.7554/eLife.43400.

135. Graf, R., Heller, H. C., Sakaguchi, S. & Krishna, S. Influence of spinal and hypothalamic warming on metabolism and sleep in pigeons. *Am. J. Physiol. - Regul. Integr. Comp. Physiol.* **252**, (1987).

136. Buck, C. L. & Barnes, B. M. Effects of ambient temperature on metabolic rate, respiratory quotient, and torpor in an arctic hibernator. *Am. J. Physiol. Integr. Comp. Physiol.* **279**, R255–R262 (2000).

137. Hudson, J. W. & Scott, I. M. Daily Torpor in the Laboratory Mouse , Mus musculus Var . Albino Author (s): Jack W . Hudson and Irena M . Scott Published by : The University of Chica. **52**, 205–218 (2016).

138. Peretti, D. *et al.* RBM3 mediates structural plasticity and protective effects of cooling in neurodegeneration. *Nature* **518**, 236–239 (2015).

139. Barnes, B. M. Freeze avoidance in a mammal: Body temperatures below 0°C in an arctic

hibernator. *Science (80-.).* (1989) doi:10.1126/science.2740905.

140. Krilowicz, B. L., Edgar, D. M. & Craig Heller, H. Action potential duration increases as body temperature decreases during hibernation. *Brain Res.* (1989) doi:10.1016/0006-8993(89)90400-9.

141. Buzatu, S. The temperature-induced changes in membrane potential. *Riv. di Biol. - Biol. Forum* (2009) doi:10.1400/122127.

142. Chanaday, N. L. & Kavalali, E. T. Time course and temperature dependence of synaptic vesicle endocytosis. *FEBS Letters* at https://doi.org/10.1002/1873-3468.13268 (2018).

143. Popov, V. I., Bocharova, L. S. & Bragin, A. G. Repeated changes of dendritic morphology in the hippocampus of ground squirrels in the course of hibernation. *Neuroscience* **48**, 45–51 (1992).

144. Von Der Ohe, C. G., Darian-Smith, C., Garner, C. C. & Heller, H. C. Ubiquitous and temperature-dependent neural plasticity in hibernators. *J. Neurosci.* **26**, 10590–10598 (2006).

145. Von Der Ohe, C. G., Garner, C. C., Darian-Smith, C. & Heller, H. C. Synaptic protein dynamics in hibernation. *J. Neurosci.* **27**, 84–92 (2007).

146. Sheroziya, M. & Timofeev, I. Moderate cortical cooling eliminates thalamocortical silent states during slow oscillation. *J. Neurosci.* (2015) doi:10.1523/JNEUROSCI.1359-15.2015.

147. Reig, R., Mattia, M., Compte, A., Belmonte, C. & Sanchez-Vives, M. V. Temperature modulation of slow and fast cortical rhythms. *J. Neurophysiol.* (2010) doi:10.1152/jn.00890.2009.

148. Drew, K. L. *et al.* Central nervous system regulation of mammalian hibernation:

Implications for metabolic suppression and ischemia tolerance. *J. Neurochem.* **102**, 1713–1726 (2007).

149. Okamoto-Mizuno, K. & Mizuno, K. Effects of thermal environment on sleep and circadian rhythm. *Journal of Physiological Anthropology* vol. 31 1–9 at https://doi.org/10.1186/1880-6805-31-14 (2012).

150. Harding, E. C., Franks, N. P. & Wisden, W. The temperature dependence of sleep. *Front. Neurosci.* **13**, 1–16 (2019).

151. Amici, R. *et al.* Cold exposure and sleep in the rat: REM sleep homeostasis and body size. *Sleep* **31**, 708–715 (2008).

152. Szymusiak, R. & Satinoff, E. Maximal REM sleep time defines a narrower thermoneutral zone than does minimal metabolic rate. *Physiol. Behav.* (1981) doi:10.1016/0031-9384(81)90145-1.

153. Parmeggiani, P. L. Rem sleep related increase in brain temperature: A physiologic problem. *Arch. Ital. Biol.* (2007) doi:10.4449/aib.v145i1.863.

154. Cerri, M., Luppi, M., Tupone, D., Zamboni, G. & Amici, R. REM sleep and endothermy: Potential sites and mechanism of a reciprocal interference. *Front. Physiol.* **8**, 1–7 (2017).

155. Komagata, N. *et al.* Dynamic REM Sleep Modulation by Ambient Temperature and the Critical Role of the Melanin-Concentrating Hormone System. *Curr. Biol.* **29**, 1976-1987.e4 (2019).

156. Lockie, S. H., McAuley, C. V., Rawlinson, S., Guiney, N. & Andrews, Z. B. Food seeking in a risky environment: A method for evaluating risk and reward value in food seeking and consumption in mice. *Front. Neurosci.* (2017) doi:10.3389/fnins.2017.00024.

157. Brown, J. C. L. & Staples, J. F. Mitochondrial metabolism during fasting-induced daily torpor in mice. *Biochim. Biophys. Acta - Bioenerg.* **1797**, 476–486 (2010).

158. Van Der Vinne, V., Bingaman, M. J., Weaver, D. R. & Swoap, S. J. Clocks and meals keep mice from being cool. *J. Exp. Biol.* (2018) doi:10.1242/jeb.179812.

159. Northeast, R. C., Vyazovskiy, V. V. & Bechtold, D. A. Eat, sleep, repeat: the role of the circadian system in balancing sleep–wake control with metabolic need. *Current Opinion in Physiology* at https://doi.org/10.1016/j.cophys.2020.02.003 (2020).

160. Walker, J. M., Haskell, E. H., Berger, R. J. & Heller, H. C. Hibernation at moderate temperatures: a continuation of slow wave sleep. *Experientia* **37**, 726–728 (1981).

161. Heldmaier, G., Ortmann, S. & Elvert, R. Natural hypometabolism during hibernation and daily torpor in mammals. *Respir. Physiol. Neurobiol.* **141**, 317–329 (2004).

162. Takahashi M., T. *et al.* A discrete neuronal circuit induces a hibernation-like state in rodents. *Nature* (2020) doi:10.1038/s41586-020-2163-6.

163. Reinertsen, R. E. & Haftorn, S. Different metabolic strategies of northern birds for nocturnal survival. *J. Comp. Physiol. B* (1986) doi:10.1007/BF00692743.

164. Porkka-Heiskanen, T. *et al.* Adenosine: A Mediator of the Sleep-Inducing Effects of Prolonged Wakefulness. *Science (80-.).* **276**, 1265–1268 (1997).

165. Huber, R., Deboer, T. & Tobler, I. Topography of EEG dynamics after sleep deprivation in mice. *J. Neurophysiol.* **84**, 1888–1893 (2000).

166. Scammell, T. E., Arrigoni, E. & Lipton, J. O. Neural Circuitry of Wakefulness and Sleep. *Neuron* **93**, 747–765 (2017).

167. Trachsel, L., Edgar, D. M. & Heller, H. C. Are ground squirrels sleep deprived during

hibernation? *Am. J. Physiol. - Regul. Integr. Comp. Physiol.* **260**, R1123–R1129 (1991).

168. Deboer, T. & Tobler, I. Slow waves in the sleep electroencephalogram after daily torpor are homeostatically regulated. *Neuroreport* **11**, 881–885 (2000).

169. Larkin, J. E. & Heller, H. C. Sleep after arousal from hibernation is not homeostatically regulated. *Am. J. Physiol. - Regul. Integr. Comp. Physiol.* **276**, 522–529 (1999).

170. Lo Martire, V. *et al.* Changes in blood glucose as a function of body temperature in laboratory mice: implications for daily torpor. *Am. J. Physiol. - Endocrinol. Metab.* **315**, E662–E670 (2018).

171. Lazarus, M., Oishi, Y., Bjorness, T. E. & Greene, R. W. Gating and the need for sleep: Dissociable effects of adenosine a1and a2areceptors. *Frontiers in Neuroscience* vol. 13 at https://doi.org/10.3389/fnins.2019.00740 (2019).

172. Basheer, R., Strecker, R. E., Thakkar, M. M., others & McCarley, R. W. Adenosine and Sleep--Wake Regulation. *Prog Neurobiol* **73**, 379–396 (2004).

173. Deboer, T. Brain temperature dependent changes in the electroencephalogram power spectrum of humans and animals. *J. Sleep Res.* **7**, 254–262 (1998).

174. Larkin, J. E. & Heller, H. C. Temperature sensitivity of sleep homeostasis during hibernation in the golden-mantled ground squirrel. *Am. J. Physiol. - Regul. Integr. Comp. Physiol.* **270**, (1996).

175. Krilowicz, B. L., Glotzbach, S. F. & Heller, H. C. Neuronal activity during sleep and complete bouts of hibernation. *Am. J. Physiol. - Regul. Integr. Comp. Physiol.* **255**, (1988).

176. Vyazovskiy, V. V. *et al.* Local sleep in awake rats. *Nature* (2011) doi:10.1038/nature10009.

177. Yarbrough, G. G. & McGuffin-Clineschmidt, J. C. In vivo bahavioral assessment of central nervous system purinergic receptors. *Eur. J. Pharmacol.* **76**, 137–144 (1981).

178. Carney, J. M., Wu Cao, Logan, L., Rennert, O. M. & Seale, T. W. Differential antagonism of the behavioral depressant and hypothermic effects of 5′-(N-ethylcarboxamide) adenosine by theobromine. *Pharmacol. Biochem. Behav.* **25**, 769–773 (1986).

179. Zarrindast, M. R. & Heidari, M. R. Involvement of adenosine receptors in mouse thermoregulation. *J. Psychopharmacol.* **7**, 365–370 (1993).

180. Carlin, J. L. *et al.* Hypothermia in mouse is caused by adenosine A1 and A3 receptor agonists and AMP via three distinct mechanisms. *Neuropharmacology* **114**, 101–113 (2017).

181. Carlin, J. L. *et al.* Activation of adenosine A 2A or A 2B receptors causes hypothermia in mice. *Neuropharmacology* **139**, 268–278 (2018).

182. Sheth, S. *et al.* Adenosine Receptors: Expression, Function and Regulation. *Int J Mol Sci* **15**, 2024–2052 (2014).

183. Swanson, T. H., Drazba, J. A. & Rivkees, S. A. Adenosine A1 receptors are located predominantly on axons in the rat hippocampal formation. *J. Comp. Neurol.* **363**, 517–531 (1995).

184. Tupone, D., Madden, C. J. & Morrison, S. F. Highlights in basic autonomic neurosciences: Central adenosine A1 receptor - The key to a hypometabolic state and therapeutic hypothermia? *Auton. Neurosci. Basic Clin.* **176**, 1–2 (2013).

185. Iliff, B. W. & Swoap, S. J. Central adenosine receptor signaling is necessary for daily torpor in mice. *Am. J. Physiol. - Regul. Integr. Comp. Physiol.* **303**, R477–R484 (2012).

186. Laughlin, B. W. *et al.* Precise control of target temperature using N6-cyclohexyladenosine and real-time control of surface temperature. *Ther. Hypothermia Temp. Manag.* **8**, 108–116 (2018).

187. Swoap, S. J., Rathvon, M. & Gutilla, M. AMP does not induce torpor. *Am. J. Physiol. - Regul. Integr. Comp. Physiol.* **293**, R468–R473 (2007).

188. Barros, R. C. H., Branco, L. G. S. & Cárnio, E. C. Respiratory and body temperature modulation by adenosine A1 receptors in the anteroventral preoptic region during normoxia and hypoxia. *Respir. Physiol. Neurobiol.* **153**, 115–125 (2006).

189. Tuovinen, K. & Tarhanen, J. Clearance of cyclopentyladenosine and cyclohexyladenosine in rats following a single subcutaneous dose. *Pharmacol. Res.* **50**, 329–334 (2004).

190. Huang, Y., Flaherty, S., Peirson, S. & Vyazovskiy, V. The relationship between fasting-induced torpor, sleep and wakefulness in laboratory mice. *Sleep Med.* **64**, S162 (2019).

191. Ciccarelli, R. *et al.* Molecular signalling mediating the protective effect of A1 adenosine and mGlu3 metabotropic glutamate receptor activation against apoptosis by oxygen/glucose deprivation in cultured astrocytes. *Mol. Pharmacol.* **71**, 1369–1380 (2007).

192. Huang, Y. G. *et al.* The relationship between fasting-induced torpor, sleep, and wakefulness in laboratory mice. *Sleep* **44**, 1–16 (2021).

193. Staples, J. F. Metabolic suppression in mammalian hibernation: The role of mitochondria. *J. Exp. Biol.* **217**, 2032–2036 (2014).

194. Morrison, S. F. & Nakamura, K. Central neural pathways for thermoregulation. *Front. Biosci.* **16**, 74–104 (2011).

195. Morrison, S. F. & Blessing, W. W. *Central Nervous System Regulation of Body Temperature*. *Central Regulation of Autonomic Functions* vol. 15 (2011).

196. Busto, R. *et al.* Small differences in intraischemic brain temperature critically determine the extent of ischemic neuronal injury. *J. Cereb. Blood Flow Metab.* **7**, 729–738 (1987).

197. Brown, J. C. L. & Staples, J. F. Mitochondrial metabolic suppression in fasting and daily torpor: Consequences for reactive oxygen species production. *Physiol. Biochem. Zool.* **84**, 467–480 (2011).

198. Winfree, C. J., Baker, C. J., Connolly, E. S., Fiore, A. J. & Solomon, R. A. Mild Hypothermia Reduces Penumbral Glutamate Levels in the Rat Permanent Focal Cerebral Ischemia Model. *Neurosurgery* (1996) doi:10.1227/00006123-199606000-00034.

199. Globus, M. Y. -., Alonso, O., Dietrich, W. D., Busto, R. & Ginsberg, M. D. Glutamate Release and Free Radical Production Following Brain Injury: Effects of Posttraumatic Hypothermia. *J. Neurochem.* (1995) doi:10.1046/j.1471-4159.1995.65041704.x.

200. Globus, M. Y. -., Busto, R., Lin, B., Schnippering, H. & Ginsberg, M. D. Detection of Free Radical Activity During Transient Global Ischemia and Recirculation: Effects of Intraischemic Brain Temperature Modulation. *J. Neurochem.* (1995) doi:10.1046/j.1471-4159.1995.65031250.x.

201. Kimura, A., Sakurada, S., Ohkuni, H., Todome, Y. & Kurata, K. Moderate hypothermia delays proinflammatory cytokine production of human peripheral blood mononuclear cells. *Crit. Care Med.* (2002) doi:10.1097/00003246-200207000-00017.

202. Goldberg, M. P., Monyer, H., Weiss, J. H. & Choi, D. W. Adenosine reduces cortical neuronal injury induced by oxygen or glucose deprivation in vitro. *Neurosci. Lett.* **89**,

323–327 (1988).

203. Gaudin, A. *et al.* Squalenoyl adenosine nanoparticles provide neuroprotection after stroke and spinal cord injury. *Nat. Nanotechnol.* **9**, 1054–1062 (2014).

204. Kitagawa, H., Mori, A., Shimada, J., Mitsumoto, Y. & Kikuchi, T. Intracerebral adenosine infusion improves neurological outcome after transient focal ischemia in rats. *Neurol. Res.* **24**, 317–323 (2002).

205. von Lubitz, D. K. J. E. & Marangos, P. J. Cerebral ischemia in gerbils: Postischemic administration of cyclohexyl adenosine and 8-sulfophenyl-theophylline. *J. Mol. Neurosci.* **2**, 53–59 (1990).

206. Choi, D. W. Possible mechanisms limiting N-methyl-D-aspartate receptor overactivation and the therapeutic efficacy of N-methyl-D-aspartate antagonists. in *Stroke* (1990).

207. Dunwiddie, T. V. Interactions between the effects of adenosine and calcium on synaptic responses in rat hippocampus in vitro. *J. Physiol.* (1984) doi:10.1113/jphysiol.1984.sp015217.

208. Olsson, R. A. Adenosine receptors in the cardiovascular system. in *Drug Development Research* (1996). doi:10.1002/(SICI)1098-2299(199611/12)39:3/4<301::AID-DDR9>3.0.CO;2-V.

209. Tawfik, H. E., Teng, B., Morrison, R. R., Schnermann, J. & Mustafa, S. J. Role of A1 adenosine receptor in the regulation of coronary flow. *Am. J. Physiol. - Hear. Circ. Physiol.* (2006) doi:10.1152/ajpheart.01319.2005.

210. Evans, M. C., Swan, J. H. & Meldrum, B. S. An adenosine analogue, 2-chloroadenosine, protects against long term development of ischaemic cell loss in the rat hippocampus.

Neurosci. Lett. **83**, 287–292 (1987).

211. Von Lubitz, D. K. J. E. *et al.* Chronic administration of selective adenosine A1 receptor agonist or antagonist in cerebral ischemia. *Eur. J. Pharmacol.* **256**, 161–167 (1994).

212. Liu, C.-W. *et al.* Hypothermia but not NMDA receptor antagonism protects against stroke induced by distal middle cerebral arterial occlusion in mice. *PLoS One* **15**, e0229499 (2020).

213. Canale, C. I. & Henry, P. Y. Energetic costs of the immune response and torpor use in a primate. *Funct. Ecol.* **25**, 557–565 (2011).

214. Bouma, H. R., Carey, H. V. & Kroese, F. G. M. Hibernation: the immune system at rest? *J. Leukoc. Biol.* **88**, 619–624 (2010).

215. Zhang, Z. huan *et al.* Circ-camk4 involved in cerebral ischemia/reperfusion induced neuronal injury. *Sci. Rep.* (2020) doi:10.1038/s41598-020-63686-1.

216. Xin, L., Junhua, W., Long, L., Jun, Y. & Xiaosu, Y. Exogenous hydrogen sulfide protects SH-SY5Y cells from OGD/R-induced injury. *Curr. Mol. Med.* (2018) doi:10.2174/1566524018666180222121643.

217. Huang, C., Zhou, H., Ren, X. & Teng, J. Inhibition of JAK1 by microRNA-708 promotes SH-SY5Y neuronal cell survival after oxygen and glucose deprivation and reoxygenation. *Neurosci. Lett.* (2018) doi:10.1016/j.neulet.2017.11.017.

218. Ruan, L. *et al.* Activation of Adenosine A1 Receptor in Ischemic Stroke: Neuroprotection by Tetrahydroxy Stilbene Glycoside as an Agonist. *Antioxidants* **10**, 1112 (2021).

219. Canals, M. *et al.* Molecular mechanisms involved in the adenosine A 1 and A 2A receptor-induced neuronal differentiation in neuroblastoma cells and striatal primary

cultures. *J. Neurochem.* **92**, 337–348 (2005).

220. Muñoz-López, S., Sánchez-Melgar, A., Martín, M. & Albasanz, J. L. Resveratrol enhances A1 and hinders A2A adenosine receptors signaling in both HeLa and SH-SY5Y cells: Potential mechanism of its antitumoral action. *Front. Endocrinol. (Lausanne).* **13**, (2022).

221. Clark, D. L., Penner, M., Orellana-Jordan, I. M. & Colbourne, F. Comparison of 12, 24 and 48 h of systemic hypothermia on outcome after permanent focal ischemia in rat. *Exp. Neurol.* **212**, 386–392 (2008).

222. Daval, J. L. & Nicolas, F. Opposite effects of cyclohexyladenosine and theophylline on hypoxic damage in cultured neurons. *Neurosci. Lett.* **175**, 114–116 (1994).

223. Xie, K. Q., Zhang, L. M., Cao, Y., Zhu, J. & Feng, L. Y. Adenosine A 1 receptor-mediated transactivation of the EGF receptor produces a neuroprotective effect on cortical neurons in vitro. *Acta Pharmacol. Sin.* **30**, 889–898 (2009).

224. Logan, M. & Sweeney, M. I. Adenosine A1 receptor activation preferentially protects cultured cerebellar neurons versus astrocytes against hypoxia-induced death. *Mol. Chem. Neuropathol.* **31**, 119–133 (1997).

225. Oyama, Y., Ono, K. & Kawamura, M. Mild hypothermia protects synaptic transmission from experimental ischemia through reduction in the function of nucleoside transporters in the mouse hippocampus. *Neuropharmacology* **163**, 107853 (2020).

226. Torlinska, T. *et al.* Effect of hypothermia on insulin-receptor interaction in different rat tissues. *Physiol. Res.* (2002).

227. Roelandse, M. & Matus, A. Hypothermia-associated loss of dendritic spines. *J. Neurosci.* **24**, 7843–7847 (2004).

228. León-Espinosa, G., Antón-Fernández, A., Tapia-González, S., DeFelipe, J. & Muñoz, A. Modifications of the axon initial segment during the hibernation of the Syrian hamster. *Brain Struct. Funct.* **223**, 4307–4321 (2018).

229. Popov, V. I. & Bocharova, L. S. Hibernation-induced structural changes in synaptic contacts between mossy fibres and hippocampal pyramidal neurons. *Neuroscience* **48**, 53–62 (1992).

230. Zhu, X., Bührer, C. & Wellmann, S. Cold-inducible proteins CIRP and RBM3, a unique couple with activities far beyond the cold. *Cell. Mol. Life Sci.* **73**, 3839–3859 (2016).

231. Jackson, T. C. & Kochanek, P. M. A New Vision for Therapeutic Hypothermia in the Era of Targeted Temperature Management: A Speculative Synthesis. *Ther. Hypothermia Temp. Manag.* **9**, 13–47 (2019).

232. Liu, A., Li, S., Jiao, Y., Kong, H. & Zhang, Z. Overexpressed cold inducible RNA-binding protein improves cell viability and EGF expression in glial cells. *BMC Mol. Cell Biol.* (2022) doi:10.1186/s12860-022-00460-3.

233. Wu, L. *et al.* Therapeutic Hypothermia Enhances Cold-Inducible RNA-Binding Protein Expression and Inhibits Mitochondrial Apoptosis in a Rat Model of Cardiac Arrest. *Mol. Neurobiol.* (2017) doi:10.1007/s12035-016-9813-6.

234. Wang, G. *et al.* Neuroprotective effects of cold-inducible RNA-binding protein during mild hypothermia on traumatic brain injury. *Neural Regen. Res.* (2016) doi:10.4103/1673-5374.182704.

235. Schmitt, K. R. L., Rosenthal, L. M., Berger, F. & Tong, G. Hypothermia after hypoxia is neuroprotective possibly via upregulation of cold shock proteins RBM3 and CIRP. *Cardiol. Young* (2012).

236. Daré, E., Schulte, G., Karovic, O., Hammarberg, C. & Fredholm, B. B. Modulation of glial cell functions by adenosine receptors. *Physiol. Behav.* **92**, 15–20 (2007).

237. Haselkorn, M. L. *et al.* Adenosine A 1 Receptor Activation as a Brake on the Microglial Response after Experimental Traumatic Brain Injury in Mice. *J. Neurotrauma* **27**, 901–910 (2010).

238. Liu, G. *et al.* Adenosine binds predominantly to adenosine receptor A1 subtype in astrocytes and mediates an immunosuppressive effect. *Brain Res.* **1700**, 47–55 (2018).

239. Björklund, O., Shang, M., Tonazzini, I., Daré, E. & Fredholm, B. B. Adenosine A1 and A3 receptors protect astrocytes from hypoxic damage. *Eur. J. Pharmacol.* **596**, 6–13 (2008).

240. Parkinson, F. E., Sinclair, C. J. D., Othman, T., Haughey, N. J. & Geiger, J. D. Differences between rat primary cortical neurons and astrocytes in purine release evoked by ischemic conditions. *Neuropharmacology* **43**, 836–846 (2002).

241. Parkinson, F. E., Xiong, W. & Zamzow, C. R. Astrocytes and neurons: Different roles in regulating adenosine levels. *Neurol. Res.* **27**, 153–160 (2005).

242. Bynoe, M. S., Viret, C., Yan, A. & Kim, D.-G. Adenosine receptor signaling: a key to opening the blood–brain door. *Fluids Barriers CNS* **12**, 20 (2015).

243. Van Der Worp, H. B. *et al.* Hypothermia in animal models of acute ischaemic stroke: A systematic review and meta-analysis. *Brain* **130**, 3063–3074 (2007).

244. Shankaran, S. *et al.* Whole-Body Hypothermia for Neonates with Hypoxic–Ischemic Encephalopathy. *N. Engl. J. Med.* **353**, 1574–1584 (2005).

245. Tahir, R. A. & Pabaney, A. H. Therapeutic hypothermia and ischemic stroke: A literature review. *Surg. Neurol. Int.* **7**, S381–S386 (2016).

246. Hirsch, K. G. & Callaway, C. W. Translating Protective Hypothermia During Cardiac Arrest Into Clinical Practice. *Jama* **321**, 1673–1675 (2019).

247. Van Der Worp, H. B. *et al.* Therapeutic hypothermia for acute ischaemic stroke. Results of a European multicentre, randomised, phase III clinical trial. *Eur. Stroke J.* **4**, 254–262 (2019).

248. Warner, D. S. Lack of effect of induction of hypothermia after acute brain injury. *J. Neurosurg. Anesthesiol.* **13**, 343–344 (2001).

249. Schwab, S., Schwarz, S., Aschoff, A., Keller, E. & Hacke, W. Moderate Hypothermia and Brain Temperature in Patients with Severe Middle Cerebral Artery Infarction. *Acta Neurochir. Suppl.* **1998**, 131–134 (1998).

250. Geurts, M., Macleod, M. R., Kollmar, R., Kremer, P. H. C. & Van Der Worp, H. B. Therapeutic hypothermia and the risk of infection: A systematic review and meta-analysis. *Crit. Care Med.* **42**, 231–242 (2014).

251. Kuczynski, A. M. *et al.* Therapeutic Hypothermia in Acute Ischemic Stroke—a Systematic Review and Meta-Analysis. *Current Neurology and Neuroscience Reports* at https://doi.org/10.1007/s11910-020-01029-3 (2020).

252. Geurts, M., Macleod, M. R., Kollmar, R., Kremer, P. H. C. & Van Der Worp, H. B. Therapeutic hypothermia and the risk of infection: A systematic review and meta-analysis. *Critical Care Medicine* at https://doi.org/10.1097/CCM.0b013e3182a276e8 (2014).

253. Liddle, L. J. *et al.* Targeting focal ischemic and hemorrhagic stroke neuroprotection: Current prospects for local hypothermia. *J. Neurochem.* **160**, 128–144 (2022).

254. Huber, C., Huber, M. & Ding, Y. Evidence and opportunities of hypothermia in acute

ischemic stroke: Clinical trials of systemic versus selective hypothermia. *Brain Circ.* **5**, 195 (2019).

255. Song, S. S. & Lyden, P. D. Overview of therapeutic hypothermia. *Curr. Treat. Options Neurol.* **14**, 541–548 (2012).

256. Keller, E. *et al.* Theoretical evaluations of therapeutic systemic and local cerebral hypothermia. *J. Neurosci. Methods* **178**, 345–349 (2009).

257. Sun, Y. J., Zhang, Z. Y., Fan, B. & Li, G. Y. Neuroprotection by therapeutic hypothermia. *Front. Neurosci.* **13**, 1–11 (2019).

258. Liu, K., Khan, H., Geng, X., Zhang, J. & Ding, Y. Pharmacological hypothermia: A potential for future stroke therapy? *Neurol. Res.* **38**, 478–490 (2016).

259. Broadley, K. J., Broome, S. & Paton, D. M. Hypothermia-induced supersensitivity to adenosine for responses mediated via A1receptors but not A2-receptors. *Br. J. Pharmacol.* **84**, 407–415 (1985).

260. Melani, A., Pugliese, A. M. & Pedata, F. Adenosine receptors in cerebral ischemia. *Int. Rev. Neurobiol.* **119**, 309–348 (2014).

261. Reinhard, J. F., Galloway, M. P. & Roth, R. H. Noradrenergic modulation of serotonin synthesis and metabolism. II. Stimulation by 3-isobutyl-1-methylxanthine. *J. Pharmacol. Exp. Ther.* **226**, 764–769 (1983).

262. Rudolphi, K. A., Schubert, P., Parkinson, F. E. & Fredholm, B. B. Neuroprotective role of adenosine in cerebral ischaemia. *Trends in Pharmacological Sciences* vol. 13 439–445 at https://doi.org/10.1016/0165-6147(92)90141-R (1992).

263. Shefner, S. A. & Chiu, T. H. Adenosine inhibits locus coeruleus neurons: an intracellular study in a rat brain slice preparation. *Brain Res.* **366**, 364–368 (1986).

264. Williams-Karnesky, R. & Stenzel-Poore, M. Adenosine and Stroke: Maximizing the Therapeutic Potential of Adenosine as a Prophylactic and Acute Neuroprotectant. *Curr. Neuropharmacol.* **7**, 217–227 (2009).

265. Martire, A. *et al.* Neuroprotective potential of adenosine A 1 receptor partial agonists in experimental models of cerebral ischemia. *J. Neurochem.* **149**, 211–230 (2019).

266. Cantor, S. L., Zornow, M. H., Miller, L. P. & Yaksh, T. L. The Effect of Cyclohexyladenosine on the Penischemic Increases of Hippocampal Glutamate and Glycine in the Rabbit. *J. Neurochem.* **59**, 1884–1892 (1992).

267. Daval, J. L., Von Lubitz, D. K. J. E., Deckert, J., Redmond, D. J. & Marangos, P. J. Protective effect of cyclohexyladenosine on adenosine A1-receptors, guanine nucleotide and forskolin binding sites following transient brain ischemia: a quantitative autoradiographic study. *Brain Res.* **491**, 212–226 (1989).

268. Zhou, J. G., Meno, J. R., Hsu, S. S. F. & Winn, H. R. Effects of theophylline and cyclohexyladenosine on brain injury following normo- and hyperglycemic ischemia: A histopathologic study in the rat. *J. Cereb. Blood Flow Metab.* **14**, 166–173 (1994).

269. Liston, T. E. *et al.* Adenosine A1R/A3R (Adenosine A1 and A3 Receptor) Agonist AST-004 Reduces Brain Infarction in a Nonhuman Primate Model of Stroke. *Stroke* **53**, 238–248 (2022).

270. Kent, T. A. & Mandava, P. Embracing Biological and Methodological Variance in a New Approach to Pre-Clinical Stroke Testing. *Transl. Stroke Res.* **7**, 274–283 (2016).

271. Yanamoto, H. *et al.* Prolonged mild hypothermia therapy protects the brain against permanent focal ischemia. *Stroke* **32**, 232–239 (2001).

272. Liddle, L. J. *et al. Infusion of Cold Saline into the Carotid Artery Does Not Affect*

Outcome after Intrastriatal Hemorrhage. *Therapeutic Hypothermia and Temperature Management* vol. 10 (Ther Hypothermia Temp Manag, 2020).

273. Longa, E. Z., Weinstein, P. R., Carlson, S. & Cummins, R. Reversible middle cerebral artery occlusion without craniectomy in rats. *Stroke* **20**, 84–91 (1989).

274. Colbourne, F., Sutherland, G. R. & Auer, R. N. An automated system for regulating brain temperature in awake and freely moving rodents. *J. Neurosci. Methods* **67**, 185–190 (1996).

275. Wan, Y. H., Nie, C., Wang, H. L. & Huang, C. Y. Therapeutic hypothermia (different depths, durations, and rewarming speeds) for acute ischemic stroke: A meta-analysis. *J. Stroke Cerebrovasc. Dis.* **23**, 2736–2747 (2014).

276. Colbourne, F., Li, H. & Buchan, A. M. Indefatigable CA1 sector neuroprotection with mild hypothermia induced 6 hours after severe forebrain ischemia in rats. *J. Cereb. Blood Flow Metab.* **19**, 742–749 (1999).

277. Clark, D. L., Penner, M., Wowk, S., Orellana-Jordan, I. & Colbourne, F. Treatments (12 and 48 h) with systemic and brain-selective hypothermia techniques after permanent focal cerebral ischemia in rat. *Exp. Neurol.* **220**, 391–399 (2009).

278. MacLellan, C. L. *et al.* Gauging recovery after hemorrhagic stroke in rats: Implications for cytoprotection studies. *J. Cereb. Blood Flow Metab.* **26**, 1031–1042 (2006).

279. MacLellan, C. L., Clark, D. L., Silasi, G. & Colbourne, F. Use of prolonged hypothermia to treat ischemic and hemorrhagic stroke. *J. Neurotrauma* **26**, 313–323 (2009).

280. Plahta, W. C., Clark, D. L. & Colbourne, F. 17β-estradiol pretreatment reduces CA1 sector cell death and the spontaneous hyperthermia that follows forebrain ischemia in the gerbil. *Neuroscience* **129**, 187–193 (2004).

281. Sessler, D. I. Complications and treatment of mild hypothermia. *Anesthesiology* **95**, 531–543 (2001).

282. Sessler, D. I. Defeating normal thermoregulatory defenses: Induction of therapeutic hypothermia. *Stroke* **40**, 11 (2009).

283. Latini, S. & Pedata, F. Adenosine in the central nervous system: Release mechanisms and extracellular concentrations. *J. Neurochem.* **79**, 463–484 (2001).

284. Morrison, S. F. Central neural control of thermoregulation and brown adipose tissue. *Autonomic Neuroscience: Basic and Clinical* at https://doi.org/10.1016/j.autneu.2016.02.010 (2016).

285. Fu, K. *et al.* Torpor-like Hypothermia Induced by A1 Adenosine Receptor Agonist: A Novel Approach to Protect against Neuroinflammation. *Int. J. Mol. Sci.* (2023) doi:10.3390/ijms241311036.

286. Eisenach, J. C., Hood, D. D. & Curry, R. Phase I safety assessment of intrathecal injection of an american formulation of adenosine in humans. *Anesthesiology* (2002) doi:10.1097/00000542-200201000-00010.

287. Richter, M. M. *et al.* Thermogenic capacity at subzero temperatures: How low can a hibernator go? *Physiol. Biochem. Zool.* **88**, 81–89 (2015).

288. Yoo, H.-J., Ham, J., Duc, N. T. & Lee, B. Quantification of stroke lesion volume using epidural EEG in a cerebral ischaemic rat model. *Sci. Rep.* **11**, 2308 (2021).

289. O'Regan, M. Adenosine and the regulation of cerebral blood flow. *Neurol. Res.* **27**, 175–181 (2005).

290. Daviaud, N., Garbayo, E., Schiller, P. C., Perez-Pinzon, M. & Montero-Menei, C. N. Organotypic cultures as tools for optimizing central nervous system cell therapies. *Exp.*

Neurol. **248**, 429–440 (2013).

291. Antonow-Schlorke, I., Ehrhardt, J. & Knieling, M. Modification of the Ladder Rung Walking Task—New Options for Analysis of Skilled Movements. *Stroke Res. Treat.* **2013**, 1–11 (2013).

292. Zhang, F. *et al.* When hypothermia meets hypotension and hyperglycemia: The diverse effects of adenosine 5'-monophosphate on cerebral ischemia in rats. *J. Cereb. Blood Flow Metab.* **29**, 1022–1034 (2009).